# Meiosis made simple:

# Mechanisms of meiotic chromosome dynamics elucidated in somatic cells

DISSERTATION

zur Erlangung des Grades
- Doktor der Naturwissenschaften -
der Fakultät für Biologie, Chemie und Geowissenschaften
der Universität Bayreuth

Vorgelegt von

**Peter Gerhard Wolf**

aus Wohlmannsgesees

Bayreuth 2017

Die vorliegende Arbeit wurde in der Zeit von April 2013 bis Februar 2017 in Bayreuth am Lehrstuhl für Genetik unter der Betreuung von Herrn Prof. Dr. Olaf Stemmann angefertigt.

Vollständiger Abdruck der von der Fakultät für Biologie, Chemie und Geowissenschaften der Universität Bayreuth genehmigten Dissertation zur Erlangung des akademischen Grades eines Doktors der Naturwissenschaften (Dr. rer. nat.)

Dissertation eingereicht am: 06.02.2017

Zulassung durch die Promotionskommission: 15.02.2017

Wissenschaftliches Kolloquium: 28.03.2017

Amtierender Dekan: Prof. Dr. Stefan Schuster

Prüfungsausschuss:

| | |
|---|---|
| Prof. Dr. Olaf Stemmann | (Erstgutachter) |
| Prof. Dr. Benedikt Westermann | (Zweitgutachter) |
| Prof. Dr. Klaus Ersfeld | (Vorsitz) |
| Dr. Claus-Dieter Kuhn | |

## Table of contents

## Summary

After DNA replication in S-phase sister chromatids are held together by a mechanism termed sister chromatid cohesion, which ensures accurate chromosome segregation in both mitosis and meiosis. Cohesion is mediated by the ring-shaped multimeric protein complex cohesin. Mitotic cells employ a cohesin complex composed of Smc1, Smc3, Scc1 and Stag1 or Stag2. To allow segregation of the sister chromatids in mitosis cohesin is removed from chromosomes in two steps. The protein Wapl dissociates the interface of two cohesin subunits allowing cohesin removal along chromosome arms. At the centromere cohesin is preserved since Sgo1 locally counteracts Wapl activity. Centromeric cohesin is ultimately removed by the protease Separase, which cleaves the subunit Scc1. Meiocytes express meiosis-specific cohesin subunits besides the above mentioned canonical cohesin proteins. Research indicates that during meiosis most cohesin complexes contain the meiosis-specific Rec8 instead of Scc1. Homologous chromosomes are tethered via chiasmata and Separase-dependent cleavage of Rec8 at chromosome arms allows their separation in meiosis I. Centromeric Rec8 is protected by Sgo2 until also this pool is cleaved in meiosis II facilitating sister chromatid distribution. Proper chromosome cohesion and correct cohesion resolution in germ cells is critical to prevent the formation of aneuploid gametes, trisomies, and infertility. Despite its importance for human health many features of meiotic cohesin complexes remain uncharacterized. In this study we use the advantage of cultured somatic cells over germ cells regarding biochemical accessibility to unravel fundamental aspects of meiosis-specific cohesin. When expressed in Hek 293 cells, Rec8 displays virtually no affinity for the cohesin subunits Stag1 or Stag2 but strongly interacts with the usually germ cell-specific Stag3. Accordingly, Rec8 is granted access to the nucleus and is loaded onto chromatin only upon co-expression of Stag3. Importantly, co-expression of Rec8 and Stag3 rescues a Sgo1 knockdown but only if Sgo2 is present. Similarly, premature loss of cohesion in response to overexpression of a hypermorphic Separase allele is suppressed by Rec8-Stag3 in a Sgo2-dependent manner. Together with additional functional assays, this indicates that centromeric Rec8 can be protected by Sgo2 from the cohesin antagonists Wapl and Separase. Our data suggest that Sgo1 exclusively protects Scc1-Stag1/2 containing cohesin, whereas Sgo2 is only competent to protect Rec8-Stag3 containing cohesin. However, under non-physiological conditions, i.e. overexpression, the Sgo proteins might be more promiscuous. Our finding that meiotic cohesin complexes are susceptible to prophase pathway signaling raises the interesting question of how cohesin

dynamics is regulated in germ cells (especially during the long dictyate arrest in oocytes) in which Wapl is present.

Studies in mouse oocytes revealed that Cyclin A is required for sister chromatid separation (SCS) in meiosis II probably by inactivating Sgo2 at the centromere. We asked whether standard cell culture cell lines can help to understand Cyclin A's meiotic function. Under physiological conditions Cyclin A is degraded in early mitosis. When we overexpressed a non-degradable variant of Cyclin A we were able to observe premature SCS in mitotically arrested cells. We speculated that this effect might be due to Sgo1 inactivation. In the following we created a stably transgenic cell line that inducibly expresses non-degradable Cyclin A and also observed precocious loss of cohesion upon induction of the transgene. This cell line can be used in subsequent studies to unravel the mechanism of Cyclin A's activity regarding chromosome cohesion control. Induction of Cyclin A can be combined with depletion or overexpression of other proteins and changes in the level of cohesion loss would indicate an involvement of the corresponding protein in the Cyclin A pathway.

## Zusammenfassung

**Meiose mal einfach:**
**Die Verwendung von somatischen Zellen zur Aufklärung von Mechanismen der meiotischen Chromosomensegregation**

Nach der Replikation der DNA sorgt die Schwesterchromatid-Kohäsion für die physikalische Verbindung der Schwesterchromatiden und gewährleistet deren korrekte Segregation in Mitose und Meiose. Die Kohäsion wird durch den ringförmigen Proteinkomplex Cohesin vermittelt, der in mitotischen Zellen aus den Untereinheiten Smc1, Smc3, Scc1 und Stag1 oder Stag2 besteht. Während der Mitose wird Cohesin auf zwei unterschiedlichen Wegen von den Chromosomen entfernt. Zunächst löst Wapl die Kohäsion entlang der Chromosomenarme auf, indem es die Interaktionsstelle zweier Cohesin-Untereinheiten öffnet. Centromerische Kohäsion bleibt erhalten, da an dieser Stelle Sgo1 die Aktivität von Wapl neutralisiert. Die Verteilung der Chromatiden wird initiiert, wenn die Protease Separase die Untereinheit Scc1 von centromerischem Cohesin schneidet. In meiotischen Zellen kann der Cohesin-Ring anders zusammengesetzt sein als oben beschrieben, da in entstehenden Keimzellen zusätzliche meiose-spezifische Untereinheiten exprimiert werden. Man geht davon aus, dass die meisten Cohesin-Ringe in meiotischen Zellen das meiose-spezifische Rec8 anstatt Scc1 enthalten. In Meiose I werden die über Chiasmata verknüpften homologen Chromosomen getrennt, indem Rec8 an den Armen der Chromosomen von Separase gespalten wird. Rec8 am Centromer wird von Sgo2 geschützt bis in Meiose II auch diese Fraktion von Cohesin durch Separase geöffnet wird. Die Chromosomen-Kohäsion und deren Auflösung ist entscheidend für eine korrekte Chromosomensegregation in der Meiose und entsprechende Fehler stellen eine Ursache für Trisomie, Fehlgeburten und Unfruchtbarkeit dar. Die Eigenschaften von meiose-spezifischen Cohesin-Komplexen besser zu verstehen erscheint daher äußerst relevant. Die Charakterisierung von Cohesin in der Meiose von Säugern wurde bisher hauptsächlich mit Oozyten bzw. Spermatozyten von Mäusen durchgeführt. Da biochemische Experimente in diesen Systemen nur schwer durchführbar sind, wurde in der vorliegenden Arbeit eine standardmäßig verwendete somatische Zelllinie benutzt, um meiotisches Cohesin zu untersuchen. Rec8 wird in Hek 293 Zellen exprimiert und durch anschließende Immunpräzipitation gezeigt, dass Rec8 nicht mit Stag1 oder Stag2, sondern nur mit dem meiose-spezifischen Stag3 interagiert. Eine Kernlokalisation von Rec8 ist auch nur zu beobachten, wenn zusätzlich Stag3 exprimiert wird. Eine RNAi-vermittelte Depletion von Sgo1

induziert einen Kohäsionsdefekt in mitotisch-arretierten Zellen, der durch die Anwesenheit von Rec8 und Stag3 aufgehoben wird. Auch die Expression einer hyperaktiven Separase Variante führt zu vorzeitiger Schwesterchromatid-Trennung, die durch Rec8 und Stag3 reduziert wird. Die durch Rec8-Stag3 vermittelte Verringerung der vorzeitigen Schwesterchromatid-Trennung im Fall der Sgo1 Depletion und auch im Fall der Separase Expression, kann aufgehoben werden, wenn die zelluläre Proteinmenge von Sgo2 durch siRNA verringert wird. Diese Befunde deuten darauf hin, dass Rec8 durch Sgo2 vor den Cohesin-Antagonisten Wapl und Separase geschützt werden kann und, dass Sgo1 ausschließlich Scc1-Stag1/2 enthaltendes Cohesin schützt, während Sgo2 nur in der Lage ist, Rec8-Stag3 enthaltende Cohesin-Komplexe zu schützen. Liegt die Konzentration der Sgo-Proteine durch Überexpression deutlich über der physiologischen Menge, scheint die Spezifität für einen bestimmten Cohesin-Komplex abzunehmen. Da in dieser Arbeit gezeigt wird, dass meiotische Cohesin-Komplexe von Wapl geöffnet werden können, sollten zukünftige Studien untersuchen wie Wapl während der Meiose reguliert wird.

Untersuchungen an Maus-Oozyten konnten zeigen, dass Cyclin A für die Schwesterchromatid-Trennung in der Meiose II erforderlich ist – wahrscheinlich, weil es Sgo2 inaktiviert. Unter physiologischen Bedingungen wird Cyclin A in der frühen Mitose abgebaut. Im Rahmen dieser Arbeit konnte gezeigt werden, dass mitotisch arretierte Hek 293 Zellen unter vorzeitiger Schwesterchromatid-Trennung leiden, wenn die Zellen eine nicht abbaubare Variante von Cyclin A exprimieren. Es ist denkbar, dass dieser Effekt ähnlich wie in Meiose durch die Inaktivierung von Sgo1 ausgelöst wird und daher wiederum eine Zellkultur Zelllinie verwendet werden kann, um den Mechanismus von Cyclin A bezüglich der Chromosomen-Segregation aufzuklären. Im Folgenden wurde eine stabile transgene Zelllinie erzeugt, die nicht-abbaubares Cyclin A induzierbar exprimiert und auch hier wurde nach der Induktion des Transgens ein frühzeitiger Verlust der Kohäsion beobachtet. Diese Zelllinie soll in weiteren Experimenten Verwendung finden, in denen z.B. die Induktion von Cyclin A mit einer Depletion oder Überexpression anderer Proteine kombiniert wird. Ändert sich der Kohäsionsverlust relativ zur alleinigen Cyclin A Expression kann angenommen werde, dass das entsprechende depletierte oder überexprimierte Protein mit Cyclin A zusammenwirkt.

# 1. Introduction

## 1.1. The cell cycle

The reproduction of cells is one of the fundamental features of life. The highly ordered process that leads to the formation of two daughter cells from one mother cell in eukaryotes is called the cell cycle (Figure 1). In order to generate two identical progeny cells the genetic material has to be correctly duplicated and equally distributed onto the newly forming daughter cells. The duplication of the DNA takes place in S-phase where each chromatid is replicated forming two sister chromatids. These sister chromatids are segregated in mitosis before the cytoplasm of the mother cell is divided by cytokinesis. When referred to mitosis and cytokinesis the term M-phase is frequently used. S-phase and M-phase are mostly separated by two gap-phases (G1-phase between M-phase and S-phase and G2-phase between S-phase and M-phase), which allow cell growth and organelle multiplication. Together the gap-phases and S-phase are referred to as interphase (Klug, 2012; Morgan, 2007).

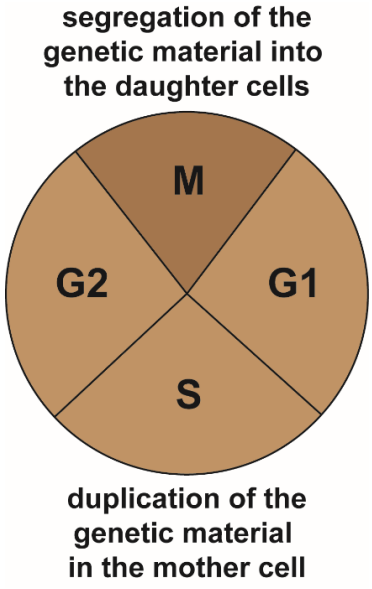


**Figure 1: The eukaryotic cell cycle**
The graphics shows the four phases of the cell cycle (M: M phase, S: S phase, G1/2: gap phase 1/2). DNA is duplicated in S-phase. Segregation of the DNA and cell division take place in M-phase. Light brown denotes the period of the cell cycle termed interphase.

## 1.2. Mitosis

During mitosis the genetic material of the mother cell is equally distributed to the daughter cells (Figure 2). The sister chromatids are separated and transported to opposite cell poles by the mitotic spindle apparatus. The main component of this machinery are mircotubules that emanate from microtubule organizing centers (called centrosomes in higher eukaryotes), which localize to the opposite poles of the cell providing the bipolarity of the spindle. Mitosis is subdivided in prophase, prometaphase, metaphase, anaphase and telophase. In prophase the chromosomes condense, the mitotic spindle begins to form and the nuclear envelope starts to dissolve. The subsequent prometaphase is characterized by the complete disintegration of the nuclear envelope and the congression and alignment of the chromosomes. Metaphase marks the time, at which the chromosomes are correctly aligned at the so-called metaphase plate between the two spindle poles. The physical linkage between the sister chromatids is resolved and the individual chromatids are segregated during anaphase. In telophase the chromosomes decondense, the microtubules of the spindle depolymerize and the nuclear envelope reforms around the chromatin masses (Klug, 2012; Morgan, 2007).

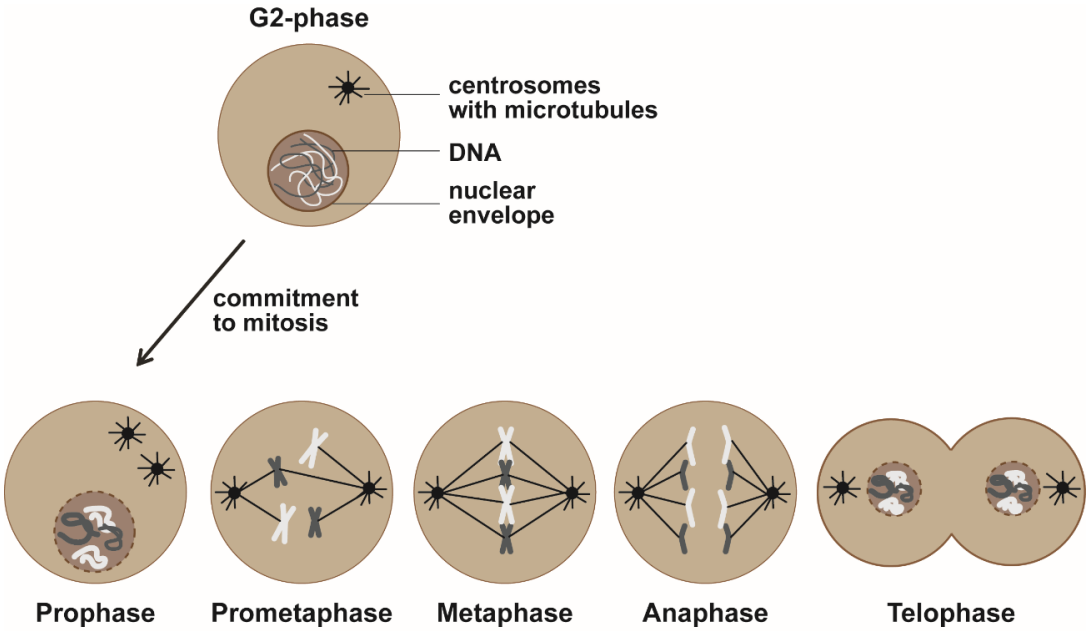


**Figure 2: Scheme of mitosis**
A cell in G2-phase decides to divide and starts the mitotic program. The centrosomes split, the chromosomes condense and the nuclear envelope breaks down. The chromosomes attach to the mitotic spindle and congress until they align at the metaphase plate. After their segregation the sister chromatids decondense again and nuclear envelope reformation takes place. See text for details.

### 1.2.1. Cell cycle regulators and mitotic entry

Besides the modification of proteins with ubiquitin, phosphorylation is the most important mechanism in cell cycle regulation. Very prominent players are the cyclin-dependent kinases (Cdks), which are activated upon binding of cyclins and are additionally controlled by inhibiting and activating phosphorylations (Lindqvist et al., 2009; Murray, 2004). As the name implies cyclins are typically regulated by periodic cycles of transcription and degradation. The fluctuations in the levels of cyclins control the activity of their associated Cdks and, hence, the corresponding events during the cell cycle (Lindqvist et al., 2009; Murray, 2004). Since there are several cyclins and Cdks in humans, we will focus on the factors that are relevant for this work, namely Cyclin B, Cyclin A and Cdk1.

The maturation promoting factor was described as an activity that drives mitotic entry and was later characterized as a complex of Cyclin B and Cdk1 (Gautier et al., 1990; Gautier et al., 1988; Lindqvist et al., 2009; Masui and Markert, 1971). Cyclin B-Cdk1 triggers several mitotic events like chromosome condensation, nuclear envelope breakdown and spindle formation (Crasta et al., 2006; Heald and Mckeon, 1990; Shintomi et al., 2015; Ward and Kirschner, 1990). Association with Cyclin B is not sufficient for Cdk1 to become active, since Myt1 and Wee1 modify the kinase with inhibitory phosphorylations (Mueller et al., 1995b; O'Farrell, 2001; Parker et al., 1992). Therefore, for mitotic entry the phosphatase Cdc25 has to be activated, which removes the inhibitory phosphates from Cdk1 (Gautier et al., 1991; Kumagai and Dunphy, 1992). Once active, Cyclin B-Cdk1 further activates Cdc25 while simultaneously inhibiting Wee1 and Myt1 by phosphorylation (Booher et al., 1997; Hoffmann et al., 1993; McGowan and Russell, 1995; Mueller et al., 1995a). This positive feedback loop amplifies Cyclin B-Cdk1 activity and triggers a switch-like progression into mitosis (Lindqvist et al., 2009; O'Farrell, 2001).

Another player that drives the cell cycle is Cyclin A, which can activate Cdk1 and Cdk2. Higher eukaryotes possess Cyclin A1 and Cyclin A2 whereas the former one is most likely only expressed in germ cells and a distinct set of stem cells (Liu et al., 1998; Miftakhova et al., 2015; Ravnik and Wolgemuth, 1999; Yang et al., 1999). The only essential function of cyclin A1 seems to be in spermatogenesis (Liu et al., 1998). Cyclin A2, however, is present in proliferating somatic cells and its ablation causes early embryonic lethality (Murphy et al., 1997). From now on we will only use the term Cyclin A but always refer to Cyclin A2. The synthesis of Cyclin A starts at the onset of S-Phase and, consistent with its role in DNA replication control,

microinjection of anti-Cyclin A antibodies in cells blocks their progression through S-phase (Cardoso et al., 1993; Girard et al., 1991; Pagano et al., 1992; Sobczakthepot et al., 1993; Zindy et al., 1992). Conversely, an additional task of cyclin A is probably to restrict re-replication. Cyclin A was shown to phosphorylate the pre-replicative complex subunit Cdc6, which triggers its relocalization from the nucleus to the cytoplasm and its subsequent destruction (Coverley et al., 2000; Petersen et al., 1999). Besides this, Cyclin A inactivates the priming polymerase α-primase and the DNA helicase Mcm4-Mcm6-Mcm7 (Ishimi et al., 2000; Voitenleitner et al., 1997).

Once replication is complete Cyclin A is required for mitosis, since RNAi mediated depletion of Cyclin A in HeLa cells causes a substantial delay in mitotic entry most likely induced by a slowed activation of Cyclin B1-Cdk1 complexes (De Boer et al., 2008; Fung et al., 2007; Gong et al., 2007). Since Cyclin A was shown to activate Cdc25, it was proposed that the Cyclin A-Cdk complex provides a basal level of Cdk activity that lowers the threshold of Cyclin B-Cdk1 necessary to sustain the feedback loop required for the commitment to mitosis (Lindqvist et al., 2009; Mitra and Enders, 2004).

### 1.2.2. Mitotic exit and the ubiquitin proteasome system

Ubiqutin is a highly conserved protein of 76 amino acids. It received its name due to its ubiquitous expression in all eukaryotic cells. Ubiquitin gets covalently attached to other proteins via an isopeptide bond between its C-terminal glycine and the ε-amino group of a lysine residue of a target protein (Finley et al., 2012). This process is called ubiquitylation. Ubiquitylation requires a cascade of enzymatic activities mediated by the ubiquitin-activating enzymes (E1s), ubiquitin-conjugating enzymes (E2s), and ubiquitin ligase enzymes (E3s). E1 uses ATP to form a thioester bond between the sulfhydryl group of its active-site cysteine and the C-terminal carboxyl group of ubiquitin. Subsequently the ubiquitin molecule is transferred to the active-site cysteine of an E2. Finally, it is conjugated to the substrate via the action of an E3 (Finley et al., 2012; Komander and Rape, 2012). Two main classes of E3 enzymes are known: The HECT domain-containing E3s and the RING motif-containing E3s. Ring E3s act as adaptors by binding an E2 loaded with ubiquitin and a substrate protein, thereby facilitating the transfer of ubiquitin by positioning the substrate lysine close to the reactive E2-ubiquitin thioester bond (Finley et al., 2012). The mechanism of conjugation involving a HECT ubiquitin

ligase is different. In this case the ubiquitin molecule is first transferred from the E2 to an active-site cysteine in the HECT domain of the E3. In the next step the ubiquitin molecule is passed from the E3 to the lysine residue of the substrate (Finley et al., 2012; Kerscher et al., 2006; Komander and Rape, 2012). Substrate proteins can be modified with single ubiquitin molecules (monoubiquitylation) either at one lysine residue or at multiple lysine residues. Furthermore, a polyubiquitin chain can be formed by successive addition of ubiquitin molecules to the N-terminus or to the ε-amino group of one of the seven lysine residues of the previously attached ubiquitin (Komander and Rape, 2012). This allows the formation of differently linked polyubiquitin chains. Monoubiquitylation and all possible polyubiquitin chains have been detected in cells. The best characterized function of ubiquitylation is the targeting of proteins to the 26S proteasome (Finley et al., 2012). The role in proteasomal targeting was first assigned to Lys48-linked chains, however, also other chain types especially Lys11 can mediate proteasomal degradation (Chau et al., 1989; Jin et al., 2008; Saeki et al., 2009; Xu et al., 2009a).

The 26S proteasome is found in all eukaryotes and is organized into two subassemblies, the regulatory particle and the core particle. The regulatory particle recognizes polyubiquitylated substrates, while the core particle contains the proteolytic active sites (Finley, 2009). Proteasomal degradation has several important cellular functions, including protein quality control, generating peptides for antigen presentation and degradation of regulatory proteins (Hershko and Ciechanover, 1998).

A RING motif-containing ubiquitin ligase with utmost importance for cell cycle regulation is the anaphase promoting complex/cyclosome (APC/C). This complex ligase consists of 15-17 subunits depending on the organism and is inactive from late G1-phase until mitosis, which allows the accumulation of its substrates (Pines, 2011). Most important among these substrates are the Separase inhibitor Securin and Cyclin B (Pines, 2011). In early mitosis APC/C is activated by phosphorylation, which facilitates binding of the co-activator Cdc20 (Kraft et al., 2003; Rudner and Murray, 2000). APC/C-Cdc20 binds to a degron motif in its substrates called the D-box and mediates ubiquitylation (Pines, 2011). Since the spindle assembly checkpoint (SAC) inhibits the APC/C, its substrates are not degraded in early mitosis. However, there are a few exceptions of proteins, including Cyclin A, that are degrade in an APC/C dependent manner despite SAC activity (discussed below). When all chromosomes are properly attached to the mitotic spindle the SAC is satisfied and the APC/C mediated

degradation of Securin and Cyclin B initiates anaphase. Another co-activator of the APC/C, Cdh1, is kept inactive during mitosis by Cyclin B1-Cdk1 dependent phosphorylation (Jaspersen et al., 1999). After a sufficient amount of Cyclin B is degraded, Cdh1 binds the APC/C and the resulting complex marks additional mitotic proteins for proteolysis including Cdc20 (Hagting et al., 2002; Lindon and Pines, 2004; Robbins and Cross, 2010). In G1-phase APC/C-Cdh1 is important for the prevention of premature initiation of S-phase (Sigl et al., 2009). When cells have committed to a new round of the cell cycle APC/C-Cdh1 is inactivated through phosphorylation by distinct cyclins and binding of inhibitors (Hsu et al., 2002; Pines, 2011).

### 1.2.3. Attachment of chromosomes to the mitotic spindle and the spindle assembly checkpoint

At the beginning of mitosis centrosomes and microtubules form a bipolar spindle. The spindle microtubules are highly dynamic and are responsible for capture and congression of mitotic chromosomes. The attachment between spindle microtubule plus ends and chromosomes is mediated by a large protein structure assembled on centromeric chromatin called the kinetochore (Westhorpe and Straight, 2013). Prior to the onset of anaphase, chromosomes have to align at the spindle midzone and generate amphitelic kinetochore attachments, in which each sister kinetochore is connected to microtubules from opposing poles of the spindle (Santaguida and Musacchio, 2009; Westhorpe and Straight, 2013).

Besides this correct attachment three erroneous modes of connection can form between kinetochores and the spindle. Monotelic attachment produces mono-oriented chromosomes in which only one sister kinetochore is attached to one spindle pole. Another type of attachment is called syntelic. Here, both sister kinetochores are associated with microtubules emanating from the same spindle pole (Gregan et al., 2011). These linkages are in contrast to the amphitelic attachment not stable i.e. they are permanently cleared. A current model suggests that the centromeric kinase Aurora B continuously phosphorylates outer kinetochore proteins resulting in a low affinity for the spindle microtubules. Correctly attached bi-oriented sister kinetochore pairs, however, create inter-kinetochore tension that physically separates the outer kinetochore proteins from Aurora B leading to a tight binding of the microtubules to the chromosome (Gregan et al., 2011). The third type of incorrect attachments is called merotelic. The kinetochores of a chromosome displaying merotelic attachment are both

attached to opposite sides of the spindle but at least one kinetochore shows additional syntelic attachment. Since these linkages create inter-kinetochore tension and are, thus, highly dangerous for cells, researchers still discuss about how merotelic attachments are prevented or corrected. One straightforward explanation is that the structural organization of the kinetochores simply suppresses the formation of merotely (Gregan et al., 2011).

Only when all kinetochores are correctly attached the cell will initiate mitotic exit and segregate the chromatids. The mechanism that monitors and responds to kinetochore-microtubule attachment is the SAC. The SAC components inhibit the APC/C by binding to its co-activator Cdc20 (Foley and Kapoor, 2013; Lara-Gonzalez et al., 2012; Musacchio, 2015; Sacristan and Kops, 2015). The core component of the SAC is the protein Mad2, which exists in two conformations: a “closed” conformation that is competent to bind Cdc20 and an “open” conformation that does not associate with Cdc20. The current model suggests that Mad2 is recruited to unattached kinetochores where the conformational change from “open” to “closed” state of Mad2 is catalyzed and the Mad2-Cdc20 complex is formed. After association with additional SAC proteins Cdc20 is bound in the so called mitotic checkpoint complex (MCC). Cdc20 molecules in MCCs can still interact with the APC/C but do not mediate the ubiquitylation of the substrates (Foley and Kapoor, 2013; Lara-Gonzalez et al., 2012; Musacchio, 2015; Sacristan and Kops, 2015). As mentioned above Cyclin A is an exception since its APC/C-dependent degradation takes place in early mitosis when the SAC is active. Available data imply that Cyclin A has a very high affinity for Cdc20 and can, thus, compete with the SAC proteins for Cdc20 interaction leading to its degradation at a time when Cdc20 is engaged in MCCs (Di Fiore and Pines, 2010).

## 1.3. Cohesin in mitosis

As pointed out above, accurate attachment of the chromosomes to the mitotic spindle requires opposition to the separation force of the microtubules. Key to this process is the physical linkage between sister chromatids called cohesion. One molecular explanation for cohesion is catenation generated during replication when sister DNAs are wound around one another. However, decatenation is mediated by topoisomerase 2, which is constitutively active and not the time limiting factor of anaphase onset. (Koshland and Hartwell, 1987; Nasmyth and Haering, 2009). Screens in yeast for mutants that displayed premature

separation of sister chromatids identified genes required for cohesion. Today we know that the multiprotein complex cohesin provides cohesion between sister chromatids from their generation in S-phase until their distribution in anaphase (Michaelis et al., 1997; Nasmyth and Haering, 2009).

### 1.3.1. The cohesin ring

The multimeric cohesin complex consists of an integral tripartite ring structure and associated proteins. The integral ring is formed by Smc1, Smc3 and the kleisin protein Scc1 (Nasmyth, 2011; Nasmyth and Haering, 2009). Smc proteins show a highly elongated rod-like shape. At the center of the polypeptide Smc proteins fold back onto themselves, which allows the formation of a 50 nm long, antiparallel, intramolecular coiled-coil (Haering et al., 2002; Melby et al., 1998). The region where the folding occurs is called the hinge domain, which is one end of the coiled-coil. At the other end of the coiled-coil N-terminal and C-terminal amino acids form an ATP nucleotide-binding domain (NBD) of the ABC family (Figure 3). Heterotypic interactions between the hinge domains of Smc1 and Smc3 lead to the formation of a Smc1/3 heterodimer. The NBDs of Smc1 and Smc3 in a cohesin ring can associate with each other to form two ATPase sites. One ATPase site is formed by the signature motif and D-loop of Smc1 and the Walker A and Walker B motifs of Smc3, whereas the second site harbors the Walker A and Walker B motifs of Smc1 and the signature motif and D-loop of Smc3 (Haering et al., 2004; Lammens et al., 2004).

Scc1 interacts with Smc1's NBD via its C-terminus and with the coiled coil emerging from Smc3’s NBD via its N-terminus (Gligoris et al., 2014; Haering et al., 2004; in 't Veld et al., 2014). The middle region of Scc1 provides a binding platform for an additional subunit termed Scc3 in *Saccharomyces cerevisiae* (Haering et al., 2002). Somatic cells of higher eukaryotes express two variants of Scc3 known as Stag1 and Stag2 (Losada et al., 2000). Cohesin complexes containing Stag1 as well as rings containing Stag2 are competent to provide cohesion whereas Stag1 seems to be especially important for telomeric sister chromatid cohesion in mammalian cells (Canudas and Smith, 2009). An additional peripheral subunit of the cohesin ring is Pds5 (Panizza et al., 2000). While Scc3 is an integral subunit of the cohesin complex Pds5 might be a substoichiometric cohesin component (Sumara et al., 2000). Pds5 mediates the interaction

of the cohesin complex with the regulatory proteins Eco1, Sororin and Wapl (Minamino et al., 2015; Nishiyama et al., 2010; Shintomi and Hirano, 2009; Vaur et al., 2012).

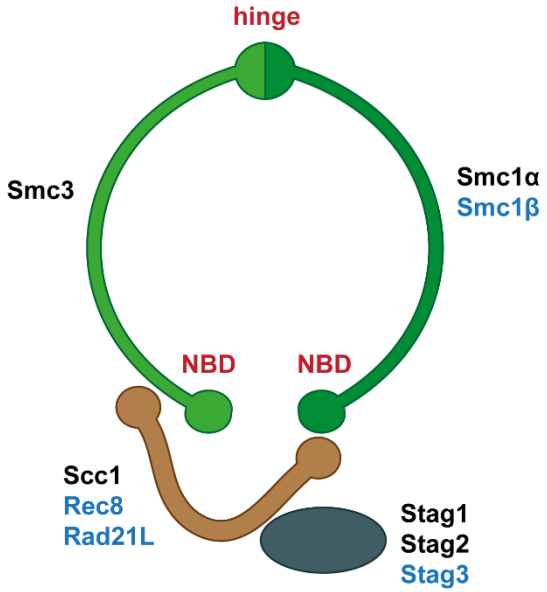


| | ubiquitous | meiosis-specific |
|---|---|---|
| Smc proteins | Smc1α, Smc3 | Smc1β |
| kleisins | Scc1 | Rec8, Rad21L |
| kleisin-binding subunits | Stag1, Stag2 | Stag3 |

**Figure 3: Composition of the cohesin ring in vertebrates**
The figure shows a greatly simplified model of the cohesin ring. For all subunits except Smc3 paralogs have been identified some of which are exclusively expressed in meiocytes. Note that the NBDs of the Smc proteins can associate and form an additional gate. Regulatory proteins are omitted for clarity. Pds5, Wapl and Sororin bind in the lower region of the complex where the kleisin and the kleisin-binding subunit reside.

The notion that Smc1, Smc3 and Scc1 form a ring has led to the proposal of the ring (or embrace) model. According to this model a single monomeric cohesin ring traps the two sister chromatids inside its lumen. This implies that cohesin holds sister chromatids together employing a topological principle rather than physical binding to DNA (Nasmyth and Haering, 2009). In strong support of this model it has been shown that artificial cleavage of the cohesin ring containing engineered Scc1 or Smc3 induces cohesin's dissociation from chromatin and loss of sister chromatid cohesion (Gruber et al., 2003; Uhlmann et al., 2000). Additional important experiments performed in yeast to shed light on cohesin's mechanism of action employed small circular minichromosomes. The minichromosomes are replicated during S-

phase and the duplicated products are held together by cohesin. In accordance with the ring model, cleavage of the cohesin ring or linearization of the DNA with a restriction enzyme abolishes the interaction of cohesin with the minichromosomes (Ivanov and Nasmyth, 2005, 2007). Furthermore, introducing covalent bonds between the three subunits of the cohesin ring rendered the association of cohesin and minichromosomes resistant against protein denaturation with sodium dodecyl sulfate (SDS) indicating that cohesin acts via a topological mechanism (Haering et al., 2008). The ring model also implies that cohesin should be capable of sliding along chromatin fibers once it has entrapped them. Such a movement was indeed observed *in vivo* and *in vitro* (Davidson et al., 2016; Lengronne et al., 2004). Since it is widely accepted among cell cycle researchers, we will use the described ring model as an intellectual framework throughout this thesis.

### 1.3.2. Establishment of cohesion

In human cells cohesin starts to re-associate with chromosomes in telophase, a process known as cohesin loading. This loading of cohesin onto chromosomes is facilitated by a heterodimeric complex formed by Scc2 and Scc4. Initially, Scc2 has been found to be essential for proper sister chromatid cohesion in yeast and subsequent work identified Scc4 as a binding partner of Scc2 (Ciosk et al., 2000; Furuya et al., 1998; Michaelis et al., 1997). Later it was demonstrated that homologs of Scc2 and Scc4 are also required for association of cohesin with chromosomes in mammalian cells (Seitan et al., 2006; Watrin et al., 2006). In 2006 the Ellenberg group determined the binding stability of cohesin on DNA and found that most chromosomal cohesin has a mean residence time of less than 25 min in both G1 and G2 cells (Gerlich et al., 2006). In G2 cells, however, a pool of cohesin corresponding to one-third of the total amount of cohesin complexes shows a much longer residence time. This fraction probably represents the cohesin pool actually mediating sister chromatid cohesion (Gerlich et al., 2006). A key question for a long time was whether the short residence time cohesin is topologically associated with DNA. Very recent *in vitro* work by Uhlmann and co-workers provides important clues to answer that question. The group incubated the purified cohesin complex (Smc1, Smc3, Scc1 and Scc3) from *Schizosaccharomyces pombe* with circular plasmid DNA obtained from bacteria. They found that cohesin bound the plasmid DNA in a topological fashion and that this interaction was strongly enhanced by addition of the loader complex

Scc2-Scc4 (Murayama and Uhlmann, 2014). This observation indicates that also in cells all cohesin that is loaded onto chromatin is topologically engaged with the DNA fiber.

It is obvious that topological association of DNA and cohesin requires opening of the ring by transient dissociation of one of its three interfaces. In elegant experiments the cohesin ring subunits were modified by fusion to proteins, which dimerize in presence of a distinct ligand allowing the controlled tethering of the interfaces. This artificial locking of the gates led to the proposal that DNA enters the ring through the hinge interface of Smc1 and Smc3 (Buheitel and Stemmann, 2013; Gruber et al., 2006). *In vitro* experiments reconstituting the loading reaction, however, challenged this view (Murayama and Uhlmann, 2015). Those experiments imply that the cohesin ring folds in a way that the hinge domain makes contacts with the ATPase domain. The NBDs of Smc1 and Smc3 disengage while hydrolyzing ATP and the DNA is trapped within the small ring formed by Scc1 and the Smc heads. In a second step the interface between Smc3 and Scc1 or Smc1 and Scc1 dissociates and the chromatid enters the ring (Murayama and Uhlmann, 2015). The authors speculated that the protein insertions for the ligand induced dimerization interfere with the folding of the cohesin ring required for DNA entry. This effect might have lead to the loading defects observed upon hinge interface locking. Closing the gate between Scc1 and Smc1 or Smc3 might not lead to a loading phenotype since opening of any of the two gates could facilitate proper topological engagement once DNA is trapped between the ATPase head and Scc1 (Murayama and Uhlmann, 2015). The unloading of cohesin requires similar events. ATP hydrolysis leads to dissociation of the interface between the NBDs and in the second step the protein Wapl opens the gate between Smc3 and Scc1 (Murayama and Uhlmann, 2015). For the DNA exit reaction it was convincingly shown the Smc3-Scc1 interface opens both *in vivo* and *in vitro* (Beckouet et al., 2016; Buheitel and Stemmann, 2013; Chan et al., 2012; Eichinger et al., 2013; Murayama and Uhlmann, 2015). *In vitro* Wapl can also stimulate the loading reaction of cohesin onto DNA probably by opening the Smc3-Scc1 gate (Murayama and Uhlmann, 2015). However, the phenotype of Wapl depletion in mammalian cells increases the level of cohesin on chromatin, a phenotype that is consistent with an anticohesive function of Wapl (Gandhi et al., 2006; Haarhuis et al., 2013; Kueng et al., 2006; Tedeschi et al., 2013). Remarkably, although the loading and the unloading of cohesin require the disengagement of the NBDs, ATP hydrolysis seems to be more important for DNA exit than for entry (Elbatsh et al., 2016; Murayama and Uhlmann, 2015). The authors speculated that for an unknown reason ATP hydrolysis might be

rate limiting for the unloading but not for loading reaction (Murayama and Uhlmann, 2015). As noted above, cohesin associates with chromosomes before S-phase but undergoes constant dissociation from and reloading onto chromosomes (Gerlich et al., 2006). During DNA replication a fraction of the highly dynamic cohesin complexes are converted into a stable pool that holds sister chromatids together, the actual cohesion establishment. A crucial player involved in cohesin stabilization, namely Eco1, is physically coupled to the DNA polymerase co-factor PCNA and, hence, travels with the replication fork along chromosomes in S-phase (Moldovan et al., 2006). Eco1 is an acetyl transferase and has been shown to acetylate two adjacent lysine residues (K105/106 in humans) in Smc3 (Ben-Shahar et al., 2008; Unal et al., 2008; Zhang et al., 2008b). The region of Smc3 containing the lysine residues points to the center of the cohesin ring and the newest model proposes that interaction of this surface with entrapped DNA stimulates ATP hydrolysis triggering dissociation of the NBDs (Gligoris et al., 2014; Murayama and Uhlmann, 2015). Lysine acetylation by Eco1 blocks the DNA mediated stimulation of ATP hydrolysis. Furthermore, there is evidence that acetylation of the two lysine residues in Smc3 is involved in the recruitment of Sororin, a positive regulator of cohesion in vertebrates (Ladurner et al., 2016; Lafont et al., 2010; Liu et al., 2013b; Nishiyama et al., 2010; Nishiyama et al., 2013; Rankin et al., 2005; Schmitz et al., 2007). Sororin most likely competes with Wapl for binding to cohesin and, hence, inhibits Wapl's ring opening activity (Nishiyama et al., 2010).

### 1.3.3. The resolution of cohesion

In many eukaryotic cells cohesin is removed from chromosomes during two phases of mitosis. During prophase the bulk of cohesin is removed by an activity known as the prophase pathway (Sumara et al., 2000; Waizenegger et al., 2000). The phosphorylation of Stag2 and Sororin allow the replacement of Sororin by Wapl, which in turn leads to ring opening and dissociation of the cohesin complex from DNA (Gandhi et al., 2006; Hauf et al., 2005; Kueng et al., 2006; Liu et al., 2013b; Nishiyama et al., 2013). The prophase pathway removes cohesin from chromosome arms but spares centromeric cohesin. At the centromere shugoshin 1 (Sgo1) recruits the protein phosphatase 2 A (PP2A) to cohesin (Figure 4). The phosphatase keeps Stag2 and Sororin in a dephosphorylated state and neutralizes Wapl activity locally at the centromere (Liu et al., 2013b; McGuinness et al., 2005; Shintomi and Hirano, 2009). At the

metaphase to anaphase transition APC/C-mediated degradation of Securin activates the protease Separase, which opens the cohesin ring by cleavage of Scc1 facilitating the segregation of the sister chromatids (Hauf et al., 2001; Sun et al., 2009; Uhlmann et al., 1999; Uhlmann et al., 2000; Yamamoto et al., 1996; Zou et al., 1999). In addition to Securin Separase can be inhibited by binding to Cyclin B-Cdk1 (Gorr et al., 2005; Stemmann et al., 2001). Cyclin B-Cdk1 phosphorylates Separase at serine 1126, which triggers the Pin1 catalyzed prolyl cis-trans isomerization of proline 1127. Only after the isomerization of Separase the Cyclin B-Cdk1 complex can bind and inhibit the protease until Cyclin B is degraded after ubiquitylation by the APC/C (Hellmuth et al., 2015). Research indicates that different tissues and cell types rely differently on the two inhibition mechanisms. Whereas Securin knockout mice are phenotypically normal, the activation of an allele encoding a Cyclin B-Cdk1 resistant Separase variant in the germ line leads to complete sterility in both sexes. The Cyclin B-Cdk1 resistant Separase but not the absence of Securin induces severe developmental failures of postmigratory primordial germ cells (Huang et al., 2008).

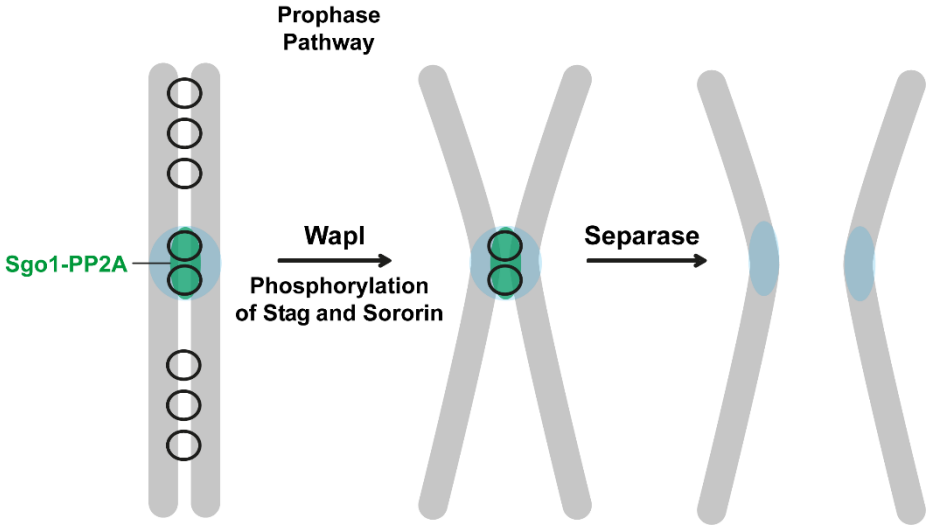


**Figure 4: Sgo1 protects centromeric cohesin in mitotic prophase**
During prophase of mitosis subunits of cohesin complexes on chromosome arms are phosphorylated allowing Wapl to open the cohesin ring in a non-proteolytic manner. Centromeric cohesin is spared from removal since it is resistant against Wapl activity due to de-phosphorylation by the Sgo1-PP2A complex. At the metaphase to anaphase transition Separase becomes active and cleaves Scc1 of cohesin at the centromers facilitating distribution of the sister chromatids. Black circles illustrate cohesin rings and the light blue parts of the chromatids represent centromeric chromatin.

## 1.4. Meiosis

Sexual reproduction represents a key event in evolution, since it greatly increases genetic diversity thereby accelerating the development of complex life (Colegrave, 2012). The characteristic of sexual reproduction is the fusion of gametes (egg and sperm in vertebrates) to recombine the parental genomes into a new genotype. Upon fertilization of an egg with a sperm the two haploid sets of chromosomes from father and mother fuse to form a diploid zygote. In order to keep the chromosome set of a diploid organism constant a prerequisite for sexual reproduction is the formation of haploid gametes via a specialized cell division called meiosis (Morgan, 2007). Among eukaryotes one can find substantial differences in the structures and mechanisms involved in the production of germ cells (Loidl, 2016). In the following we describe the mammalian meiosis.

### 1.4.1. Specific features of meiosis

Meiosis allows the formation of haploid gametes from a diploid precursor cell by one round of DNA replication followed by two successive rounds of chromosome segregation (Figure 5). In the first round of chromosome distribution (meiosis I) the homologous chromosomes are segregated reducing the ploidy of the daughter cells. The sister chromatids are segregated in the second meiotic division (meiosis II). For separation of the homologous chromosomes in meiosis I the sister kinetochores attach to one pole of the spindle. How this so-called mono-orientation is exactly achieved remains to be determined but probably involves the physical fusion of the kinetochores (Duro and Marston, 2015). Recently Kim et al. identified the protein Meikin, which localizes to kinetochores exclusively in meiosis I and seems to be involved in the kinetochore fusion. Mice lacking Meikin are completely infertile and have severe defects in mono-orientation (Kim et al., 2015). In contrast to mitosis, the homologous chromosomes have to be physically linked to allow their correct distribution in meiosis I. During prophase of the first meiotic division the homologs align and recombination events between paternal and maternal chromosomes form chiasmata, which tether the chromosomes (Klug, 2012; Morgan, 2007).

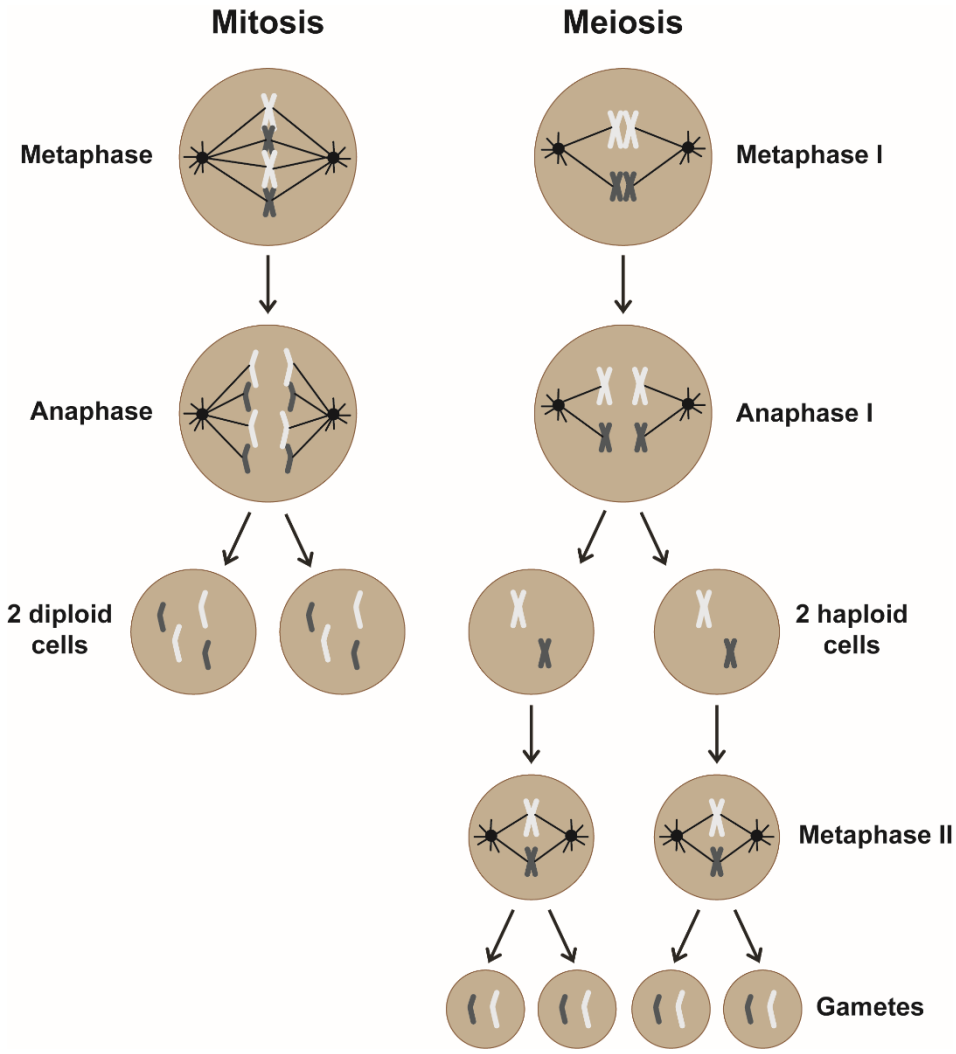


**Figure 5: Overview of mitosis and meiosis**
In mitosis one round of chromosome segregation produces two diploid cells. In meiosis the first of two chromosome distribution events reduces the ploidy as the homologous chromosomes are segregated into the daughter cells. For details see text.

The changing shapes of the chromosomes observable by light microscopy during prophase I led to its subdivision into distinct stages. In the first stage of prophase I, the so called leptonema, chromosomes start to condense and to pair. In the following zygonema the chromosomes are shortened and the synaptonemal complex (SC) starts to form. The SC is a proteinaceous structure, which tethers the homologous chromosomes together and facilitates generation of chiasmata (Zickler and Kleckner, 1999). Additional compaction of the chromosomes and disassembly of the SC occurs in pachynema. In the next step, the diplonema, the distance between chromosomes increases. The final stage is characterized by nuclear envelope breakdown and formation of the meiotic spindle and is termed diakinesis

(Klug, 2012). In the following metaphase I the homologs are oriented for the correct segregation in anaphase I. The spindle microtubules depolymerize, the nuclear envelope may re-form (depending on the organism) and cytokinesis takes place in telophase I. The following meiosis II begins with nuclear envelope breakdown in prophase II followed by alignment of the chromosomes in metaphase II and segregation of sister chromatids in anaphase II. It ends up with 4 haploid cells in telophase II.

There are profound differences in meiosis of male (spermatogenesis) and female (oogenesis) mammals. Cells that currently pass through meiosis are called spermatocytes or oocytes, respectively. The initiation of spermatogenesis takes place during puberty and the production of sperm continues the complete life span of the male individual. Spermatogenesis is a continuous process that ends up with four haploid, functional sperm cells. Oogenesis in contrast, produces only one functional egg, since both meiotic divisions are highly asymmetric. During telophase I one set of homologs is abscised with a very small amount of cytoplasm forming the first polar body. A subsequent asymmetric cell division in meiosis II forms the second polar body and the actual egg containing most of the cytoplasm (Klug, 2012). Furthermore, oogenesis is not a continuous process but interrupted by a long arrest stage. During embryogenesis of females oocytes undergo prophase I and arrest in diplonema. This phase of cellular quiescence is called dictyate arrest and lasts at least until puberty. Upon hormone stimulation one or few oocytes exit from the arrest, undergo meiosis until metaphase II and differentiate into a fertilizable eggs. Meiosis II is only completed upon fertilization (Klug, 2012). The later in life of a female an egg is released by ovulation the longer it has been arrested in prophase I.

### 1.4.2. Pairing of the homologous chromosomes and the synaptonemal complex

Recombination events between homologous chromosomes in meiosis increase genetic diversity since it creates chromosomes that contain a mix of paternal and maternal alleles. In addition, recombination facilitates the pairing of the homologs. The programmed DNA double strand breaks (DSB) are induced in leptonema by the topoisomerase-like protein Spo11 and in its absence the alignment of the homologs is severely inhibited (Zickler and Kleckner, 2015). DSB repair by homologous recombination starts with the resection of the DNA at the break creating single stranded DNA, which gets covered with a distinct set of proteins. In mitotic G2

cells this DNA-protein complex invades the undamaged sister chromatid during the process of repair and pairs with the complementary sequence. The current model suggests that strand exchange between homologous chromosomes and not between sister chromatids in prophase I facilitates pairing of the homologs. Usually the invading strand returns to where it came from after it was extended by DNA synthesis using the complementary sequence of the homolog. However, some of the lesions are repaired in a way that creates lasting interhomolog connections, so called crossovers. The outcome is that one sister chromatid of the parental homolog is ligated to one sister of the maternal homolog (Figure 6). The cohesin rings embracing the sister chromatids distal form the crossover, hence, also tether the homologous chromosomes together (Zickler and Kleckner, 1999, 2015).

In leptonema the chromosomes consist of chromatin loops emanating from a basis formed by proteins that are later part of the SC and called the axial element (AE). After the homologs have aligned along their AEs the distance between the homologs decreases in zygonema in a process called synapsis. Synapsis coincides with the formation of the SC between the homologs. The two AEs of the homologs get connected by transverse filaments consisting of dimers of a large coiled-coil protein. Along these transverse filaments additional proteins accumulate forming the central element. When integrated in the SC the AEs are termed lateral elements. At the end of pachynema the repair of the DSBs is finished and the SC is disassembled. In diplonema the distance between the homologs increases and the chiasmata resulting from crossover events become visible (Figure 6) (Morgan, 2007; Zickler and Kleckner, 1999, 2015).

## 1.5. Cohesin in meiosis

Like in mitosis the cohesin complex provides cohesion of chromatids in meiosis. Due to chiasmata formed in prophase I the cohesion established in premeiotic S-phase also holds homologous chromosomes together. Meiotic cell divisions require special regulation of the cohesin rings, since separation of the homologs and separation of the sister chromatids occurs in a timely separated manner. Furthermore, cohesin is important for proper SC assembly in germ cells. It is hardly surprising that cohesin subunits evolved that are exclusively required for gametogenesis. Germ cells, thus, contain the general cohesin subunits, which mediate cohesion in mitosis and, in addition, the meiosis-specific subunits (McNicoll et al., 2013).

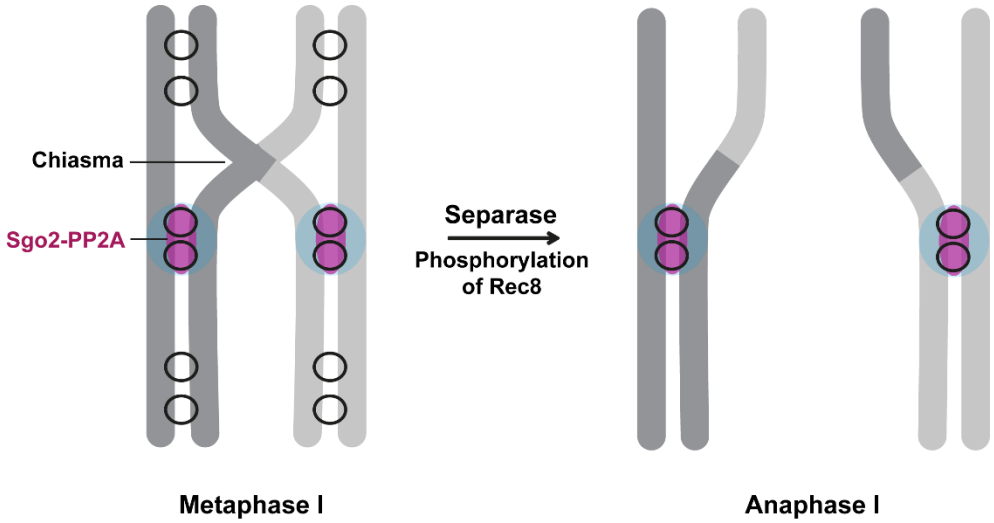


**Figure 6: Sgo2 protects centromeric cohesin from Separase cleavage in meiosis I**
The meiotic kleisin Rec8 has to be phosphorylated in order to become a substrate for Separase. In meiosis I Rec8 on chromosome arms is phosphorylated and cleaved allowing segregation of the homologous chromosomes. Centromeric Rec8 is kept in a dephosphorylated state by the Sgo2-PP2A complex. In meiosis II Sgo2-PP2A is inactivated by an incompletely understood mechanism (not depicted). Black circles illustrate cohesin rings and the light blue parts of the chromatids represent centromeric chromatin.

### 1.5.1. The meiosis-specific cohesin subunits

Whereas Baker's yeast expresses only one meiosis-specific cohesin subunit, a paralog of Scc1 called Rec8, humans express four different cohesin subunits specific for gametogenesis (Figure 3). Although human germ cells express two paralogs of Scc1, Rec8 and Rad21L, and, hence, contain three kleisins, only Rec8 seems to be required for cohesion (Tachibana-Konwalski et al., 2010). Cohesion defects are also observed in germ cells lacking a meiosis-specific form of Smc1 termed Smc1β (Biswas et al., 2013; Revenkova et al., 2004). Additionally, the meiotic cell divisions in mammals require Stag3, which is also exclusively expressed during gametogenesis. Stag3 knockout mice show severe defects in meiotic cohesion and recombination (Hopkins et al., 2014; Winters et al., 2014). Our knowledge about meiosis-specific cohesin is still very limited. The additional meiosis-specific cohesin subunits would allow meiocytes to form a great number of differently composed cohesin rings. However, we are quite ignorant how many different cohesin rings exist in germ cells and which subunits are at all competent to interact with each other. In addition, we are far from understanding

whether the regulatory proteins, which control the function of cohesin in mitosis, also interact with germ cell cohesin.

### 1.5.2. The resolution of cohesion in meiosis

As stated above cohesin removal in meiosis occurs in two steps, which both depend on Separase activity. In anaphase I the protease cleaves cohesin at the chromosome arms allowing segregation of the homologous chromosomes (Figure 6). Centromeric cohesin, in contrast persists until anaphase II and is only then removed by Separase. The current model implies that the cleavage of cohesin is controlled by phosphorylation since the kleisin Scc1 is functionally exchanged to Rec8. In *in vitro* cleavage assays phosphorylation merely enhances the Separase dependent proteolysis of Scc1 whereas it is essential for Rec8 cleavage (Hauf et al., 2005; Kudo et al., 2009). Accordingly, Rec8 phosphorylation is crucial for correct chromosome distribution in meiosis whereas Scc1 phosphorylation seems to be dispensable for correct mitotic progression (Brar et al., 2006; Hauf et al., 2005; Katis et al., 2010). As described above cohesion resolution in mitosis is also a two-step process, while the first step is phosphorylation regulated. Although the mechanism of cohesin ring opening is distinct in mitotic prophase and meiosis I the protection of centromeric cohesion seems to be very similar. In meiosis a paralog of Sgo1, namely Sgo2, recruits PP2A to centromeric cohesin and antagonizes Rec8 phosphorylation (Lee et al., 2008; Llano et al., 2008). Hypophosphorylated centromeric Rec8 is spared from Separase cleavage in meiosis I and maintains cohesion between sister chromatids. A key question is how Sgo2-PP2A is inactivated after meiosis I to allow Rec8 phosphorylation and subsequent cleavage by Separase in meiosis II. Sgo2, which is also expressed in somatic cells was shown to relocalize from the cohesin sites at the inner centromere towards the kinetochore upon chromosome bi-orientation in metaphase of mitosis and meiosis II. A straightforward model suggests that relocalization of the Sgo2-PP2A complex leads to de-protection and subsequent phosphorylation of Rec8 (Gomez et al., 2007; Lee et al., 2008). However, other studies suggest that relocalization of Sgo2 might not be sufficient to render Rec8 sensitive to cleavage. Ricke et al. showed a Sgo1 independent localization of PP2A to the centromere in mitosis (Ricke et al., 2012). Additionally, cytological analysis from the Wassmann group demonstrated co-localization of PP2A and Rec8 in metaphase of meiosis II (Chambon et al., 2013). Another recent study from the Wassmann lab

described a crucial function of Cyclin A2 for SCS in meiosis II. Inactivation of Cyclin A in oocytes by antibody injection blocked distribution of sister chromatids in anaphase II but not distribution of the homologs in anaphase I. This segregation defect in anaphase II can be rescued by chemical inhibition of PP2A. Remarkably, overexpression of Cyclin A induced precocious loss of cohesion between sister chromatids in meiosis I (Touati et al., 2012). These data strongly indicate that Cyclin A is required for Sgo2-PP2A inactivation in meiosis II.

### 1.5.3. Implications for human health

As women age the frequency of infertility, miscarriages and developmental disorders like trisomy 21 of the progeny increases. Statistics demonstrates the dramatic effect of womens' age on aneuploidy. Around 2 percent of all clinically recognized pregnancies of women under the age of 25 years are trisomic. However, among women over 40 years one-third of the pregnancies are affected by trisomy (Hassold and Hunt, 2001). Several studies suggest that a premature separation of chromosomes lead to incorrect segregation in the meiotic divisions and, hence, to aneuploidy in the eggs (Webster and Schuh, 2016). Research indicates that cohesin complexes are lost from chromosomes during the dictyate arrest leading to weakening of cohesion as oocytes age. The comparison of oocytes from young and aged mice showed a clearly reduced level of chromosomal cohesin in the latter (Lister et al., 2010). A similar age-related decrease of cohesin was also observed in human oocytes (Tsutsumi et al., 2014). Furthermore, when compared to oocytes of young mice the distance between sister kinetochores was increased in old oocytes indicating a weakened centromeric cohesion. Most importantly, the chromosome segregation steps were indeed more error-prone in oocytes derived from aged females (Chiang et al., 2010; Lister et al., 2010). Understanding the features of cohesin in meiocytes is crucial to comprehend the above mentioned medical problems associated with meiosis. This is especially important since the number of babies delivered to women aged 35 and older is constantly increasing (Webster and Schuh, 2016).

## 1.6. Aims of this work

Mammalian meiosis research is mostly restricted to sophisticated microscopic analysis and genetics of transgenic mice. We wondered whether one could use a simple cell culture system to study features of meiosis-specific cohesin and mechanisms of meiotic chromosome segregation. At first, we wanted to observe the behavior of the meiosis-specific kleisin Rec8 when expressed in the standard cell line Hek 293. This might help us to clarify whether Rec8 is functional in combination with the general cohesin subunits present in mitotic cells or whether Rec8 functionality requires association with the meiosis-specific subunits Stag3 or Smc1β. Since cultured cells are not limiting in amount and, thus, can readily be subjected to immunoprecipitation experiments, we intended to directly show interactions of meiosis-specific cohesin subunits. Knowing the interaction network of a distinct subunit can help to understand which differently composed cohesin rings form *in vivo*. With a cell line expressing functional Rec8 containing cohesin we sought to investigate whether Rec8 cohesin is susceptible to the cohesin antagonist Wapl and whether it relies on Sororin and/or Sgo for functionality.

Research in mouse oocytes indicates an involvement of Cyclin A in meiotic inactivation of Sgo2-PP2A. In somatic cells Cyclin A is usually rapidly degraded at the beginning of mitosis. We asked whether overexpression of a non-degradable variant of Cyclin A in mitotic cells will induce sister chromatid cohesion defects. Such an observation would suggest that Cyclin A is also competent to inactivate the Sgo1-PP2A complex. Again the cultured cells would be perfectly suited to unravel the mechanism of Cyclin A's action, since they are easily amenable to biochemical experiments.

# 2. Results

## 2.1. Elucidating features of meiotic cohesin subunits using somatic cells

### 2.1.1. Rec8 requires association with Stag3 to become functional

Despite its importance for human health, several features of cohesin subunits that are specific for germ cells are not understood at all. To unravel novel aspects of meiotic cohesin we created a cell line that has the Rec8 gene stably and inducibly integrated in the genome. Upon addition of doxycycline (Dox) to the culture medium the cells produce Rec8 C-terminally fused to GFP. As a control, we also created a cell line that inducibly expresses a Scc1-GFP fusion construct. Immunoblotting for GFP on cell lysates of the corresponding cells cultivated either in medium lacking or containing Dox showed bands whose intensity significantly increased in presence of Dox and therefore represent Scc1-GFP or Rec8-GFP, respectively (Figure 7A). Notably, in all clones analyzed the levels of Scc1-GFP were lower than Rec8-GFP (data not shown). Also previous experiments conducted in the Stemmann lab indicated that cells try to keep a constant Scc1 concentration (Schockel et al., 2011). This regulation mechanism, however, seems not to apply to Rec8 at least when expressed in a somatic cell. At first, we wanted to know whether the presence of Rec8 influences the effect of a Sgo1 depletion. A siRNA-mediated knockdown of Sgo1 in mitotic cells leads to premature SCS due to inactivation of Sgo1-mediated protection of centromeric cohesion from prophase pathway activity (McGuinness et al., 2005). When we depleted Sgo1 by RNAi in Hek 293 FlpIns expressing Scc1-GFP, arrested the cells in prometaphase by nocodazole treatment and performed chromosome spreading, we observed, as expected, a severe premature SCS. Cells harboring Rec8-GFP showed a similar percentage of SCS separation suggesting that Rec8 is either not functional or sensitive to prophase pathway activity and protected by Sgo1 (Figure 7B). To assess the functionality of Rec8 in somatic cells we performed immunofluorescence microscopy (IFM) using the cell line inducibly expressing GFP tagged Scc1 as a positive control to reveal the behaviour of functional cohesin. When we compared the cellular localization of the GFP fusion proteins in both cell lines, we found that Rec8, in contrast to Scc1, is excluded from the nucleus and is therefore most likely not associated with chromatin (Figure 7C).

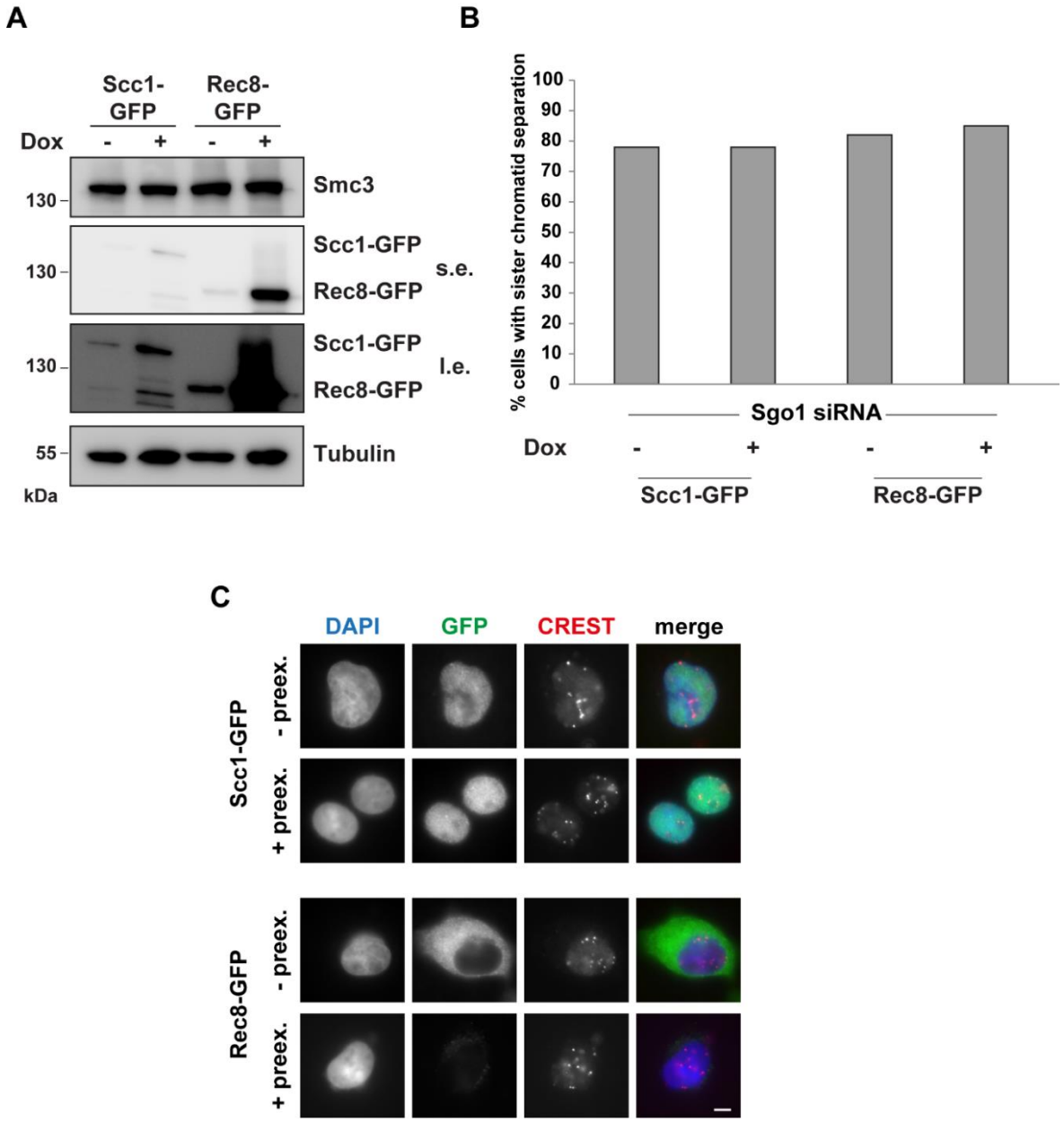


**Figure 7: Rec8 is not functional in mitotic cells**

**(A, B)** Transgenic cell lines were treated with Dox to induce the expression of Scc1-GFP or Rec8-GFP or were left untreated. **(A)** Cells were boiled in SDS sample buffer, subjected to SDS-PAGE followed by Western blotting using the indicated antibodies. The GFP blot is shown in a short (s.e.) and a longer (l.e.) exposure time **(B)** The cells were transfected with siRNA targeting Sgo1. 12h later nocodazole was added and after additional 15 h cells were harvested for chromosome spreading. 100 cells were counted per sample. **(C)** Transgenic cell lines expressing either Scc1-GFP or Rec8-GFP after induction with Dox were subjected to IFM and probed with antibodies recognizing CREST as a centromere marker or GFP. Cells were where indicated treated with the detergent Triton X-100 prior to fixation in order to remove soluble proteins (+preex.). The scale bar represents 5 µm.

We reasoned that another meiosis-specific cohesin subunit might be necessary for Rec8 to become functional. First, we asked whether Rec8 is competent for the association with all components that are required for a functional cohesin ring. To address this question we performed immunoprecipitation (IP) experiments that revealed a robust interaction of Rec8 with both SMC3 and SMC1α (Figure 8). Importantly, we co-isolated virtually no SA1 or SA2 when we immunoprecipitated Rec8 (Figure 9). A subsequent IP experiment revealed, interestingly, that Stag3, in contrast to Stag2, strongly interacts with Rec8 (Figure 10).

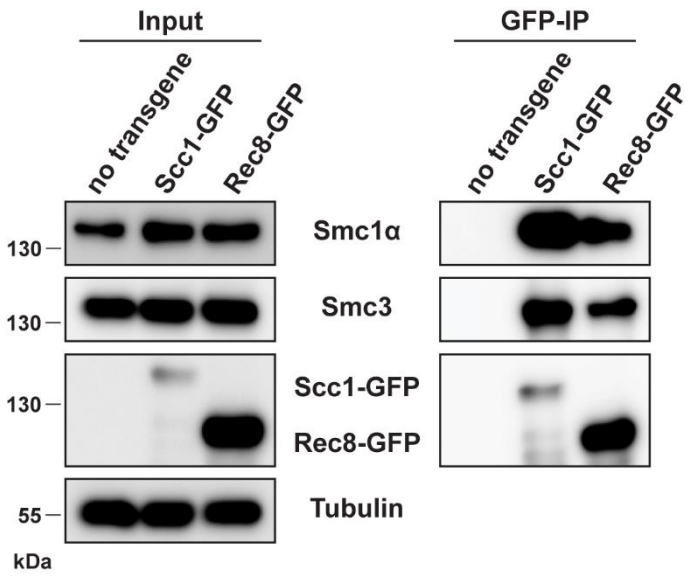


**Figure 8: Rec8 interacts with Smc1α and Smc3**
Transgenic cell lines induced to express either Scc1-GFP or Rec8-GFP and a none transgenic cell line were treated for 12 h with nocodazole and then collected. Lysates were prepared and subjected to IP with beads coupled to single chain camel GFP antibodies (nanobodies). Inputs and immunoprecipitates were finally analyzed by Western blotting using the indicated antibodies.

From this finding we concluded that Rec8 has to associate with the meiosis-specific cohesin subunit Stag3 to form a functional cohesin complex. Indeed, we found that the coexpression of Stag3 was sufficient to trigger Rec8's nuclear localisation (Figure 11). In addition, the nuclear signal of Rec8-GFP upon Stag3 coexpression was resistant to preextraction, which lead us to the conclusion that Rec8 is not only present in the nucleus but also loaded on chromatin (Figure 11B). As a control, we ectopically expressed Stag2 and this did not change the localization of Rec8 as expected (Figure 11B).

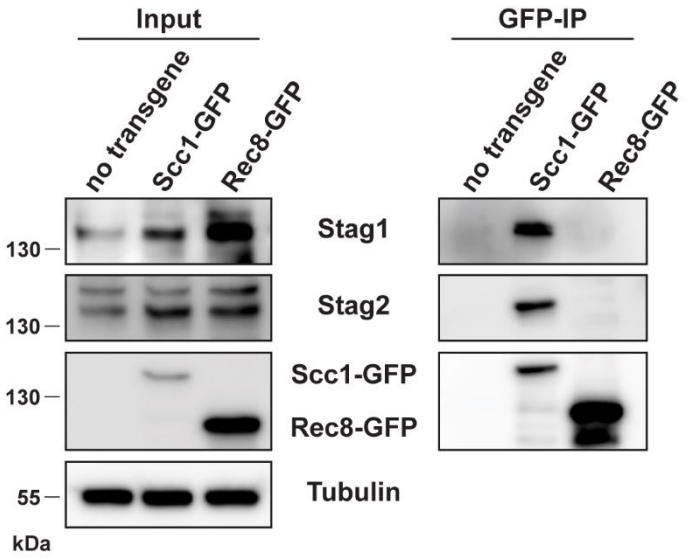


**Figure 9: Rec8 does not interact with Stag1 and Stag2**
The experiment was performed as described in Figure 8 but analyzed with different antibodies.

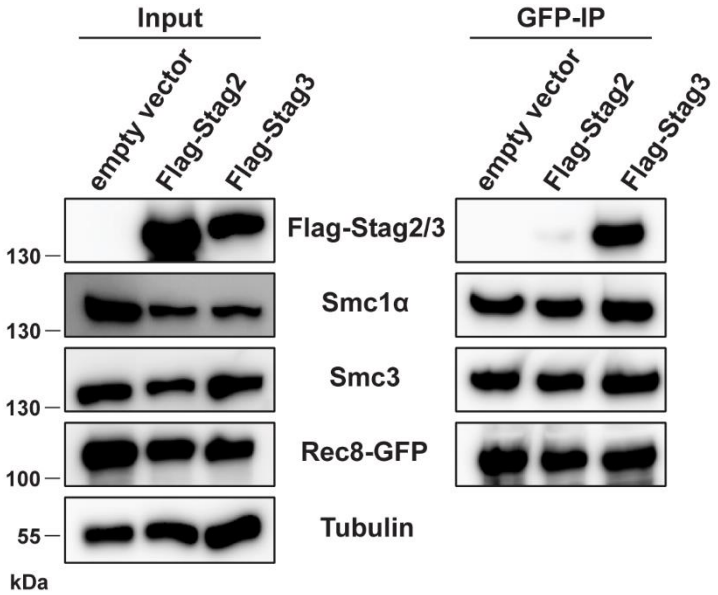


**Figure 10: Rec8 robustly interacts with Stag3**
The cell line expressing Dox-induced Rec8-GFP was transfected with plasmids encoding Flag-Stag2 or Flag-Stag3. After 36 h cells were treated with nocodazole for 12 h and harvested. Lysates were prepared and subjected to IP with beads coupled to GFP nanobodies. Inputs and immunoprecipitates were finally analyzed by Western blotting using the indicated antibodies.

Taken together our data suggest that Rec8 is functional only when assembled in a cohesin complex that contains also Stag3. This finding is in accordance with other studies showing that Stag3 is a component of all meiosis-specific cohesin complexes in mice. Since Rec8 is essential

for chromatid cohesion in meiosis, our data clearly explain the cohesion defects in germ cells lacking Stag3 (Hopkins et al., 2014).

For further experiments we generated doubly transgenic cell lines harboring the Rec8 and either the Stag2 (as a control) or the Stag3 gene under control of an inducible promotor. Consistent with the earlier transient transfection experiment only Stag3 and not Stag2 was competent to trigger Rec8's nuclear localization despite similar expression levels (Figure 12).

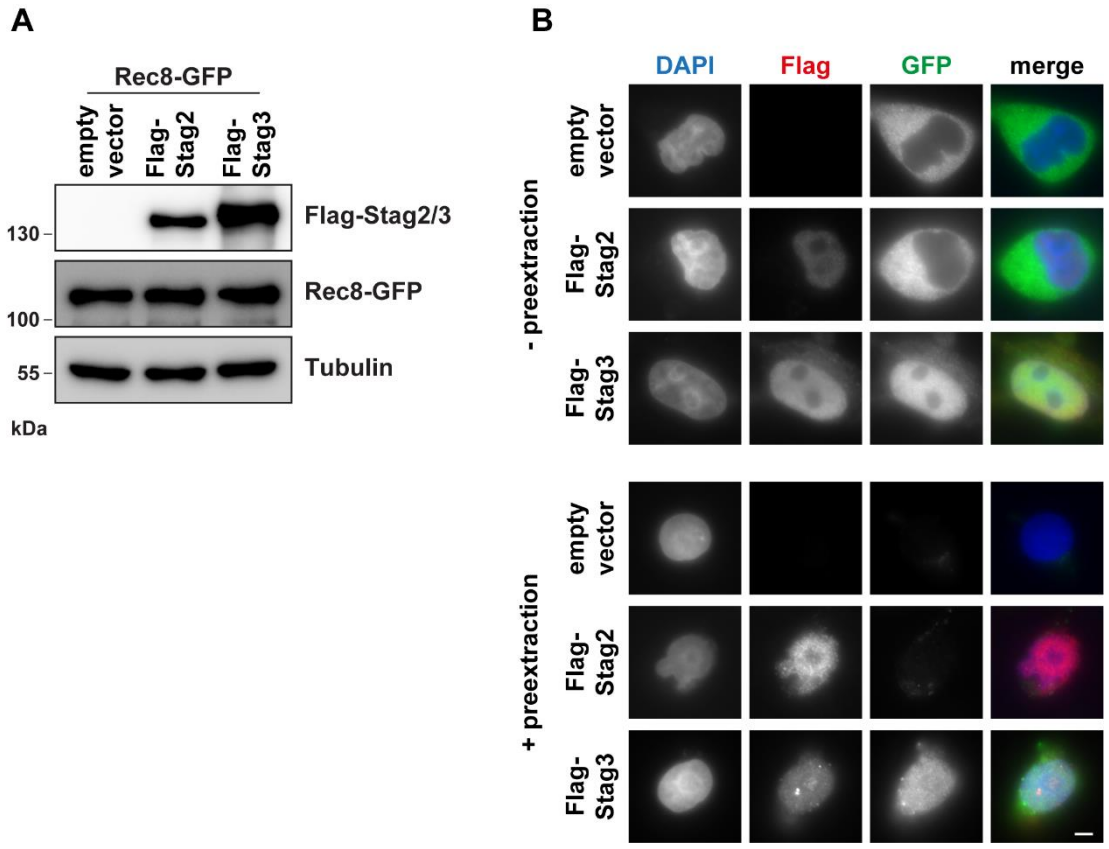


**Figure 11: Stag3 expression is sufficient to promote nuclear localization of Rec8**

**(A, B)** The Rec8-GFP expressing cell line was transfected with plasmids encoding Flag-Stag2 or Flag-Stag3. **(A)** 48 h after transfection the cells were boiled in SDS sample buffer and analyzed by Western blotting using antibodies as indicated. **(B)** 48 h following transfection cells were subjected to IFM and probed with antibodies recognizing Flag or GFP. Cells were either treated with the detergent Triton X-100 prior to fixation in order to remove soluble proteins (+preextraction) or were left untreated (-preextraction). The scale bar represents 5 µm.

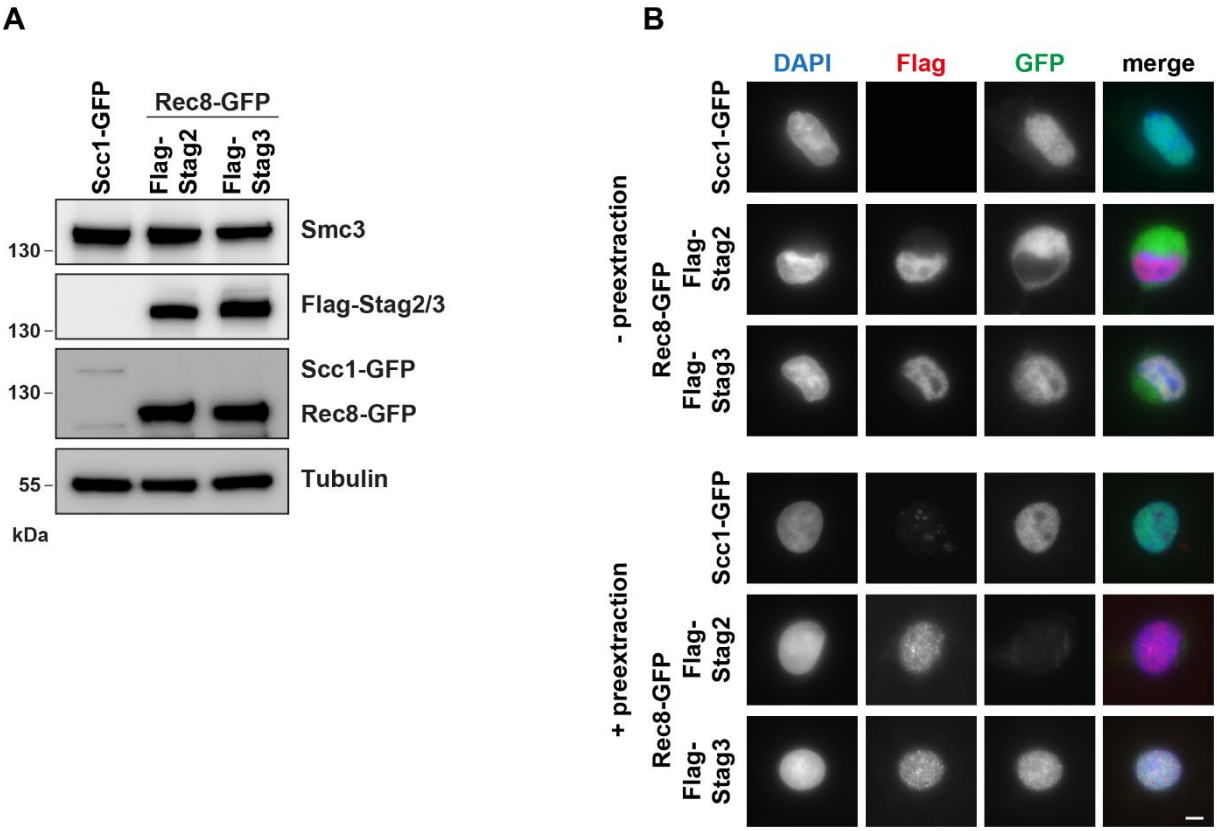


**Figure 12: A doubly transgenic cell line inducibly expressing two meiotic cohesin subunits**
**(A, B)** Transgenic cell lines were induced to express Scc1-GFP or Rec8-GFP and Flag-Stag2 or Flag-Stag3, respectively. **(A)** 48 h after induction the cells were boiled in SDS sample buffer and analyzed by Western blotting using antibodies as indicated. **(B)** 48 h following induction cells were subjected to IFM and probed with antibodies recognizing Flag or GFP. Where indicated cells were treated with the detergent Triton X-100 prior to fixation in order to remove soluble proteins (+preextraction). The scale bar represents 5 µm.

### 2.1.2. The deleterious effect of hyperactive Separase is reduced in Rec8-Stag3-cells

Next, we designed experiments helping us to further proof the functionality of Rec8 containing cohesin in our Rec8-Stag3-cell line. In mammals, Sgo1 and Sgo2 protect centromeric cohesin throughout early mitosis and meiosis I, respectively. However, despite this apparent division of labor, mammalian Sgo2 is expressed in the soma, where its function is still under discussion. The natural function of Sgo2 is the protection of Rec8 from Separase cleavage in meiosis 1. It was demonstrated that Rec8 gets phosphorylated in order to become a substrate for Separase (Brar et al., 2006; Katis et al., 2010; Kudo et al., 2009). Since the expression of functional Rec8-containing cohesin is not toxic in our cells, we propose that Rec8 gets properly phosphorylated once Sgo2 shifts from centromeric cohesin towards the kinetochore when centromeres are pulled to opposite poles at metaphase. Thus, we designed an experiment creating a situation in which Separase is active but Sgo2 is still associated with centromeric cohesin due to lack of spindle tension on centromeres. When Separase is overexpressed Securin becomes limiting. However, in this case Cyclin B-Cdk1 binding to Separase will inhibit the protease (Boos et al., 2008; Holland and Taylor, 2006). Therefore, we transfected a variant of Separase that is resistant to Cyclin B-Cdk1 mediated inhibition (Hellmuth et al., 2015) and subjected the cells to chromosome spreading after a prolonged prometaphase arrest induced by nocodazole treatment. When we expressed this hyperactive Separase in Hek 293 FlpIns (the parental cell line without a transgene) and the Rec8-Stag2-cell line, we observed that around 40 % of the cells showed separated sister chromatids despite being arrested in prometaphase (Figure 13). This finding is in sharp contrast to a previous study showing that centromeric cohesin is preserved when Separase is activated in prometaphase arrest (Lee et al., 2008). Most importantly, when expressed in Rec8-Stag3-cells Separase only induces premature SCS separation in 10 % of the cells, indicating that Rec8 is a poor substrate for Separase. A simultaneously RNAi-mediated depletion of Sgo2 (but not Sgo1) and expression of hyperactive Separase triggers SCS to an extent identical to Hek 293 FlpIns and Rec8-Stag2-cells (Figure 13). From this observation, however, one cannot unambiguously deduce that Sgo2 protects Rec8 from Separase dependent cleavage. In the following we show that Rec8 cohesin is susceptible to Wapl dependent ring opening and that Sgo2 renders centromeric Rec8 cohesin resistant against Wapl activity. Upon Sgo2 depletion the prophase pathway can remove centromeric Rec8 cohesin and expression of the hyperactive Separase induces disjunction of the

chromatids. Nevertheless, the reduction of hyperactive Separase induced premature SCS by Rec8 and Stag3 clearly demonstrates that functional meiotic cohesin rings form in our cell line.

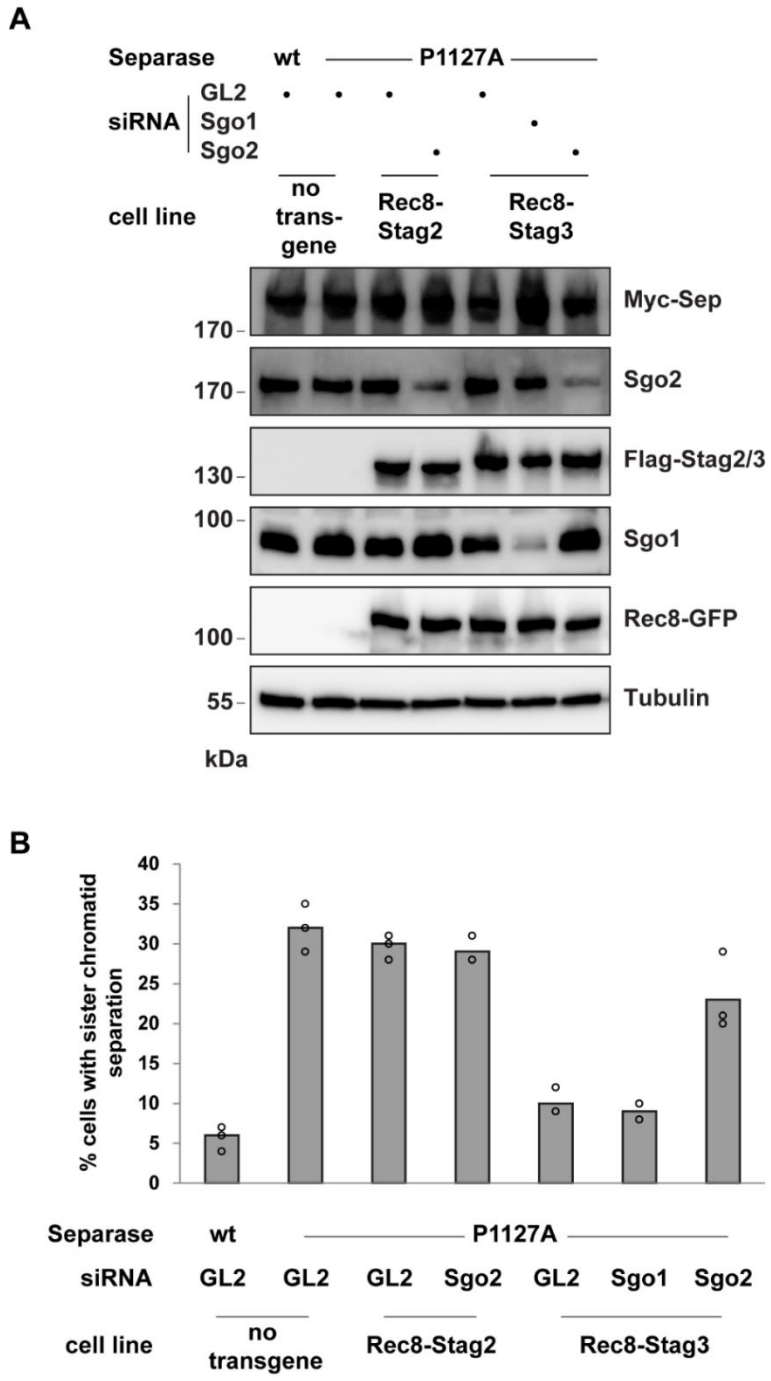


**Figure 13: The deleterious effect of hyperactive Separase is reduced in Rec8-Stag3-cells**
**(A, B)** Dox treated cells containing no transgene, Rec8 and Stag2 or Rec8 and Stag3 were transfected with a plasmid encoding wild type Separase (wt) or a hyperactive Separase variant (P1127A) and siRNA directed against GL2, Sgo1 or Sgo2. 12h thereafter cells were arrested in metaphase by nocodazole treatment and harvested 15 h later. **(A)** A fraction of the cells was boiled in SDS sample buffer and subjected to immunoblotting using the indicated antibodies to verify Separase expression and knockdown efficiencies. **(B)** Cells were subjected to chromosome spreading and analyzed for premature SCS. 100 cells were counted per sample. Averages (grey bars) of three independent experiments (spheres) are shown.

### 2.1.3. Rec8 cohesin is susceptible to the cohesion antagonist Wapl

With a standard cell line harboring meiosis-specific cohesin in hand, we started to elucidate as yet unexplored features of Rec8 containing cohesin. Since the cohesin antagonist Wapl is present in germ cells, an obvious and very interesting question is whether Rec8 containing cohesin is susceptible to Wapl activity (Kuroda et al., 2005; Zhang et al., 2008a). In mitosis of higher eukaryotes, two distinct pathways are responsible for dissolution of sister chromatids (Waizenegger et al., 2000). During prophase the bulk of cohesin is removed from chromosome arms by dissociation of Scc1 from Smc3. This non-proteolytic ring opening requires the activity of Wapl. A siRNA-mediated depletion of Wapl extends cohesin's residence time on chromatin that it can now be detected at prometaphase chromosomes until cleaved by Separase in metaphase (Buheitel and Stemmann, 2013). If the Rec8 containing cohesin is resistant to Wapl and, hence, to the prophase pathway, one would expect GFP-positive prometaphase chromosomes in our Rec8-Stag3-cells, mimicking a Wapl depletion. Interestingly, we found no difference regarding the GFP signal on mitotic chromosomes when we compared Rec8-Stag3-cells and cells expressing GFP-tagged Scc1. Surprisingly, we were not able to detect GFP stained mitotic chromosomes in Rec8-Stag3-cells when we inactivated Wapl by siRNA (Figure 14). We speculated that the increased chromosomal level of endogenous Scc1 in Rec8-Stag3-cells upon Wapl knockdown might outcompete Rec8-GFP from chromatin and thus mask a potential effect of Wapl depletion. Indeed, when we co-depleted Wapl and Scc1 by RNAi we readily observed a significantly increased GFP signal on mitotic chromosomes of prometaphase arrested Rec8-Stag3-cells (Figure 14B). We conclude that Wapl is able to remove these Rec8-containing cohesin complexes from chromatin. Given its ability to displace meiotic cohesin it will be very interesting to elucidate the function and, especially, the regulation of Wapl in germ cells of vertebrates.

Proper cohesion mediated by Scc1 cohesin requires the protein Sororin to counteract Wapl activity (Nishiyama et al., 2010). Since we demonstrated that also Rec8 cohesin is susceptible to Wapl, we wanted to test whether Sororin protects Rec8 cohesin complexes from this cohesion antagonist. An RNAi mediated depletion of Sororin leads to unscheduled SCS in mitosis due to failures in protection of centromeric cohesin. We hypothesized that presence of Rec8-Stag3 in cells should rescue the cohesion defect if Rec8 containing cohesin is protected from Wapl activity by a mechanism independent of Sororin.

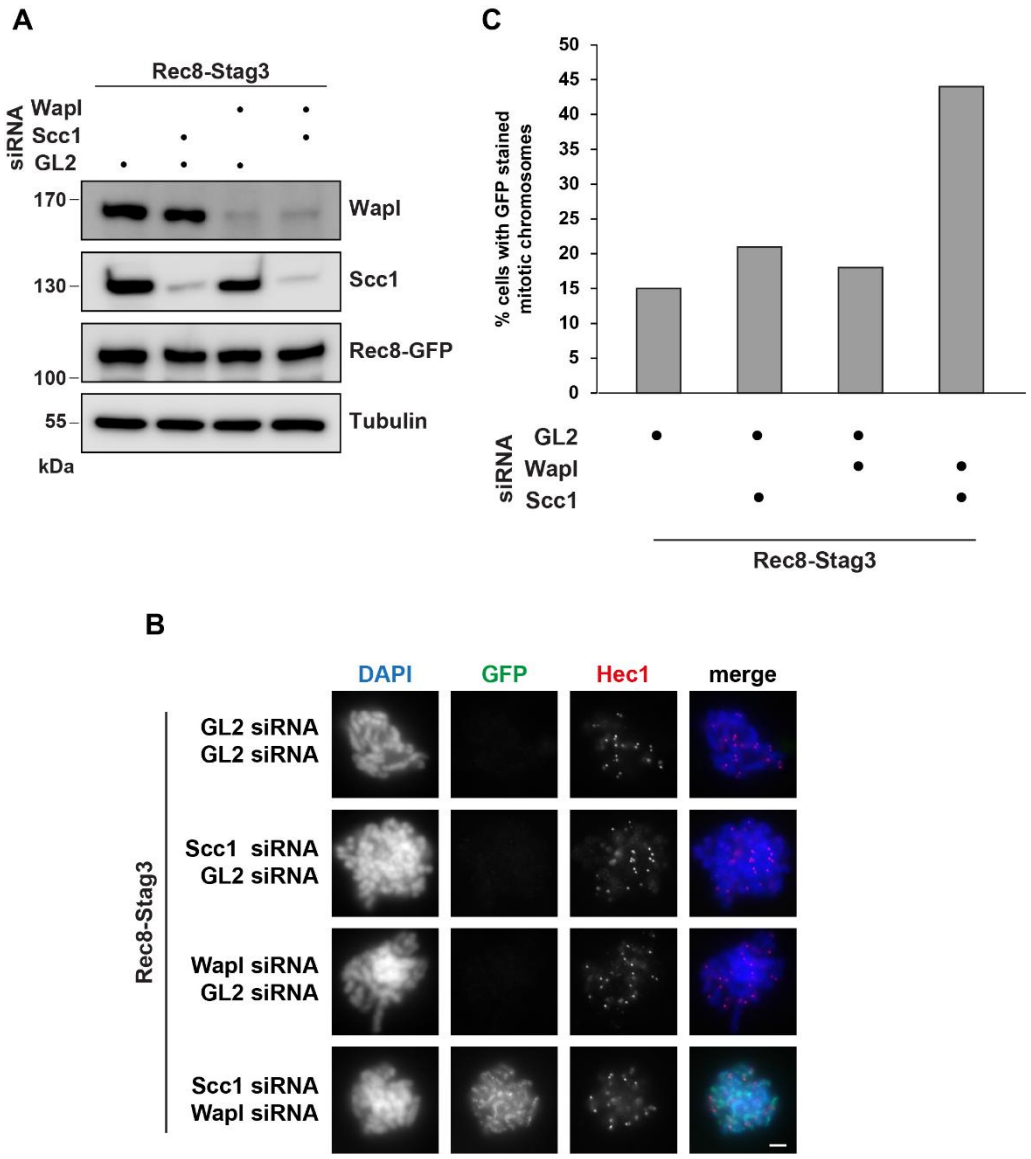


**Figure 14: Rec8 cohesin is susceptible to cohesion antagonist Wapl**

**(A, B, C)** Dox treated transgenic cells expressing Rec8-GFP and Flag-Stag3 were transfected with siRNAs targeting Scc1 or Wapl or both. 60 h later cells were treated with nocodazole for 6 h. **(A)** A fraction of the cells was boiled in SDS sample buffer and subjected to immunoblotting using the indicated antibodies to verify knockdown efficiencies. **(B)** Cells were subjected to IFM and stained for DNA, Rec8-GFP and the mitotic kinetochore marker Hec1. The samples were analyzed for GFP positive mitotic chromosomes due to incomplete removal of Rec8 cohesin. Representative images for each sample are shown. The scale bar represents 5 µm. **(C)** Quantification of mitotic chromosomes coated with Rec8-GFP. 100 mitotic cells were analyzed for each condition.

We transfected Rec8-Stag3 expressing and control cells with siRNA targeting Sororin, arrested the cells in metaphase and performed chromosome spreads. As expected, control cells showed severe premature SCS (Figure 15). Importantly, Rec8-Stag3 expressing cells also suffered from a cohesion defect when Sororin was depleted although to a lower extent than

control cells that did not overexpress any cohesin (Figure 15). We speculate that this does not represent an incomplete rescue since the cohesion failure caused by hyperactive Separase (Figure 13) and Sgo1 knockdown (Figure 16) was completely rather than partially supressed by Rec8-Stag3. Hence, we propose that Wapl can remove Rec8 cohesin from chromatin and that this process is antagonized by Sororin.

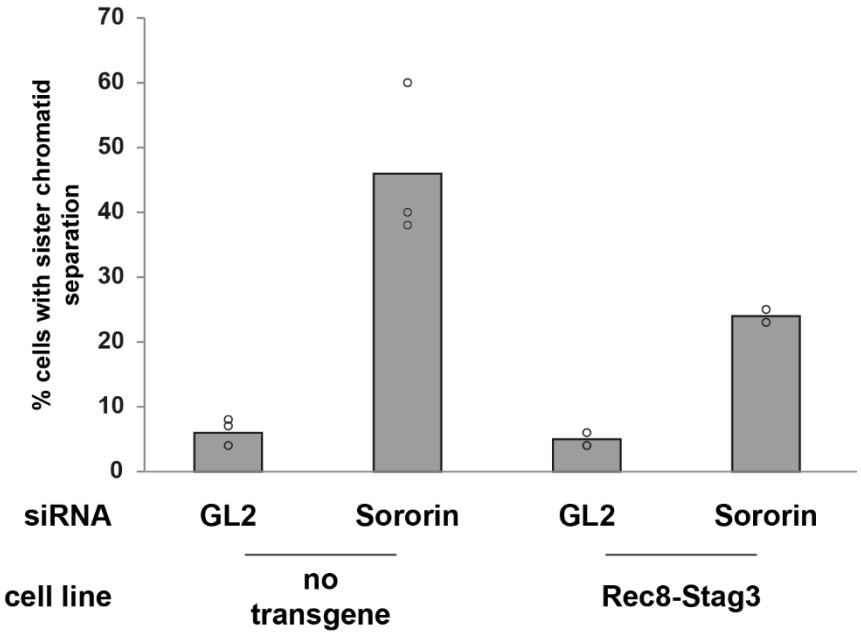


**Figure 15: Rec8 mediated cohesion requires Sororin**
Cell lines expressing no transgene or Rec8 and Stag3 were first treated with Dox and then transfected with GL2 or Sororin siRNA. 36 h after addition of the transfection mix nocodazole was added and 15 h later cells were harvested, subjected to chromosome spreading and analyzed for premature SCS. 100 cells were counted per sample. Averages (grey bars) of three independent experiments (spheres) are shown.

### 2.1.4. Rec8 cohesin is protected by Sgo2 from Wapl activity

Since our data and data from others suggest that mammalian Rec8 is protected from Separase cleavage by Sgo2, we speculated that Sgo2 is also competent to protect Rec8 cohesin from Wapl activity and wondered how a depletion of Sgo1 affects our Rec8-Stag3-cell line (Lee et al., 2008; Llano et al., 2008). Usually a siRNA-mediated knockdown of Sgo1 in mitotic cells leads to premature SCS due to inactivation of Sgo1-mediated protection of centromeric cohesion from prophase pathway activity (McGuinness et al., 2005). If Rec8 containing cohesin mediates cohesion at centromeres, and is thus functional, sister chromatid cohesion should

only be affected by a co-depletion of Sgo1 and Sgo2 but not by knockdown of Sgo1 alone. When we depleted Sgo1 by RNAi in Hek 293 FlpIns and in the Rec8-Stag2-cell line, arrested the cells in prometaphase by nocodazole treatment and performed chromosome spreading, we observed, as expected, a severe premature SCS (Figure 16).

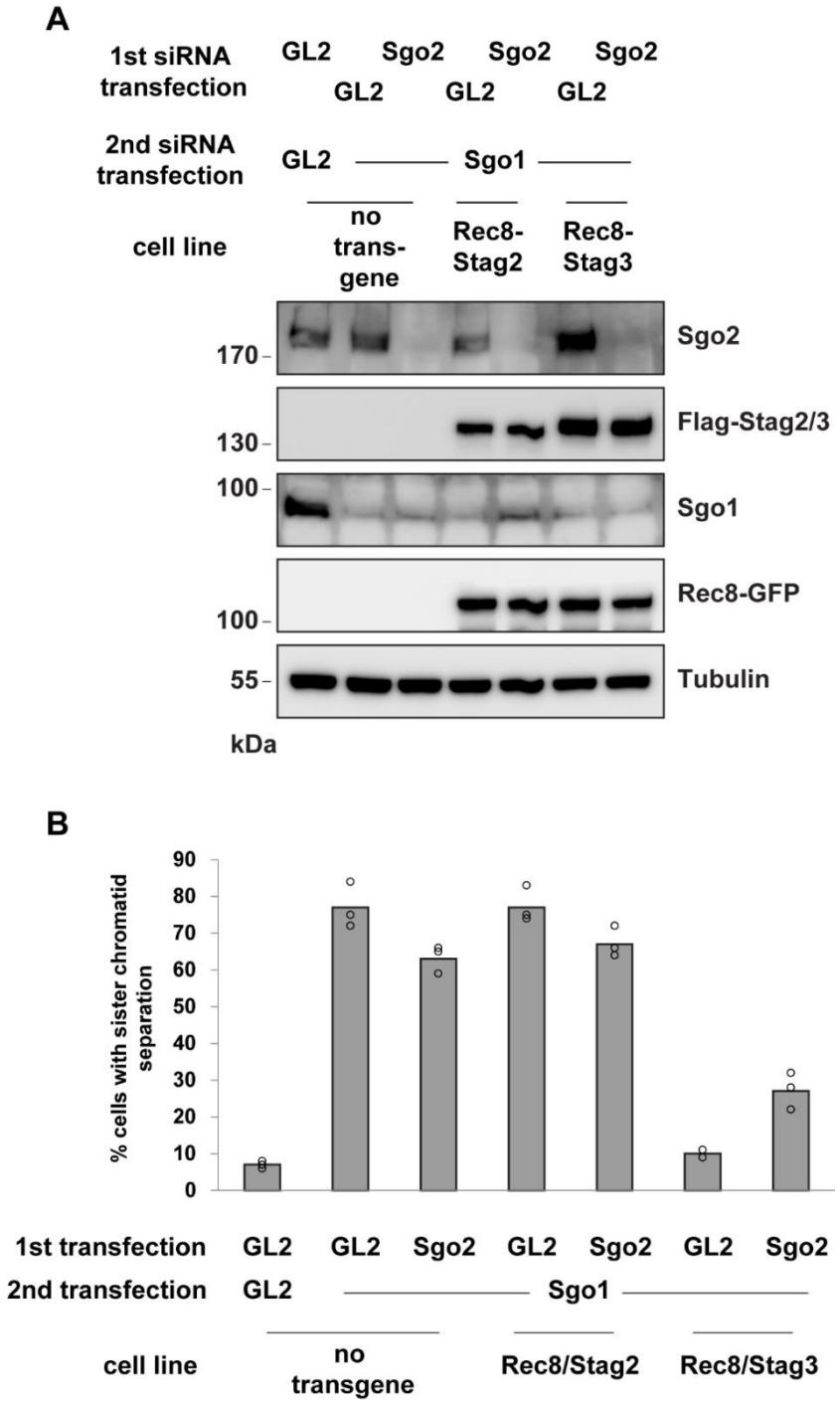


**Figure 16: Rec8 cohesin protected from Wapl activity**

**(A, B)** Dox treated cells containing no transgene, Rec8 and Stag2 or Rec8 and Stag3 were transfected with GL2 or Sgo2 siRNA. 24 h after addition of the first transfection mix, cells were transfected with siRNA targeting Sgo1. 12h later nocodazole was added and after additional 15 h cells were harvested.

**Figure 16 continued (A)** A fraction of the cells was boiled in SDS sample buffer and subjected to immunoblotting using the indicated antibodies to verify knockdown efficiencies. **(B)** Cells were subjected to chromosome spreading and analyzed for premature SCS. 100 cells were counted per sample. Averages (grey bars) of three independent experiments (spheres) are shown.

Intriguingly, expression of Rec8-Stag3 completely suppressed the precocious dissolution of sister chromatids. Most importantly, a concomitant depletion of both Sgo1 and Sgo2 lead to a premature separation of sisters in Rec8-Stag3-cells (Figure 16). Research from Yu and coworkers indicate that Sgo1 binds to the interface of Scc1 and Stag2 (Hara et al., 2014). In co-IP experiments Stag3 interacted with Scc1 (Data not shown). Thus, the rescue effect of Sgo1 depletion could be explained by the remote possibility that cohesin molecules containing Scc1 and Stag3 are protected by Sgo2. To formally prove that Rec8-Stag3 cohesin molecules rescue the effect of Sgo1 knockdown we performed the same experiment with cell lines expressing Stag3 as the only meiotic cohesin subunit. Notably, a prominent Stag3 signal, which was resistant against preextraction was observable in the nucleus even when Rec8 was not present indicating the formation of a functional cohesin ring containing Stag3 and Scc1 (Figure 17A). However, expression of Stag3 did not reduce the cohesion defect caused by Sgo1 depletion confirming that it is indeed Rec8 cohesin that rescues Sgo1 ablation in an Sgo2 dependent manner (Figure 17B).

From these findings we drew two conclusions. First, we indeed created somatic cells that hold functional meiotic cohesin, i.e. they exploit meiotic cohesin complexes for sister chromatid cohesion. Second, Sgo2 is able to protect meiosis-specific cohesin from Wapl activity. This is the first report showing that Sgo2 can counteract Wapl activity on meiotic cohesin. Strikingly, depletion of Sgo2 alone has no effect on sister dissolution in all cell lines examined (data not shown). This result is inconsistent with reports suggesting that Sgo2 has a substantial role in mitosis and participates in the protection of mitotic cohesin from the prophase pathway (Kitajima et al., 2006; Lee et al., 2008).

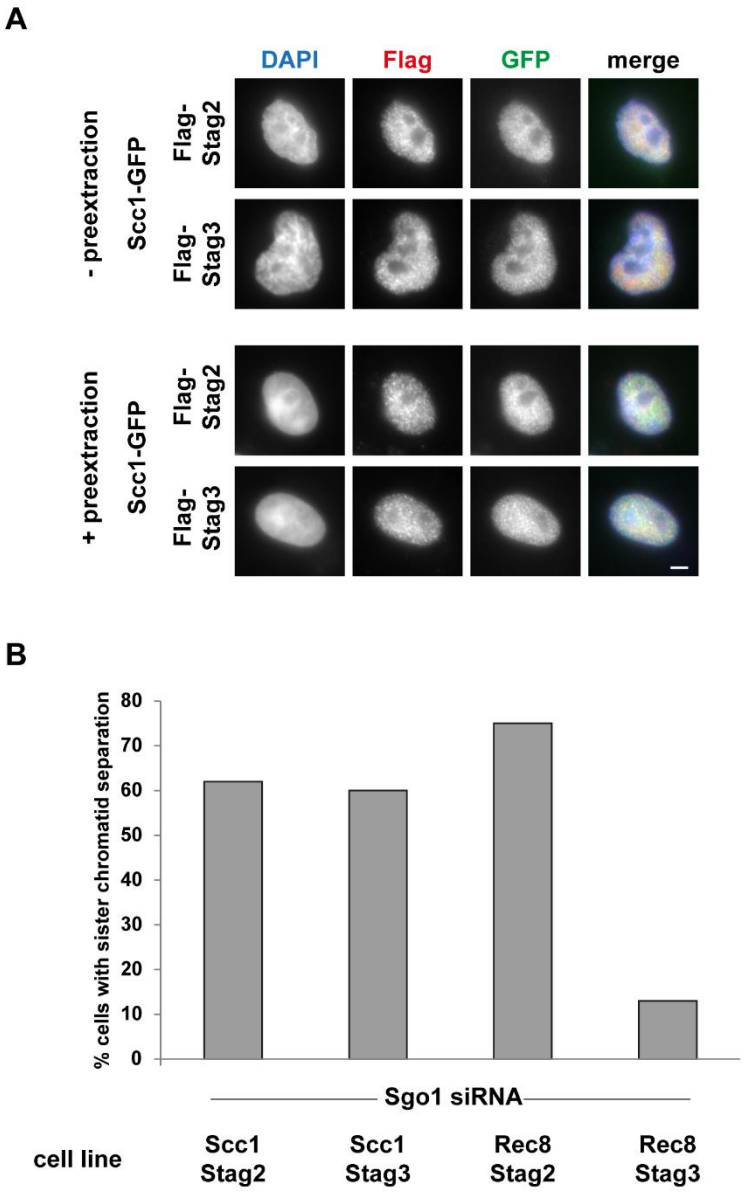


**Figure 17: In the absence of Rec8-Stag3 associates with chromatin but does not rescue the cohesion defect resulting from Sgo1 depletion**

**(A)** Transgenic cell lines were induced to express Scc1-GFP and Flag-Stag2 or Flag-Stag3, as indicated. 48 h after induction cells were subjected to IFM and probed with antibodies recognizing Flag or GFP. Cells were either treated with the detergent Triton X-100 prior to fixation in order to remove soluble proteins (+preextraction) or left untreated (-preextraction). The scale bar represents 5 µm. **(B)** Cell lines producing the indicated proteins after induction with Dox were transfected with Sgo1 siRNA. 12h later nocodazole was added and after additional 15 h cells were harvested. Cells were subjected to chromosome spreading and analyzed for premature SCS. 100 cells were counted per sample.

### 2.1.5. The substrate specifity of human Sgo1 and Sgo2

Encouraged by the finding that there seems to be a division of labor between Sgo1 and Sgo2, i.e. the substrate specificity of two shugoshin proteins in humans might be clearly defined, we wanted to further illuminate the features of Sgo1 and Sgo2. Former work demonstrated that Sgo1's localization on chromosomes is no longer restricted to centromeres when strongly overexpressed. In this case Sgo1 can be detected along the whole chromosome length in prometaphase accompanied by persisting cohesin on chromosome arms protected from prophase pathway activity by mislocalized Sgo1 (Liu et al., 2013b). We believed that we could take advantage of this observation to show the specificity of the human shugoshins. First, we transfected cells expressing Scc1-GFP with a plasmid either encoding Sgo1 or Sgo2, arrest the cells in prometaphase via nocodazole and performed a combination of chromosome spreading and IFM. Notably, when we overexpressed Sgo1, we readily observed, as expected, Sgo1 and Scc1-GFP signals on chromosome arms (Figure 18). However, we never found chromosomes with Scc1-GFP stained arms upon overexpression of Sgo2 indicating that Sgo2 is incompetent to protect Scc1 containing cohesin from Wapl activity. Next, we wanted to test the effect of overexpression of both shugoshins in the Rec8-Stag3-cell-line. We expected a GFP signal on chromosome arms in prometaphase, in contrast to Scc1-GFP expressing cells, upon overexpression of Sgo2 but not upon overexpression of Sgo1. Indeed, we frequently found mitotic chromsomes showing a Sgo2 and a Rec8-GFP signal along the whole chromosome length suggesting that Sgo2 protects Rec8 cohesin from prophase pathway activity at the arms (Figure 18). Surprisingly, we also found Sgo1 stained chromosome arms accompanied by a Rec8 signal. We think that the massive overexpression of Sgo1 leads to levels of Sgo1-PP2A at chromosome arms that can protect Rec8 cohesin although this type of cohesin is not a substrate under physiological conditions. This result is in line with observations made by Xu et al. when they overexpressed Sgo1 in mouse oocytes and observed a persistence of Rec8 at the chromosome arms beyond anaphase I (Xu et al., 2009b). Most likely we did not observe the same effect for Sgo2 and Scc1, since the Sgo2 expression level is substantially lower than the Sgo1 expression level (Figure 18A). Taken together, we believe that under regular conditions Sgo1 protects Scc1 containing cohesin whereas Sgo2 is responsible for Rec8 containing rings. When heavily overexpressed, however, Sgo1 seems to be more promiscuous. Hongtao Yu and coworkers demonstrated that Sgo1 physically interacts with cohesin (Liu et al., 2013b). It is conceivable that upon overexpression of the shugoshin

proteins unspecific interactions between Sgo1 and Rec8 cohesin recruit PP2A to the corresponding cohesin ring thereby providing protection activity. Interestingly, Sgo can be present along chromosome arms without detectable amounts of cohesin, since we observed Sgo2 covered metaphase chromosomes without a Scc1-GFP signal. Bub1 phosphorylates histone H2A at the centromere allowing Sgo1's binding to the histone and its subsequent recruitment to centromeric cohesin (Liu et al., 2013a). We believe that the Sgo proteins can also bind to unmodified histone when overexpressed and can, hence, cover whole chromosomes without cohesin being present.

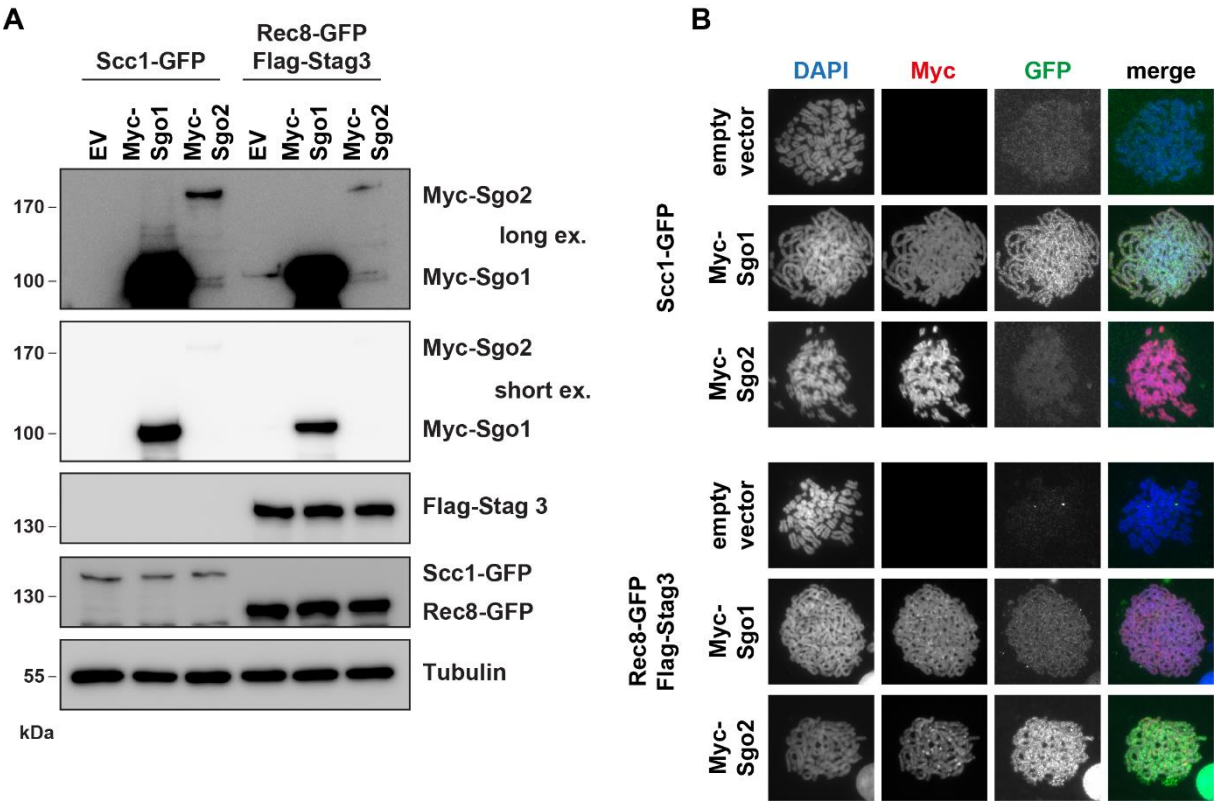


**Figure 18: The human Shugoshins are more promiscuous when overexpressed**
**(A, B)** Transgenic cell lines were treated with Dox to induce the expression of Scc1-GFP or Rec8-GFP and Flag-Stag3. Subsequently, cells were transfected with plasmids encoding Myc-Sgo1 or Myc-Sgo2 or an empty vector (EV). 12h later thymidin was added and cells were arrested for 20h. 13h after thymidin washout and nocodazole addition cells were harvested. **(A)** Cells were boiled in SDS sample buffer and analyzed by Western blotting using the indicated antibodies to examine Myc-Sgo1 and Myc-Sgo2 expression levels. The Myc signal is shown after short and long exposure. **(B)** Cells were subjected to a method that is related to chromosome spreading but allows immunofluorescence staining of chromatin associated proteins. Cells were probed with antibodies recognizing Myc and GFP. Representative images are depicted. Note that Rec8 cohesin is at least partially protected from prophase pathway activity when Sgo1 is overexpressed as indicated by the weak but above background GFP signal on metaphase chromosomes.

### 2.1.6. Meikin localizes to centromeres in mitotic cells but is not sufficient to induce mono-oriented kinetochores

Recently a protein, Meikin, was identified that is responsible for creating monopolar attachments of sister chromatids in vertebrate meiosis (Kim et al., 2015). We wanted to know whether we can use our cell line expressing functional meiotic cohesion to elucidate Meikin's mechanism of action. At first we transiently transfected Rec8-Stag3-cells with Myc-Meikin and subjected the cells to preextraction prior to fixation (Figure 19). Here a co-localization of the centromere marker CREST and Myc-Meikin was clearly visible in interphase and mitosis. Thus, Meikin localizes to the centromere in somatic cells. However, centromeric localization of Meikin is independent of meiotic cohesin, since an identical localization pattern of Meikin was observed in Scc1-GFP cells (Figure 20B). Next, we performed immunostaining of the kinetochore marker Hec1 on chromosome spreads in Rec8-Stag3-cells to determine the effect of Meikin expression on the kinetochore in mitotic cells.

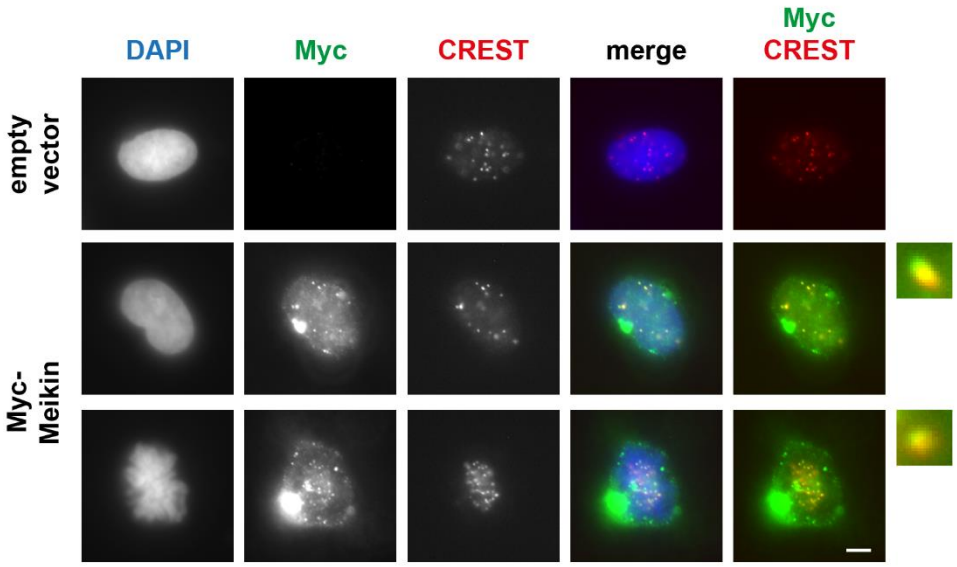


**Figure 19: Meikin localizes to the centromere in mitotic cells**
The Rec8-Stag3-cell line was transfected with an empty vector or a plasmid encoding Myc-Meikin. 24 h after transfection the cells were split on coverslips and after additional 24 h the cells were fixed after preextraction. Immunofluorescence staining was performed using antibodies against Myc and CREST as a centromere marker. A Myc-Meikin transfected cell in interphase (middle panel) and one in mitosis (bottom panel) are shown as deduced from chromosome morphology. The small images on the right-hand side show co-localizing Myc and CREST signals in a higher magnification. The very bright and large Myc signals are most likely caused by aggregated protein. The scale bar represents 5 µm.

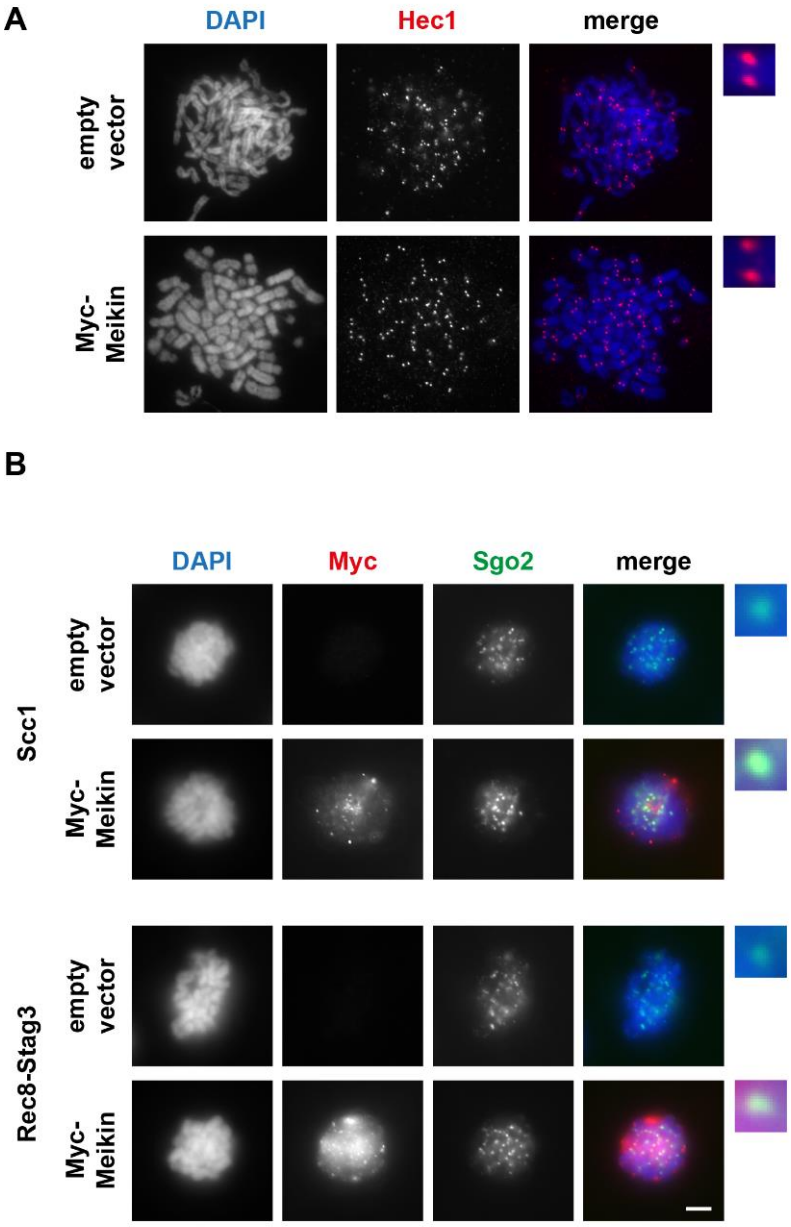


**Figure 20: Meikin does not induce monopolar kinetochors but leads to elevated Sgo2 levels at centromeres**

**(A)** Rec8-Stag3 expressing cells were transfected with an empty vector or a plasmid encoding Myc-Meikin. 24 h after transfection the cells were blocked at mitosis using nocodazole for 6 h and subjected to a method that is related to chromosome spreading but allows immunofluorescence staining of chromatin associated proteins. Hec1 was stained and the distance of the two Hec1 dots was analyzed by visual inspection. Two representative images are shown. The small images on the right-hand side show sister kinetochores in a higher magnification. **(B)** Transgenic cell lines expressing Scc1-GFP or Rec8-GFP and Flag-Stag3 were transfected with an empty vector or a plasmid encoding Myc-Meikin. 24 h after transfection the cells were split on coverslips and after additional 24 h the cells were fixed after preextraction. Immunofluorescence staining was performed using antibodies recognizing Myc and Sgo2. The intensity of the centromeric Sgo2 signal was analyzed by visual inspection. Representative images are shown. The small images on the right-hand side show magnified centromeres. The scale bar represents 5 µm.

If Meikin indeed modifies sister kinetochors in a way that they are competent for mono-orientation, one would expect a decrease in sister kinetochore distance. However, control cells and Myc-Meikin transfected cells did not show a difference in the distance between two Hec1 signals (Figure 20A). From this finding we infer that Meikin and meiotic cohesin alone is not sufficient to promote mono-orientation of sister chromatids and, furthermore, that germ cells contain additional factors required for correct chromosome segregation during meiosis I. Watanabe and colleagues also suggested that Meikin supports cohesion protection at the centromere by recruiting Sgo2, since Meikin ablation lead to a diminished centromeric Sgo2 localization (Kim et al., 2015). Consistently, when we immunostained Sgo2 in Scc1-GFP and Rec8-Stag3-cells either transfected with an empty vector or a plasmid encoding Myc-Meikin we found that expression of Meikin lead to increased Sgo2 levels at centromers in both cell lines (Figure 20). Taken together, Meikin localizes to centromeres and increases centromeric Sgo2 levels independent of additional meiotic factors, but is not sufficient to promote mono-orientation of kinetochores.

### 2.1.7. Higher eukaryotes possess two isoforms of Smc1β

When we amplified the Smc1β gene from human testis cDNA, we noticed that the PCR produces two differently sized products (data not shown). Cloning and subsequent sequencing revealed that we isolated two annotated isoforms of Smc1β, the bigger one named isoform 1 and the smaller one named isoform 2. Using an *in silico* approach we were able to find the same two isoforms of Smc1β in several mammals and higher vertebrates (data not shown). An alignment of both isoforms with Smc1α revealed that Smc1β isoform 2 lacks a region of 74 amino acids that contains crucial residues of Smc1's ATPase domain including the signature motif, the Walker B motif and the D-loop (Figure 21). We were excited by this finding, since very recent data show that Wapl dependent opening of the cohesin ring requires ATP hydrolysis mediated by the ATPase domain that contains Smc1's signature motif and D-loop (Elbatsh et al., 2016). Thus, we hypothesized that isoform 2 of Smc1β might define a pool of cohesin on meiotic chromosomes that is resistant against Wapl mediated removal. At first we wanted to observe the behavior of the two meiotic Smc1 proteins in mitotic cells. Therefore, we transfected Hek FlpIn cells with plasmids encoding the two isoforms. When we performed

IFM using the transfected cells, we found that Smc1β isoform 1 localizes to the nucleus and is resistant against preextraction (Figure 22).

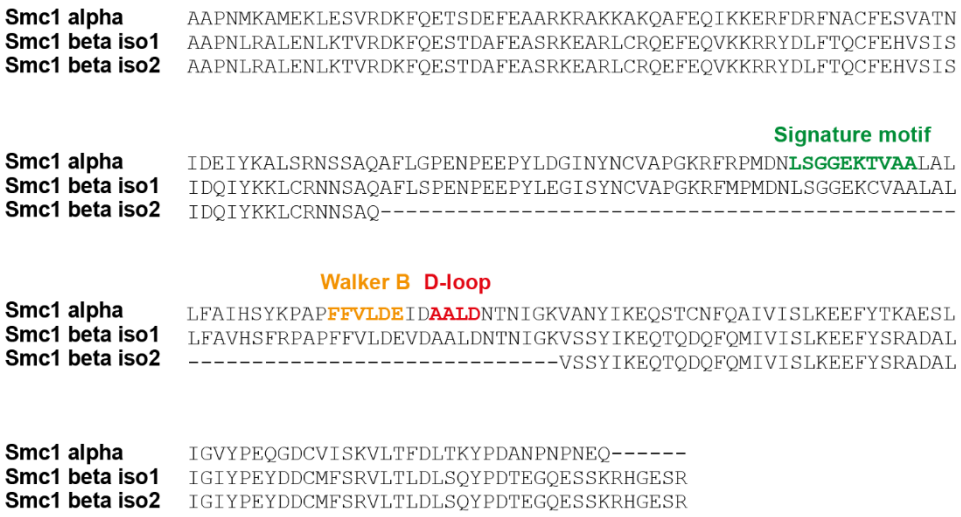


**Figure 21: Smc1β isoform 2 lacks crucial motifs in the ATPase domain**
The alignment shows the C-terminus of human Smc1α, Smc1β isoform 1 and Smc1β isoform 2. Note the 74 amino acid deletion within Smc1β isoform 2, which includes the Signature motif, the Walker B motif and the D-loop as highlighted in the Smc1α sequence.

The signal of Smc1β isoform 2, however, was clearly excluded from the nucleus and was eliminated when cells were preextracted prior to fixation. Thus, we wanted to know whether the localization of Smc1β isoform 2 changes when expressed in the Rec8-Stag3-cell line where additional meiotic cohesion subunits are present. Indeed, the presence of Rec8 and Stag3 triggered nuclear localization of Smc1β isoform 2. Intriguingly, its signal was still not resistant against treatment with detergent, but was completely absent after preextraction. This observation is consistent with published data highlighting the importance of the Walker B motif in Smc1α for cohesion establishment (Elbatsh et al., 2016). Nevertheless, both isoforms of Smc1β were included in further analysis. We speculated that nuclear localization of Smc proteins might require interaction with a kleisin and Smc1β isoform 2 is only granted access to the nucleus when co-expressed with Rec8 and Stag3 since it is not able to interact with Scc1. To test this hypothesis, we performed co-IP experiments from Scc1-GFP cells and Rec8-Stag3-cells that where transfected with plasmids encoding the corresponding Smc1 proteins. Unexpectedly, Scc1 as well as Rec8 interacted with Smc1α, Smc1β isoform 1 and Smc1β isoform 2 (Figure 23). From this observation we infer that it is not a missing kleisin-interaction that prevents nuclear localization of Smc1β isoform 2 in Hek FlpIn cells.

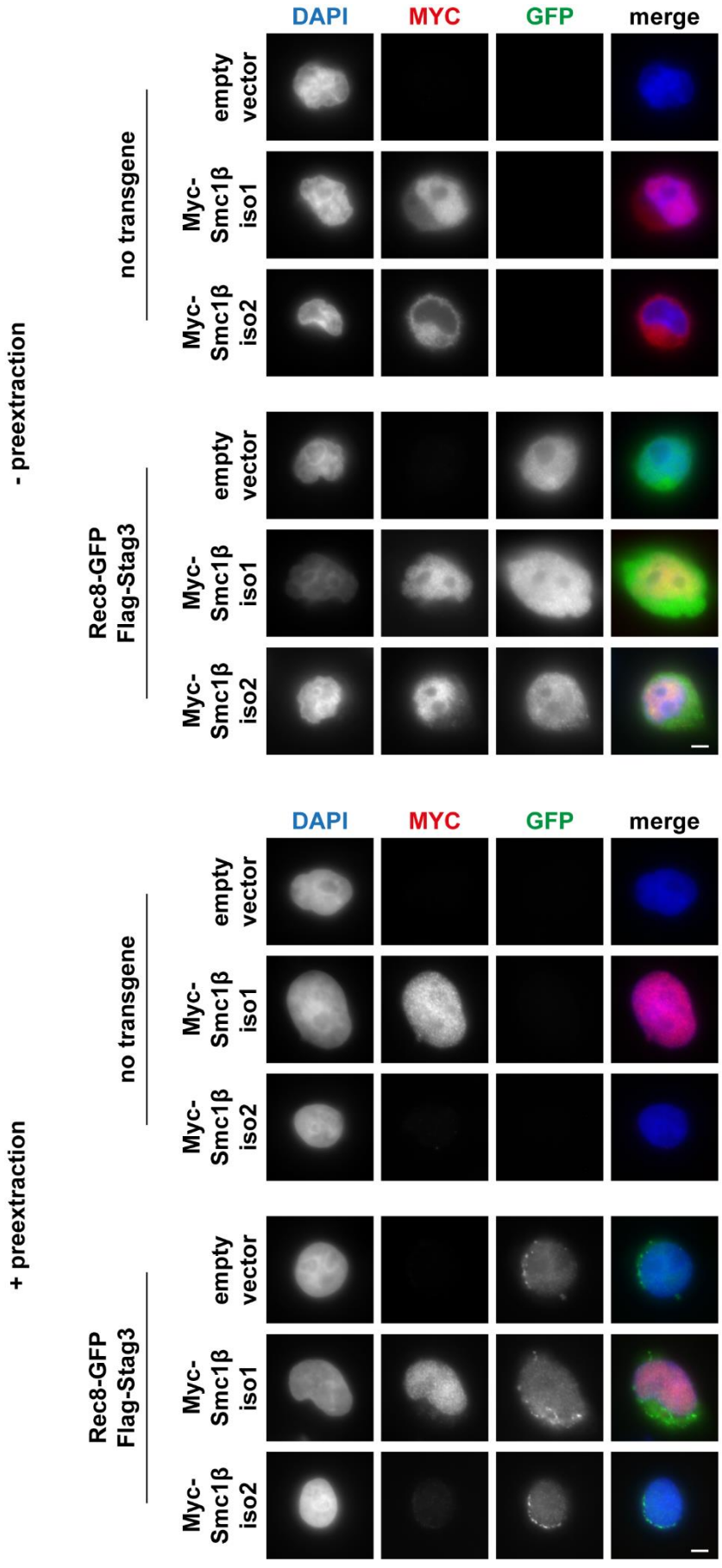


**Figure 22: The nuclear localization of Smc1β iso2 but not of Smc1β iso1 depends on Rec8 and Stag3**

**Figure 22 continued** Dox treated cell lines containing no transgene or Rec8 and Stag3 were transfected with an empty vector or plasmids encoding Myc-tagged Smc1β iso1 or iso2. 48 h after transfection the cells were fixed and subjected to IFM using the indicated antibodies. Cells were treated with the detergent Triton X-100 prior to fixation in order to remove soluble proteins (+preextraction) or were left untreated (-preextraction). The scale bar represents 5 μm.

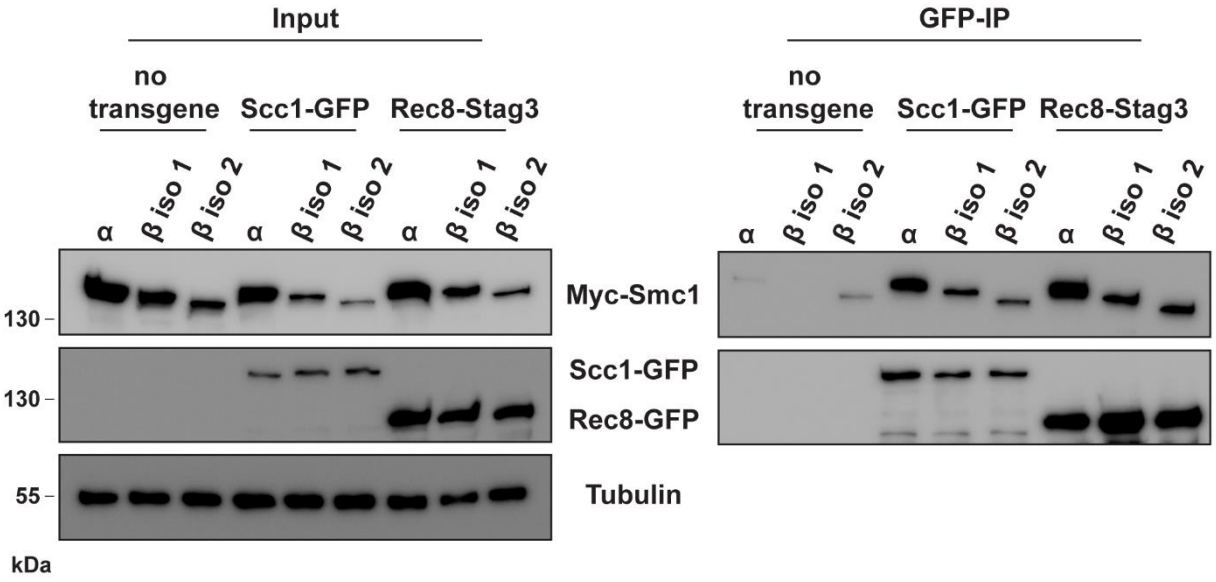


**Figure 23: Scc1 and Rec8 interact with both isoforms of Smc1β**
Transgenic cell lines induced to express Scc1-GFP or Rec8-GFP and a none transgenic cell line were transfected with plasmids encoding either Myc-tagged Smc1α, Smc1β isoform 1 or Smc1β isoform 2. 36 h after transfection nocodazole was added and after additional 12 h the cells were harvested. Lysates were prepared and subjected to IP with beads coupled to GFP nanobodies. Inputs and immunoprecipitates were finally analyzed by Western blotting using the indicated antibodies.

In the next step we wanted to know whether an isoform of Smc1β creates a cohesin ring that is resistant against Wapl activity. To this end, we created triple transgenic Hek FlpIn cell lines containing Rec8-GFP, Flag-Stag3 and Myc-tagged versions of one of the three Smc1 proteins (i.e. Smc1α, Smc1β isoform 1 and Smc1β isoform 2). In the following, mitotic chromosomes of these cell lines were observed for persistent cohesin in metaphase. A representative image of a Rec8-Stag3-Smc1α-cell in mitotic prophase (Figure 24, upper image series) shows the appearance of chromosomes completely decorated with cohesin. Here, a clear Myc and GFP signal is observable along the whole chromosome length. Importantly, the number of cells showing GFP and Myc stained mitotic chromosomes was as low in the triple transgenic cell lines expressing Smc1β isoform 1 or Smc1β isoform 2 as it was in the control cell line expressing Rec8-Stag3-Smc1α. The nuclear signals of Smc1β isoform 1 after preextraction are

similar to ectopically expressed Smc1α (Data not shown). Thus, assuming isoform 1 does mediate Wapl resistance, we would expect metaphase chromosomes showing a cohesin stain with an intensity similar to the cohesin signal of a control cell in prophase. However, this is not the case (Figure 24 shows representative images). We therefore propose that Smc1β containing cohesin molecules are not resistant to Wapl mediated ring opening.

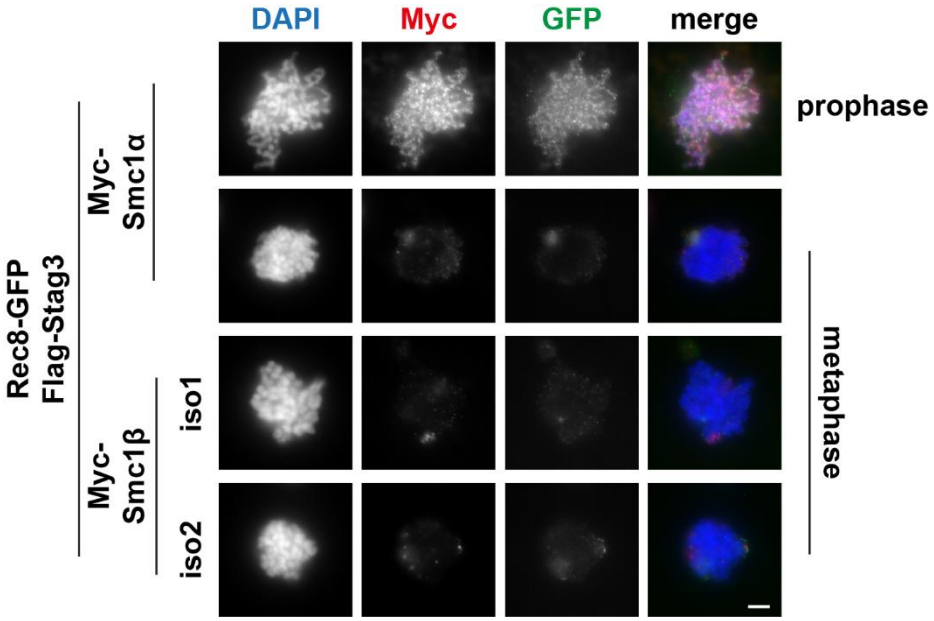


**Figure 24: Smc1β does not confer resistance against Wapl activity**
Triple transgenic cell lines were induced with Dox for 20 h to express Rec8 and Stag3 plus Smc1α, Smc1β iso1 or Smc1β iso2. Nocodazole was added and 5 h later the cells were subjected to preextraction, fixation and IFM with the indicated antibodies. The scale bar represents 5 µm.

## 2.2. Towards an understanding of the mechanism that converts Rec8 into a Separase substrate

Having shown that one can use standard cell lines to study features of meiotic cohesin subunits, we wondered if this could also help us to elucidate the mechanisms that turn Rec8 into a substrate for Separase. It was suggested that Rec8 is turned into a Separase substrate only upon its phosphorylation (Brar et al., 2006; Katis et al., 2010; Kudo et al., 2009). Rec8 and Stag3 form a functional cohesin complex in mitotic cells, however, the cells do not show any toxic effects. A non-cleavable variant of Scc1, in contrast, induces severe chromosome segregation defects and cell death (Hauf et al., 2001). From these observations, we infer that Rec8 in our Rec8-Stag3-cell line is phosphorylated in a way that allows cleavage by Separase

at the metaphase to anaphase transition followed by correct SCS. We speculated that a variant of Rec8 that cannot be properly phosphorylated and, hence, not cleaved would execute a severe cytotoxic effect. To observe such a toxic effect upon expression of a non-phosphorylatable Rec8, would add evidence to the model proposing that Separase cleaves Rec8 exclusively in a phosphorylated state.

We decided to perform the experiments using mouse Rec8 (mRec8) since the ultimate goal would be to study the effect of a non-phosphorylatable Rec8 variant in mouse oocytes. At first, we wanted to make sure that murine Rec8 is functional in concert with human cohesin subunits. We created a transgenic Hek FlpIn cell line that inducibly expresses human Stag3. This cell line and non-transgenic Hek FlpIn cells were transfected with a plasmid encoding mRec8 and subjected to IFM. Remarkably, mRec8 behaved exactly like the human homolog. In the presence of Stag3 a very pronounced signal of mRec8 was observed in the nucleus whereas in the absence of Stag3 mRec8 localized mainly to the cytosol (Figure 25). Even more importantly, the nuclear signal of mRec8 was resistant against preextraction (Figure 25). These observations strongly suggest that mRec8 in conjunction with human Stag3 is competent to form a functional cohesin complex in human cells.

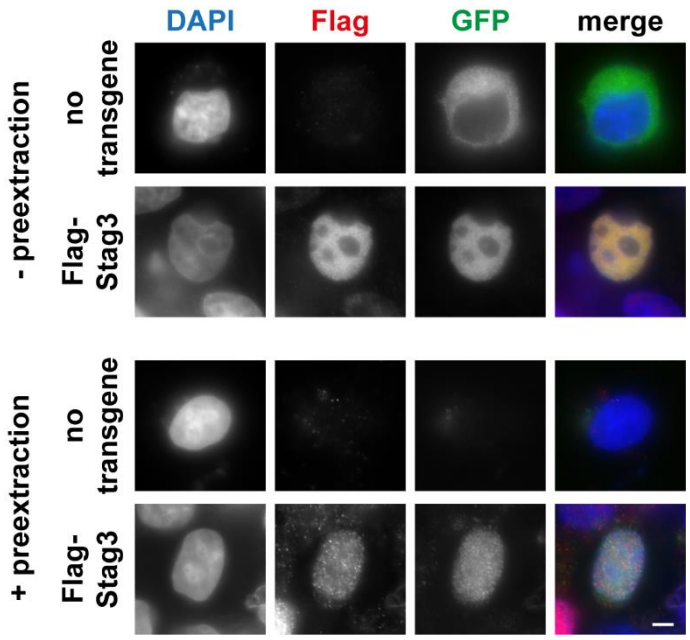


**Figure 25: Murine Rec8 behaves in human cells like human Rec8**

A transgenic cell line induced to express human Flag-Stag3 and a none transgenic cell line were transfected with a plasmid encoding murine Rec8-GFP. 48 h following transfection cells were subjected to IFM and probed with antibodies recognizing Flag or GFP. Cells were either treated with the detergent Triton X-100 prior to fixation in order to remove soluble proteins (+preextraction) or were left untreated (-preextraction). The scale bar represents 5 µm.

To gain deeper insights in the mechanism that turns Rec8 into a Separase substrate we created two phosphorylation site mutant (phosphomutant) variants of mRec8. In the first variant 39 serine and threonine residues that are in close proximity to putative Separase cleavage sites were exchanged with alanine (mRec8 39A). The second variant lacks all serine and threonine residues (mRec8 S/T-free). We created doubly transgenic cell lines containing the gene for human Stag3 and one of the three murine Rec8 variants, i.e. mRec8 wt, mRec8 39A or mRec8 S/T-free. Unexpectedly, neither the Stag3-mRec8 39A nor the Stag3-mRec8 S/T-free cell line showed a growth defect that would indicate toxicity of the Rec8 variants (data not shown).

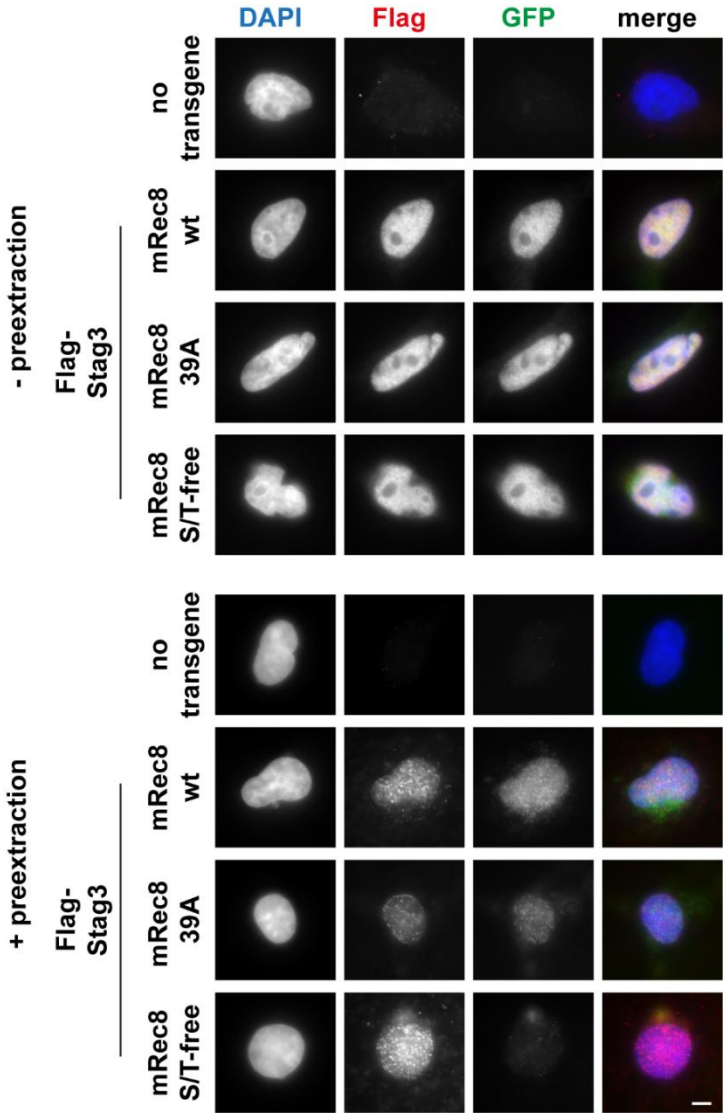


**Figure 26: The behaviour of non-phosphorylatable mRec8 variants in human cells**
A transgenic cell line induced to express human Flag-Stag3 was transfected with plasmids encoding wild type mRec8, an mRec8 variant, in which 39 serine and threonine residues were exchanged with alanine (39A) and an mRec8 variant in which all serine and threonine residues (S/T-free) were exchanged with alanine. All mRec8 proteins were GFP-tagged. 48 h after transfection cells were subjected to IFM using the indicated antibodies. Cells were either pretreated with the detergent Triton

**Figure 26 continued** X-100 in order to remove soluble proteins (+preextraction) or directly fixed (-preextraction). Cells without any transgenes were included to verify specificity of the signals. The scale bar represents 5 µm.

Therefore, we wondered whether the numerous amino acid exchanges might prevent proper folding of the protein and render the Rec8 variants non-functional. To test this hypothesis, we subjected the doubly transgenic cell lines to IFM. Both phosphomutant variants localized to the nucleus exactly like mRec8 wt, whereas only mRec8 39A was resistant to preextraction (Figure 26). A straightforward explanation of this observation is that only mRec8 39A can form a cohesive ring complex but still contains the relevant phosphorylation sites required for cleavage by Separase. In order to verify or falsify this idea, we exploited a functional assay to evaluate functionality of the phosphomutant mRec8 variants. We had shown before that the expression of human Rec8 and Stag3 completely rescues the cohesion defect generated by depletion of Sgo1 (Figure 16). So we asked now whether the mRec8 variants in combination with Stag3 are also competent to decrease the level of premature SCS upon Sgo1 knockdown. Astonishingly, even mRec8 wt was not able to reduce the effect of Sgo1 ablation (Figure 27). Taken together these data imply that mRec8 wt and mRec8 39A associate with chromatin but do not assemble cohesin rings that mediate sister chromatid cohesion (for possible explanations see Discussion).

Since mRec8 is obviously not functional in human cells, we are not able to explore potentially non-cleavable variants by cellular phenotypes (i.e. growth defects due to chromosome segregation failures). Therefore, we considered a different experimental approach to study the cleavage of our mRec8 phosphomutants. According to Kudo et al. murine Rec8 is not cleaved by active Separase *in vitro* unless it is phosphorylated (Kudo et al., 2009). We speculated that Rec8 that is purified from metaphase arrested cells should be modified with the necessary phosphorylations and, thus, be cleaved upon incubation with active Separase. For the variants with phosphorylation sites mutated, in contrast, we would expect a less efficient cleavage or no cleavage at all. We expressed the variants of mRec8 in Hek 293T cells, isolated them via IP and incubated the proteins with purified Separase *in vitro*. To our surprise, we did not detect fundamental differences in cleavage between the mRec8 variants (Figure 28). Normalized to the whole amount of mRec8 present in the reaction mRec8 39A seems to be cut as efficiently as the wild type protein. mRec8 S/T-free seems to be only marginally less efficiently cleaved by Separase compared to wild type and the 39A variant (Figure 28). In

conclusion, we reconstituted the Separase dependent Rec8 cleavage *in vitro* but were not able to demonstrate a clear correlation between cleavage efficiency and phosphorylation status of Rec8. In the discussion section, however, we suggest experiments to analyze our mRec8 phosphomutants further.

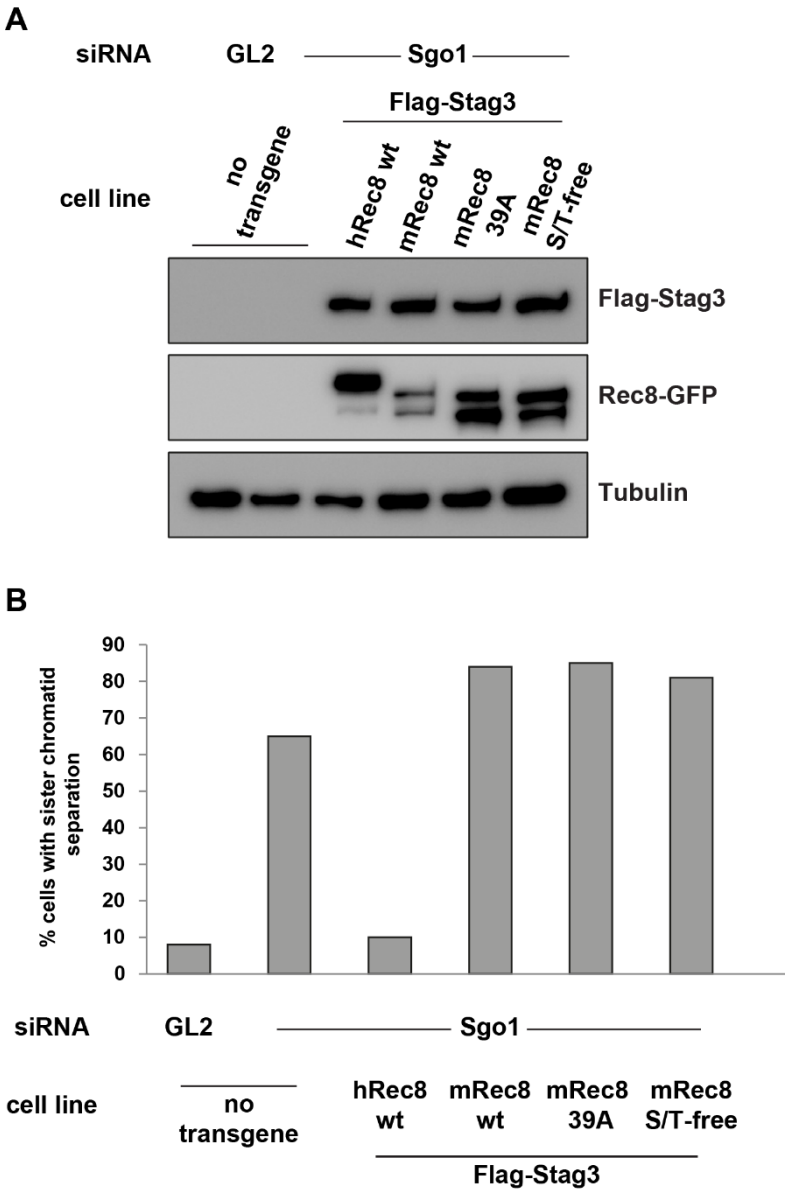


**Figure 27: Despite similar behavior to human Rec8 murine Rec8 is not functional in human somatic cells**

**(A, B)** A non-transgenic cell line and transgenic cell lines induced to express human Flag-Stag3 and human Rec8 (hRec8) or the indicated mRec8 variants were transfected with GL2 or Sgo1 siRNA. 12h later cells were arrested in metaphase by nocodazole treatment for 15h and subsequently harvested. **(A)** A fraction of the cells was boiled in SDS sample buffer and subjected to immunoblotting using the indicated antibodies to verify transgene expression. Right now we cannot explain the two bands detected by the GFP antibody **(B)** Cells were subjected to chromosome spreading and analyzed for premature SCS. 100 cells were counted per sample.

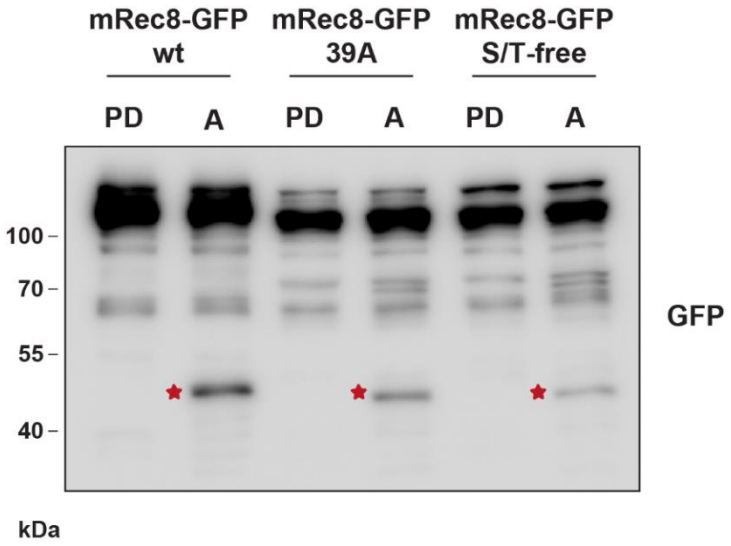


**Figure 28: mRec8 39A is cleaved by Separase as efficiently as wt mRec8 when isolated from nocodazole arrested cells**

Hek293T cells were transfected with plasmids encoding wt mRec8, mRec8 39A or mRec8 S/T-free. 36 h after transfection the cells were arrested in mitosis with nocodazole for 14 h and harvested. Lysates were prepared and subjected to IP with beads coupled to GFP nanobodies. The re-isolated beads were washed several times and incubated with active (A) or protease-dead (PD) Separase at 30°C. After 30 min the reaction was stopped by addition of SDS sample buffer. The samples were subjected to immunoblotting and probed with a GFP antibody. The red asterisks denote the C-terminal cleavage fragment of Rec8.

## 2.3. Role of Cyclin A in terms of meiotic chromosome segregation and prophase pathway activity

### 2.3.1. Non-degradable Cyclin A induces unscheduled SCS in nocodazole arrested cells

The Wassmann group could show that Cyclin A2 is necessary for SCS in meiosis II. Overexpression of Cyclin A generates single sister chromatids already during anaphase I. They speculated that Cyclin A2 somehow inhibits Sgo2 or PP2A at the centromere and thereby enables Rec8 phosphorylation and subsequent cleavage by Separase (Touati et al., 2012). In mitotic cells Cyclin A is rapidly degraded in prophase and we asked whether overexpression of non-degradable Cyclin A might trigger premature SCS in this system as well. This effect could be induced, for example, by inactivation of Sgo1-PP2A similar to the proposed mechanism in meiosis. However, we got interested in Cyclin A for a second reason. An important question is whether the prophase pathway is only active in early mitosis when it removes the bulk of cohesin from chromosomes or if it could in theory also operate later in mitosis. A possible mechanism of switching off the prophase pathway could be the degradation of a positive regulator. Thus, Cyclin A is a good candidate and the involvement of other kinases in the non-proteolytical cohesin ring opening is well established (Hauf et al., 2005; Liu et al., 2013b; Nishiyama et al., 2013). If overexpression of Cyclin A shows an effect on cohesion, it can indicate two possible explanations. First, Cyclin A is involved in prophase pathway signaling and non-physiological levels lead to hyperactivity in cohesin removal. Second, higher levels of Cyclin A inactivate the protection of centromeric cohesin as it is probably the case in meiosis II (note that in mitosis it would be deprotection from Wapl activity whereas it is deprotection from Separase cleavage in meiosis). Whatever cause might apply we would be able to learn about the regulation of the prophase pathway or study the mechanism of Cyclin A function in the second meiotic division.

To gain deeper insights into the role of Cyclin A we transfected Hek 293T cells with a plasmid encoding Δ86-Cyclin A, arrested the cells in metaphase and analyzed sister chromatid cohesion by chromosome spreading (Figure 29B). An empty vector and a Δ90-Cyclin B encoding plasmid served as controls. The truncated Cyclins are not recognized by the APC/C and, hence, not degraded (den Elzen and Pines, 2001; Murray et al., 1989). Remarkably, almost half of the cells transfected with Cyclin A showed separated sister chromatids. In contrast, cells expressing non-degradable Cyclin B exhibited only marginal loss of cohesion.

Next, we repeated the experiment with another cell line and could undoubtedly show that Cyclin A overexpression induces cohesion failure also in HeLa cells (Figure 29D). Therefore, we conclude that overexpression of Cyclin A or untimely presence of the protein in metaphase destroys centromeric cohesion.

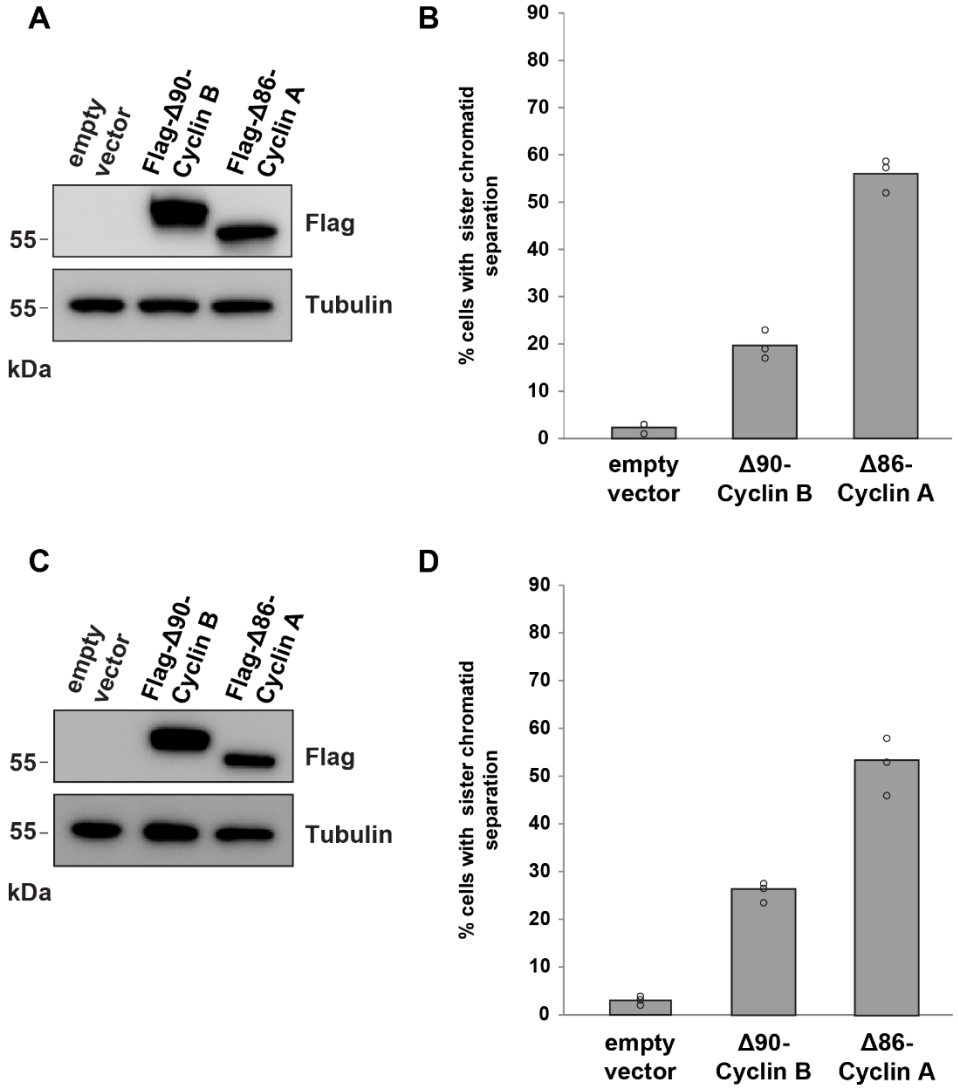


**Figure 29: Overexpression of non-degradable Cyclin A induces premature SCS in Hek 293T and HeLa cells**

**(A, B)** Hek 293T cells were transfected with an empty vector or plasmids encoding Flag-Δ90-Cyclin B or Flag-Δ86-Cyclin A. 35 h after transfection cells were arrested in metaphase by nocodazole treatment for 15h and subsequently harvested. **(A)** A fraction of the cells was boiled in SDS sample buffer and subjected to immunoblotting using the indicated antibodies to verify comparable expression levels of Cyclin B and Cyclin A. **(B)** Cells were subjected to chromosome spreading and analyzed for premature SCS. 100 cells were counted per sample. Averages (grey bars) of three independent experiments (spheres) are shown. **(C, D)** The experiments were performed as described in **(A, B)** except that HeLa cells were used.

In the next step we created transgenic Hek FlpIn cell lines that express N-terminally GFP-tagged Δ90-Cyclin B or Δ86-Cyclin A upon induction. These cell lines were treated with Dox and simultaneously blocked at mitosis by addition of nocodazole for 14 h. Western blotting confirmed comparable expression levels of both non-degradable Cyclins (Figure 30A). Importantly, chromosome spreading analysis revealed that, as before, stabilized Cyclin A but not Cyclin B triggers significant cohesion loss in a metaphase arrest (Figure 30B).

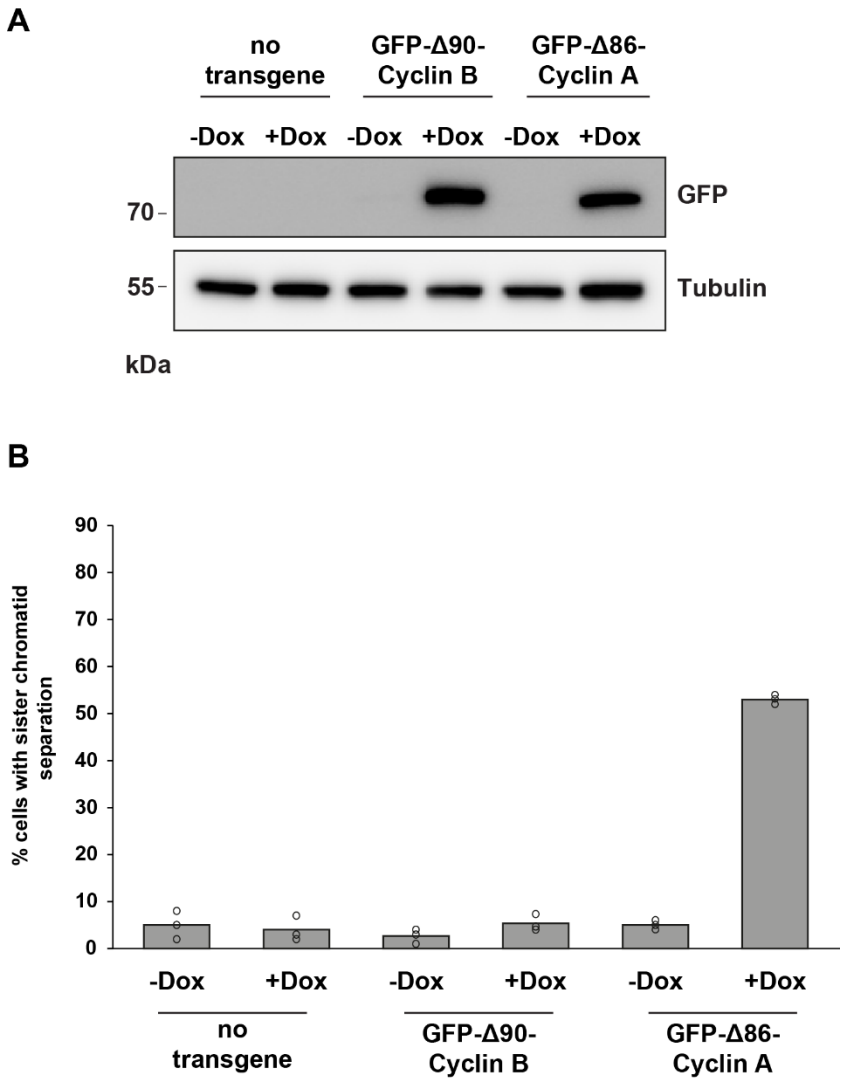


**Figure 30: Non-degradable Cyclin A induces premature SCS in Hek 293 FlpIn cells when inducibly overexpressed**

**(A, B)** Cell lines harboring GFP-Δ90-Cyclin B, GFP-Δ86-Cyclin A or no transgene were either treated with Dox or left uninduced. At the same time, nocodazole was added and cells were harvested 14 h thereafter. **(A)** A fraction of the cells was boiled in SDS sample buffer and subjected to immunoblotting using the indicated antibodies to verify correct induction and equal expression levels of transgenic Cyclin B and Cyclin A. **(B)** Cells were subjected to chromosome spreading and analyzed for premature SCS. 100 cells were counted per sample. Averages (grey bars) of three independent experiments (spheres) are shown.

In contrast to Cyclin B, Cyclin A triggers cellular events also during S-phase (Yam et al., 2002). A remote explanation for the cohesion defect observed upon Cyclin A but not Cyclin B overexpression is that non-physiological levels of Cyclin A impair correct cohesion establishment upon DNA replication. To rule out this possibility, we arrested the cells in mitosis via nocodazole and only then induced expression of the transgenes. Notably, this procedure also lead to unscheduled separation of the sister chromatids albeit with lowered penetrance (Figure 31). We, thus, conclude that non-physiological Cyclin A levels lead to ring opening of cohesin during mitosis.

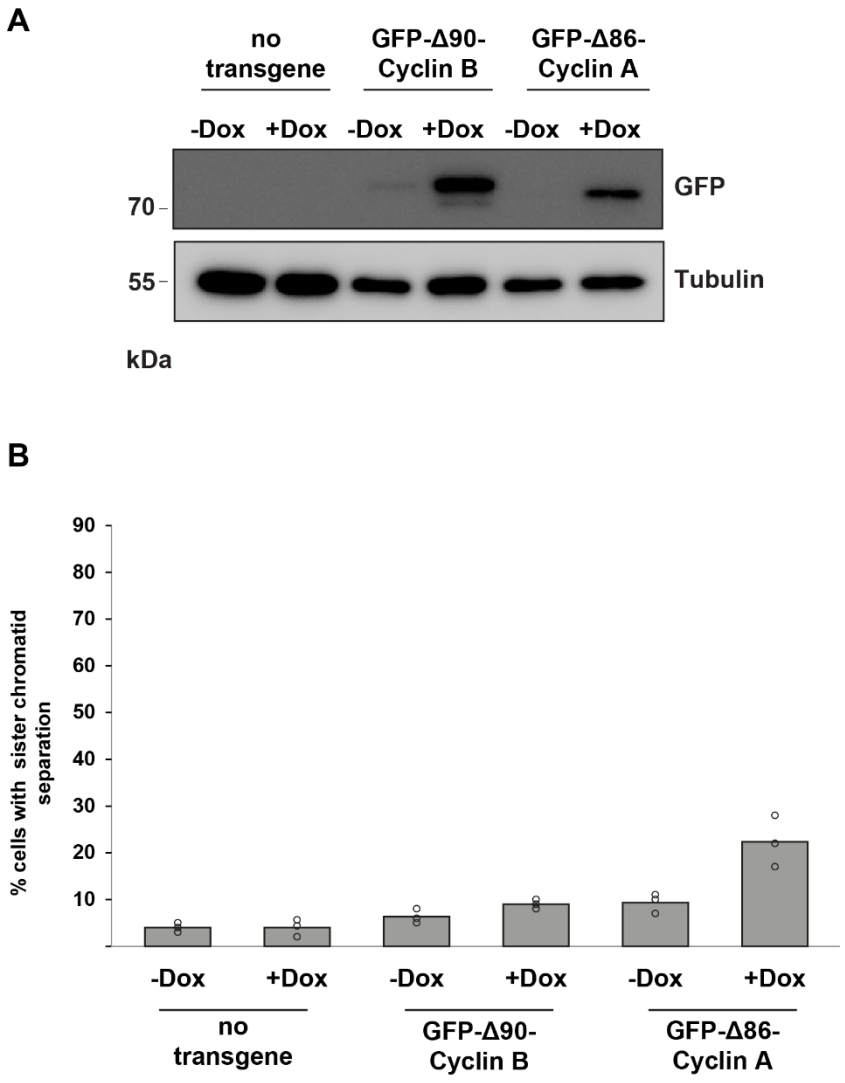


**Figure 31: Non-degradable Cyclin A leads to premature SCS in Hek 293 FlpIn when its expression is induced during metaphase arrest**

**(A, B)** Cell lines harboring no transgene, GFP-Δ90-Cyclin B, GFP-Δ86-Cyclin A were arrested in S-phase with thymidine released into fresh medium for 12 h and blocked at mitosis with nocodazole for 5 h. Then, Dox was added and after additional 5h cells were harvested. **(A)** A fraction of the cells was boiled in SDS sample buffer and subjected to immunoblotting using the indicated antibodies to verify correct

**Figure 31 continued** induction and equal expression levels of transgenic Cyclin B and Cyclin A. **(B)** Cells were subjected to chromosome spreading and analyzed for premature SCS. 100 cells were counted per sample. Averages (grey bars) of three independent experiments (spheres) are shown.

Touati et al. showed via IFM that Cyclin A localizes to the centromere in meiosis II. Therefore, we asked whether we could also detect the protein in somatic cells at the centromeric region. Cyclin B was shown before to localize to the kinetochore (Bentley et al., 2007) and was, hence, used as a positive control to proof sensitivity of our method. Indeed, a robust signal for GFP that co-localized with Hec1 was observable in our GFP-Δ90-Cyclin B expressing cell line. In contrast, we were not able to detect GFP-Δ86-Cyclin A at the centromere (Figure 32). We believe that Cyclin A executes its activity (i.e. modifying a cohesin regulator) at the centromere. A very transient association of Cyclin A with its centromeric interaction partner could explain why we were unable to stain centromeric Cyclin A.

Our cell line that inducibly expresses non-degradable Cyclin A can be used as a versatile tool to unravel Cyclin A's mechanism of cohesin release. The expression of Cyclin A can be combined with RNAi mediated knockdown of proteins that might be involved in the Cyclin A mediated SCS. A reduction in the percentage of separated sister chromatids upon knockdown of a certain protein would indicate its involvement in the Cyclin A pathway.

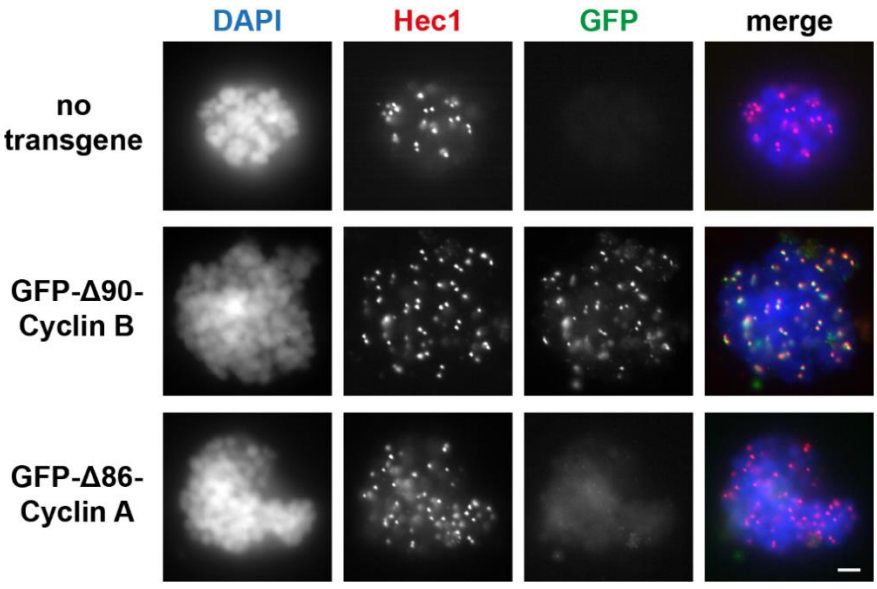


**Figure 32: Cyclin A does not significantly accumulate at centromeres in mitotic cells**
A none transgenic cell line and transgenic cell lines induced to express GFP-Δ90-Cyclin B or GFP-Δ86-Cyclin A were preextracted and fixed 12 h after induction. Then the cells were stained with Hec1 and GFP antibodies. Note that signals for Δ90-Cyclin B but not Δ86-Cyclin A were readily observable at centromeres. The scale bar represents 5 µm.

### 2.3.2. Cyclin A-Cdk is competent to phosphorylate Sororin

Recent studies proposed that prophase pathway mediated ring opening involves phosphorylation of Sororin by Cdk1 (Dreier et al., 2011; Nishiyama et al., 2010; Nishiyama et al., 2013; Zhang et al., 2011). However, it was never unambiguously shown that it is Cdk1 in combination with Cyclin B, which is solely responsible for Sororin modification *in vivo*. We speculated that Cyclin A might be even more important for enabling Wapl mediated ring opening. Thus, we planned to compare Cyclin B's and Cyclin A's capability to phosphorylate Sororin by an *in vitro* kinase assay. First, we wanted to test how to obtain active Cyclin B-Cdk1 and Cyclin A-Cdk1. We overexpressed Flag-tagged Cyclin B or Cyclin A, respectively, in Hek 293T cells, arrested the cells in metaphase and purified the proteins using anti-Flag affinity beads assuming that the Cyclins will co-purify endogenous Cdk1. To verify activity we incubated the eluates with the model Cdk1 substrate Histone H1 in presence of [γ-$^{33}$P]-labelled ATP and subjected the samples to SDS-PAGE followed by autoradiography. Indeed, in both cases we were able to observe a strong phosphorylation signal of Histone H1 that was markedly reduced when the Cdk inhibitor RO-3306 was present in the reactions indictating that Cyclin B and Cyclin A can be purified in combination with Cdk and in an active state from cell culture (Figure 33).

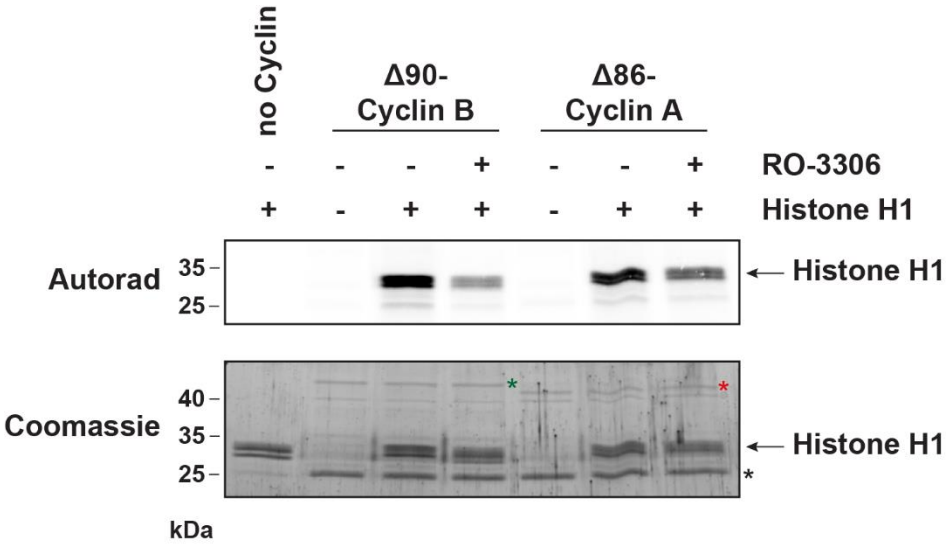


**Figure 33: Active Cyclin B-Cdk and Cyclin A-Cdk can be purified from Hek 293T cells**
Hek 293T cells were transfected with plasmids encoding Flag-Tev-Δ90-Cyclin B and Flag-Tev-Δ86-Cyclin A. 34 h after transfection the cells were blocked in mitosis for 14 h by nocodazole treatment and subsequently harvested. Lysates were prepared and incubated with anti-Flag affinity beads. The beads were re-isolated and, following extensive washing, Δ90-Cyclin B and Δ86-Cyclin A were eluted by incubation with Tev protease. The eluates were incubated with histone H1 in the presence of

**Figure 33 continued** [γ-$^{33}$P]-ATP at 30°C. After 30 min the reaction was stopped by addition of SDS sample buffer. The samples were separated by SDS-PAGE, stained with Coomassie and finally subjected to autoradiography. Coomassie staining reveals equal amounts of histone, Δ90-Cyclin B (green asterisk) and Δ86-Cyclin A (red asterisk). The CDK inhibitor RO-3306 was included to show that phosphorylation activity is CDK-dependent. The black asterisk denotes the Tev protease present in the kinase preparations.

Next, we performed a kinase assay using recombinant Sororin as a substrate. Remarkably, the $^{33}$P-signals as visualized by autoradiography were almost identical independent of whether Sororin was incubated with the Cyclin B or the Cyclin A eluate (Figure 34). This shows that Cyclin A-Cdk is competent to phosphotylate Sororin *in vitro*. Finally and most importantly, our data indicate that Sororin might be a bona fide substrate of Cyclin A and that Cyclin A might be involved in prophase pathway signaling.

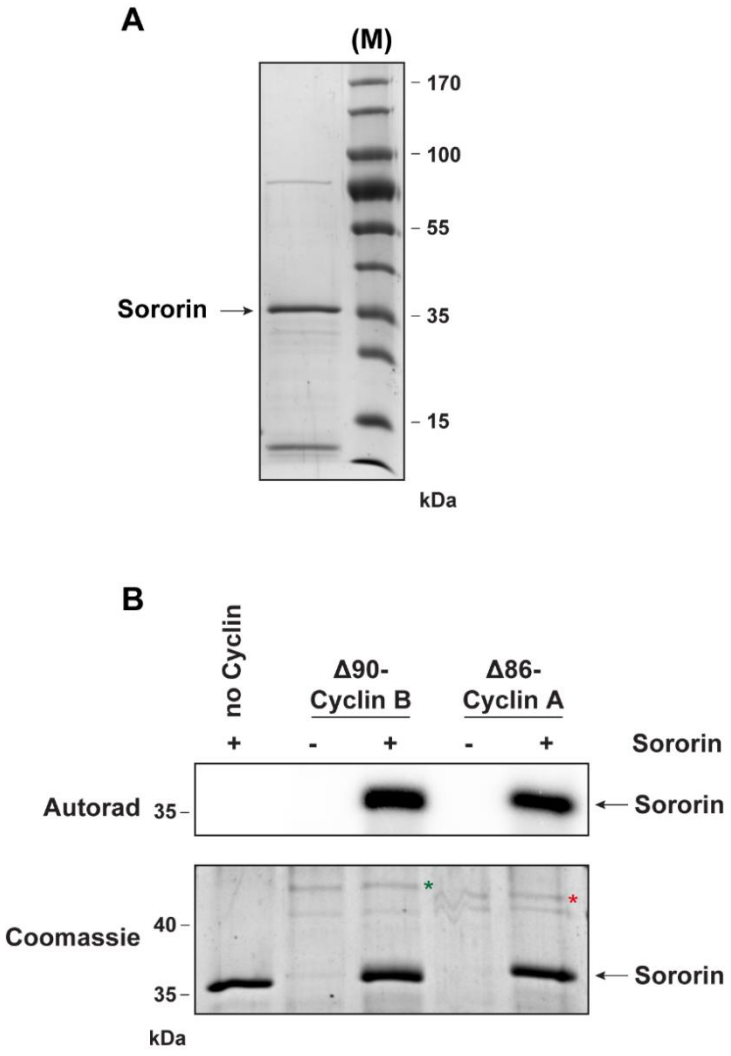


**Figure 34: Cyclin A-Cdk and Cyclin B-Cdk phosphorylate Sororin with similar efficiency**
**(A)** A coomassie stained gel of bacterially produced and subsequently purified Sororin. Marker is

**Figure 34 continued** indicated as (M). **(B)** The preparations of Δ90-Cyclin B and Δ86-Cyclin A characterized in Figure 33 were incubated with Sororin shown in **(A)** in the presence of [γ-$^{33}$P]-ATP at 30°C. After 30 minutes, the reactions were stopped by addition of SDS sample buffer. The samples were separated by SDS-PAGE, stained with Coomassie and finally subjected to autoradiography. Coomassie staining reveals comparable amounts of Δ90-Cyclin B (green asterisk) and Δ86-Cyclin A (red asterisk).

# 3. Discussion

## 3.1. How many different cohesin complexes do exist in germ cells?

In this study we employed human cell lines, which are routinely used in standard cell culture applications, to unravel unstudied and controversial characteristics of meiosis-specific cohesin subunits. We clearly show that the meiosis-specific kleisin Rec8 interacts with Smc3 and, importantly, with Smc1α (Figure 8) and that it can form a functional complex with these two Smc-proteins (Figure 13 and Figure 16). But the physiological situation in germ cells might be different. Does Rec8 associate with Smc1α *in vivo* and, if so, does this complex have a function in cohesion during gametogenesis? Even for the first question the literature provides conflicting results. The research group of Jessberger could co-isolate Rec8 when they precipitated Smc1α (Revenkova et al., 2004). This result is inconsistent with studies that found an interaction only between Rec8 and Smc1β but not with Smc1α (Ishiguro et al., 2011; Lee and Hirano, 2011). Our data, however, provide evidence that Rec8 is definitely competent to bind Smc1α.

Other experiments, also mainly performed by the Jessberger lab, showed that cohesion is primarily supported by Smc1α cohesin in prophase I. However, Smc1β seems to become essential for cohesion from late prophase until metaphase II (Biswas et al., 2013; Revenkova et al., 2004). This is in accordance with the finding that Smc1β but not Smc1α can be detected on meiotic chromsomes beyond prophase I until metaphase II (Kouznetsova et al., 2005; Revenkova et al., 2001). It was shown in rat spermatocytes that Smc1β appears only in leptonema i.e. after premeiotic S-phase (Figure 35) (Eijpe et al., 2003). Assuming that Rec8 forms cohesive cohesin complexes during premeiotic S-phase, these complexes have to contain Smc1α. Studies in which Tachibana-Konwalski and colleagues activated Rec8 at distinct timepoints during oocyte development and employed functional cohesion rescue assays suggest that Rec8 mediated cohesion cannot be established during the prolonged dictyate-stage arrest and oocyte growth (Burkhardt et al., 2016; Tachibana-Konwalski et al., 2010). However, this work cannot exclude whether Rec8 cohesin can be loaded during early prophase when DNA double-strand breaks are induced. Postreplicative cohesion establishment upon DNA breaks is well described in mitotic cells (Heidinger-Pauli et al., 2008; Heidinger-Pauli et al., 2009; Strom et al., 2007; Strom et al., 2004; Unal et al., 2004; Unal et al., 2007). Thus, it is conceivable that cohesin complexes containing Rec8 and Smc1β are

loaded and establish cohesion upon DNA damage in prophase I. Another question is whether other kleisins than Rec8 mediate cohesion during gametogenesis. In spermatocytes of Rec8 knockout mice sister chromatid cohesion is not completely abolished during early prophase I indicating that cohesin complexes containing a kleisin different than Rec8 can, at least to some extent, mediate cohesion for a short time period after premeiotic S-phase (Bannister et al., 2004; Xu et al., 2005). Therefore, it is imaginable that the Smc1α containing rings mediating cohesion in early prophase in Smc1β$^{-/-}$ mice are associated with Scc1 or Rad21L. However, this is hard to reconcile with very elegant work in mouse oocytes in which artificial cleavage of an engineered Rec8 lead to complete separation of homologes and sister chromatids in meiosis I, suggesting that cohesion is exclusively mediated by Rec8 (Tachibana-Konwalski et al., 2010). Additionally, Rad21L disappears in diplonema from chromosomes and was described not to impact centromere cohesion whereas Scc1 becomes detectable as late as pachynema (Figure 35) (Fukuda et al., 2014; Ishiguro et al., 2011; Ishiguro et al., 2014; Lee and Hirano, 2011). In conclusion, the currently available data suggest that a cohesin ring containing Rec8 and Smc1β are mainly responsible for cohesion in meiosis. However, knockout studies suggest that complexes composed of Rec8 and Smc1α are also competent to tether chromatids together in germ cells although we do not know if this is physiologically relevant. Our data now unambiguously proof that Rec8 and Smc1α form a cohesin ring that can mediate cohesion.

In the course of this work, we showed that Rec8 is only functional when associated with another meiosis-specific subunit, namely Stag3. As reviewed by Susannah Rankin one does not find evidence in the literature for a complex assembled with Stag3 and Smc1α (Rankin, 2015). Lee and Hirano rather observed an interaction of Stag3 with Smc1β but not Smc1α (Lee and Hirano, 2011). We, however, provide data showing that Rec8 and Stag3 are functional in Hek 293 FlpIn cells where most likely only Smc1 α is available to form a cohesin ring. Interestingly, our microscopy analysis demonstrating that Stag3 alone localizes to the nucleus and is resistant against preextraction indicates an interaction of Stag3 with the general kleisin Scc1 (Figure 17). This finding is consistent with co-IP experiments where Scc1 co-purified with Stag3 (Gutierrez-Caballero et al., 2011; Ishiguro et al., 2011). In contrast, there are conflicting reports on whether Rec8 and Rad21L interact with Stag1 and Stag2 or not (Gutierrez-Caballero et al., 2011; Ishiguro et al., 2011; Lee and Hirano, 2011). From our data we infer that Rec8 is not found in a complex with Stag1 and Stag2 (Figure 9 and Figure 10). Stag3$^{-/-}$ mice have a severe meiotic phenotype resembling the phenotype of the Rad21L$^{-/-}$ Rec8$^{-/-}$ double mutant

(Fukuda et al., 2014; Hopkins et al., 2014; Llano et al., 2012; Winters et al., 2014). This fact further suggests that Rec8 and Rad21L need Stag3 for functionality. Remarkably, cohesion is not completely eradicated in Stag3$^{-/-}$ spermatocytes (Winters et al., 2014). The first possible explanation is that in meiocytes, contrary to the situation in our cell line, Rec8 does form a functional complex with Stag1 or Stag2 *in vivo*. More likely, however, is the explanation that very small levels of Scc1 that are not detectable by the exploited methods mediate some cohesion.

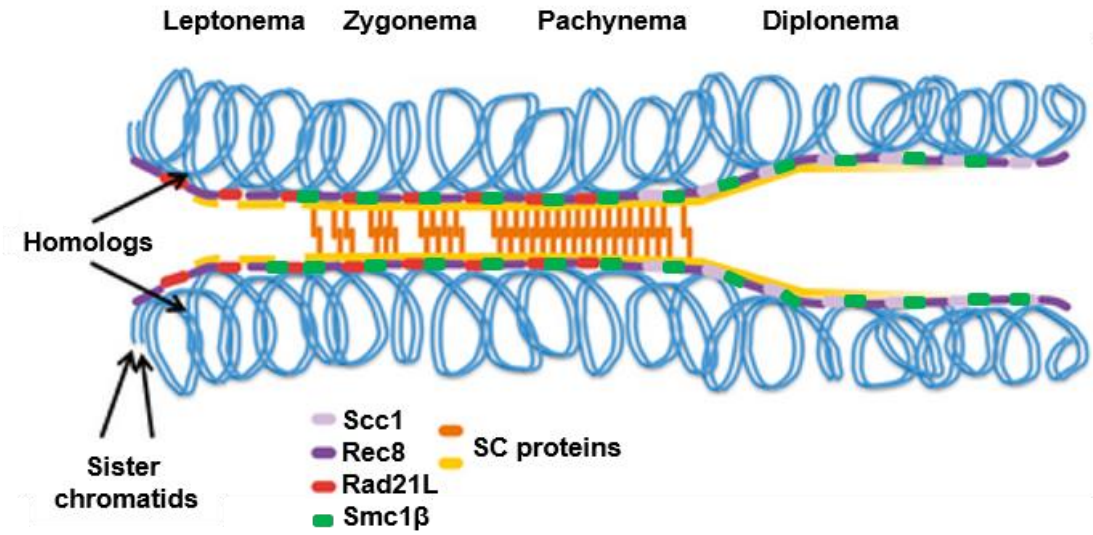


**Figure 35: Cohesin during prophase I of meiosis**
The figure shows the appearance of cohesin subunits during prophase I. Smc1β is detectable from leptonema and Scc1 from pachynema onwards (McNicoll et al., 2013). Rad21L disappears in diplonema (McNicoll et al., 2013). Some cohesin proteins are omitted for clarity: Smc1 α is present from premeiotic S-Phase onwards and disappears at the end of prophase I (Revenkova et al., 2001). Smc3 and Stag3 are present throughout meiosis. Stag1 and Stag2 were barely studied in meiosis but Stag2 was detected in early prophase I (McNicoll et al., 2013). Image taken and modified from Rankin, 2015.

We observed the localization of Rec8 in mitotic cells by IFM and demonstrated that Rec8 appears to be completely excluded from the nucleus when it is not associated with Stag3. In human cells nuclear envelope break down accompanies mitosis and proteins that are restricted to the cytosol have to be actively exported in G1-phase. Hence, we asked whether Rec8 harbors nuclear export signals (NES) and performed bioinformatical analysis using the software NESsential and NetNES (Fu et al., 2011; la Cour et al., 2004). Indeed, both tools predicted that Rec8 contains a motif in its C-terminus that very likely functions as a NES (data

not shown) explaining the predominantly cytosolic localization of Rec8. A straightforward explanation for the observation that Stag3 triggers Rec8's nuclear localization is that a nuclear localization signal (NLS) in Stag3 shuttles Rec8 into the nucleus. Interestingly, a recent study identified bona fide NLSs in the C-terminal part of Stag2 (Tarnowski et al., 2012). Using the online tool cNLS Mapper (Kosugi et al., 2009) we were able to identify a motif in the C-terminus of Stag3, which likely has a strong nuclear localization signaling activity. Importantly, when we aligned Stag2 and Stag3 the putative NLS in Stag3 overlaps with one motif in Stag2 previously identified and characterized by Tarnowski et al. (Figure 36) (Tarnowski et al., 2012). Therefore, we assume that Rec8 is not imported into the nucleus but rather exported in G1-phase when enclosed upon nuclear envelope reformation. A complex of Rec8 and Stag3, however, is imported into the nucleus due to the NLS in Stag3 and can entrap DNA during replication in S-phase. It will be interesting to investigate whether Rec8's NES is masked upon interaction with Stag3. Another possibility is that Stag3's NLS simply outcompetes the activity of the NES in Rec8.

```
Stag2  PLNLAFLDILSEFSSKLLRQDKRTVYVYLEKFMTFQMSLRREDVWLPLMSYRNSLLAGGD
Stag3  PPNLAFLELLSEFSPRLFHQDKQLLLSYLEKCLQH-VSQAPGHPWGPVTTYCHSLSPVEN
       * *****::***** :*::***: :  **** :   :*      * *: :* :**    :

Stag2  DDTMSVISGISSRGSTVRSKKSKPSTGKRKVVEGMQLSLTEESSSSDSMWLSREQTLHTP
Stag3  TAETSP--------------QVLPS-SKRRRVEGPAKPNREDVSSS------QEESLQLN
           *               :  **  **: ***      *: ***      :*::*:

Stag2  VMMQTPQLTSTIMREPKRLRPEDSFMSVYPMQTEHHQTPLDYNTQVTWMLAQRQQEEARQ
Stag3  SIPPTPTLTSTAVKSRQPLW------GLKEMEE-EDGSELDFAQGS--------QPVAGT
        :  ** **** ::  : *        :  *:     : **:            *  *

Stag2  QQE-RAAMSYVKLRT-----NLQHAIRRGTSLMEDDEEPIVEDVMMSSEGRIEDLNEGMD
Stag3  ERSRFLGPQYFQTPHNPSGPGLGNQLM-RLSLMEEDEEEELEIQDESNEERQ---DTDMQ
       ::       * :         * : :    ****:***  :*    * * *    :  *:

Stag2  FDTMDIDLPPSKNRRERTELKPDFFDPASIMDESVLGVSMF
Stag3  ASSY-----SSTS-----ERGLDL------LDSTELDIEDF
         :       *       *   *:      :* : * :  *
```

**Figure 36: Stag3 may contain a NLS**
The alignment shows the C-termini of Stag2 und Stag3. The NLS identified in Stag2 by Tarnowski et al. and the NLS in Stag3 identified by our bioinformatical analysis are highlighted in red. Asterisks indicate positions with a fully conserved residue. Colons denote residues with similar properties.

## 3.2. What is the function of Wapl in meiosis and how dynamic is meiotic cohesin?

In this study we presented results demonstrating that Rec8 containing cohesin rings can be opened by Wapl. First, siRNA mediated depletion of Wapl leads to increased Rec8 cohesin levels on mitotic chromosomes. Second, the rescue effect of Rec8-Stag3 on the cohesion defect induced by Sgo1 knockdown is abrogated when Sgo2 is co-depleted indicating that Sgo2 protects Rec8 cohesin at the centromere from prophase pathway activity. Our finding that cohesion is impaired upon Sororin depletion even when cells express Rec8 and Stag3 is precisely in line with this idea as it demonstrates that Rec8 containing cohesin rings also have to associate with Sororin to establish cohesion in S-phase. Our data that Rec8 cohesin is susceptible to prophase pathway signaling beg the question whether Wapl acts on meiotic cohesin under physiological conditions in germ cells. We have known for a long time that Wapl is clearly detectable in germ cells and two papers published very recently describe a function for the cohesin regulator in gametogenesis (Challa et al., 2016; Crawley et al., 2016; Kuroda et al., 2005; Zhang et al., 2008a). The analysis of budding yeast Wapl deletion mutants revealed that the cohesin regulator is involved in SC formation, recombination and in the control of chromosome axis compaction (Challa et al., 2016). Although the level of chromosome-associated Rec8 did not differ between wild type and Wapl knockout mutants the distribution of Rec8 along chromosomes was considerably changed. Meiotic chromosomes in wild type yeast cells contain regions with high levels as well as regions with low levels of Rec8 (Ito et al., 2014; Kugou et al., 2009; Sun et al., 2015). In the absence of Wapl, however, Rec8 was uniformly distributed along chromatin and the authors speculated that Wapl may be required for the formation of Rec8-poor regions on chromosomes (Challa et al., 2016). A study conducted in the nematode *C. elegans* attributed Wapl a function in the modulation of higher-order chromosome structure in meiosis, too (Crawley et al., 2016). Besides Rec8 *C. elegans* expresses two additional, highly homologous and functionally redundant meiosis-specific kleisins, COH-3 and COH-4. Interestingly, Crawley et al. show that, compared to wild type animals, only the chromosomal signals of COH-3 and COH-4 but not of Rec8 increase dramatically in pachynema nuclei when Wapl is missing. This work, hence, implies that only COH-3 and COH-4 containing cohesin molecules are sensitive to Wapl activity. It will be a thrilling challenge to work out why cohesin containing the Rec8 protein is protected from Wapl mediated ring opening in *C. elegans.* One could imagine that Wapl resistance is an

intrinsic feature of *C. elegans* Rec8 or that a posttranslational modification renders Rec8 insensitive towards Wapl. Additionally, a prominent role for Wapl in gametogenesis was reported in *A. thaliana* (De et al., 2014). In wild type meiocytes of the plant the bulk of the Rec8 homolog SYN1 is removed in diplonema and diakinesis. Upon Wapl inactivation, however, high amounts of SYN1 remain associated with chromosomes even in metaphase I. The authors speculated that this prolonged presence of cohesin is the reason for the chromosome bridges and mis-segregation of chromosomes, which were observed in anaphase I of Wapl mutant plants.

Most importantly, work by the Cohen laboratory described a role for the kinase Nek1 in cohesin removal during prophase in mammalian spermatogenesis (Holloway et al., 2011). In wild type males, but not in animals homozygously mutant for Nek1, the level of Smc3 decreases on chromosome cores in diplonema. In a follow-up study they propose that Nek1 activates the phosphatase PP1 by phosphorylation and that PP1 removes an inhibitory phosphate group from Wapl (Brieno-Enriquez et al., 2016) indicating that Wapl is responsible for the cohesin removal in late prophase I. Similar to the situation in *C. elegans,* the levels of Rec8 and Stag3 are not affected by Nek1 ablation implying that Wapl only acts on a distinct subset of cohesin complexes (Holloway et al., 2011). Consistent with the model that Wapl activity displaces Sororin from DNA, the chromosomal level of Sororin was elevated in Nek1 mutant mice (Brieno-Enriquez et al., 2016). Interestingly, another study dealing with the Wapl antagonist detected Sororin at the central region of the synaptonemal complex from zygonema onwards, contrary to the localization of other cohesin components in the lateral elements (Gomez et al., 2016). By late prophase I, Sororin accumulates at centromeres and remains there until anaphase II with slight localization changes relative to a kinetochore marker. The authors speculated that Sororin might not be required for cohesion maintenance during prophase but rather for cohesin protection from Separase cleavage in anaphase I (Gomez et al., 2016). Our data, however, indicate that Rec8 cohesin requires Sororin to efficiently maintain cohesion (Figure 15). Yet, it is conceivable that small and undetectable amounts of Sororin associate with cohesin complexes along lateral elements. Another interesting idea is that a meiosis specific mechanism exists, which renders Rec8 cohesin resistant against Wapl. This might explain why cohesin does not colocalize with Sororin in meiotic prophase (Gomez et al., 2016) and why the Rec8 level is not elevated in spermatocytes of Nek1 mutant mice (Holloway et al., 2011). The pronounced centromeric localization of

Sororin in spermatocytes is very interesting since we have evidence that Sororin has the ability to inhibit Separase (Brigitte Neumann, unpublished results). Therefore, it is tempting to speculate that the protection of centromeric cohesion throughout meiosis I is not exclusively achieved by local dephosphorylation of Rec8 but also by local inhibition of Separase.

Another interesting question is whether cohesin can be loaded or whether cohesion can be established from leptonema onward. As already mentioned, a replication independent cohesion establishment in prophase I probably exists for two reasons. First, Smc1β is not present during premeiotic S-phase and, yet, is required for correct chromosome cohesion during meiosis (Revenkova et al., 2004). In addition, it has been shown in plants and insects that cohesin subunits appear on meiotic chromosomes during prophase, i.e. independent of DNA replication. However, the relevance of this late loading was not investigated (Qiao et al., 2011; Valdeolmillos et al., 2007). Second, although not formally demonstrated so far, proper DNA double strand break repair in prophase of meiosis most likely requires de-novo formation of cohesion as it is the case in post-replicative mitotic cells (Bentley et al., 2007; Heidinger-Pauli et al., 2009; Strom et al., 2007; Strom et al., 2004; Unal et al., 2004; Unal et al., 2007). But beside these theoretical considerations, what data do exist about cohesion establishment beyond premeiotic S-phase? And are the factors that have been shown to be associated with cohesion formation present in germ cells at all? Indeed, it was demonstrated in *Drosophila* that the subunit Scc2 of the cohesin loader colocalizes with the synaptonemal complex and cohesin on chromosomes during meiotic prophase (Gause et al., 2008). In meiocytes of the flies mutations in Scc2 lead to cohesion defects and proper synaptonemal complex maintenance was impaired. However, the cohesion defect could be attributed to failures in cohesion establishment already during premeiotic S-phase (Gause et al., 2008). Remarkably, Weng and colleagues employed an inducible RNAi strategy that allowed them to leave Scc2 levels constant during meiotic S-phase but initiate knockdown in mid-prophase (Weng et al., 2014). Intriguingly, when Scc2 was depleted after premeiotic S-phase in *Drosophila* oocytes cohesion was lost and meiotic chromosomes mis-segregated. Furthermore, the authors also expressed shRNAs targeting Eco1 and cohesin subunits (namely SMC1, SMC3 and Stag) stage-specifically in mid-prophase. A phenotype similar to Scc2 depletion was observed in all cases suggesting that not only re-loading of cohesin in prophase I is necessary for efficient cohesion but also de-novo synthesis of cohesin subunits. Therefore, the study provided by Weng et al. strongly indicates that a rejuvenation pathway of meiotic cohesion during prophase I exists at

least in some organisms. Also in baker's yeast and in mice the presence of Scc2 on chromosomes in prophase I of meiosis was described (Kuleszewicz et al., 2013; Lin et al., 2011; Visnes et al., 2014). In the future it will be important to perform experiments involving stage-specific Scc2 inactivation during mouse meiosis to reveal its function beyond premeiotic S-phase in mammalian meiosis.

## 3.3. Why is there an obviously non-functional isoform of Smc1β?

Intrigued by the fact that a conserved isoform of Smc1β exists that lacks crucial motifs of the ATPase domain we studied its behavior in mitotic cells and found that Smc1β isoform 2 exclusively localizes to the nucleus in the presence of Rec8-Stag3 (Figure 22). Furthermore, we observed that the nuclear signal of Smc1β isoform 2 is removed by preextraction indicating that it is not stably associated with chromatin (Figure 22). There are mutations in the D-loop and the signature motif of Smc1 described that support viability (Camdere et al., 2015; Elbatsh et al., 2016). However, changes in the amino acids of Smc3's Walker B motif, which usually form an ATPase site together with the D-loop and signature motif of Smc1, are lethal (Arumugam et al., 2003; Hu et al., 2011). This fact clearly demonstrates the significance of this ATPase site for cohesin function. Furthermore, Walker B mutants of Smc1 are incompatible with life of yeast cells (Arumugam et al., 2003; Hu et al., 2011). Since Walker B domain, D-loop and signature motif are completely absent in Smc1β isoform 2, it is hardly surprising that this cohesin subunit is not functional at least in terms of cohesion. One could argue that germ cells express additional loading factors that are able to facilitate the loading of Smc1β isoform 2, but this seems to be unlikely. Therefore, the question arises what the function of this crippled cohesin subunit might be. Smc1β isoform 2 might be involved in processes different than sister chromatid cohesion since Smc1β$^{-/-}$ mice (that lack both isoforms) show a diverse phenotype including failures in synapsis. It is conceivable that there is division of labor between the two isoforms, i.e. isoform 1 is mainly responsible for cohesion whereas isoform 2 may be in charge for correct SC formation or maintenance. It will be interesting to create Smc1β$^{-/-}$ mice expressing one of the two isoforms and observe which phenotypes can be rescued in each case.

A very tempting, yet highly speculative model is that isoform 2 containing cohesin complexes are not loaded on chromatin itself but that in previously loaded cohesin molecules

topologically embracing DNA Smc1α or Smc1β isoform 1 is replaced by isoform 2. The replacement of a cohesin subunit by another seems to be difficult without dissociation from the chromosome but cannot be entirely excluded. The rationale would be to create a cohesin ring that is resistant against Wapl activity due to limitations in ATPase activity (Elbatsh et al., 2016). This could be important already in prophase I where a pool of dynamic and a pool of stably chromatin-associated cohesin might be required. Another possibility is that Wapl resistant cohesin molecules are crucial for cohesion maintenance during the long dictyate arrest in oocytes. In any case, the elucidation of the function of Smc1β isoform 2 will further expand our understanding of cohesin.

## 3.4. Why is mouse Rec8 not functional in human cells?

We showed by IFM that mouse Rec8 behaves very similar to human Rec8 in Hek 293 cells. Murine Rec8 exclusively localizes to the nucleus in the presence of Stag3 and is resistant against preextraction indicating that it is stably associated with DNA and, thus, interacts with the human cohesin subunits. The wild type and the 39A but not the S/T-free variant of mRec8 remain in the nucleus after preextraction (Figure 26). Hence, we infer that S/T-free mRec8 interacts with Stag3 because it is transported into the nucleus but that it is probably not competent to be loaded onto chromatin.

However, we were puzzled by the observation that wild type mRec8, although it behaves exactly like human Rec8 in the immunofluorescence experiments, does not rescue the cohesion defect induced by Sgo1 knockdown (Figure 27). One explanation could be that a preextraction-resistant binding of the cohesin ring with DNA does not necessarily be synonymous with topological entrapment of DNA. We consider this unlikely since recent work by the Uhlmann lab where they reconstituted cohesin loading *in vitro*, shows an intrinsic ability of cohesin to entrap DNA and indicates that association of cohesin with chromatin is invariably of topological nature. We prefer the idea that mRec8 is able to establish cohesion in human cells but that the mechanisms, which protect cohesin from Wapl activity in human cells, are not applicable to the murine kleisin. It might be imaginable that Sororin does not interact with cohesin molecules containing mRec8. We showed that human Rec8 requires Sororin to build robust cohesion. Furthermore, we demonstrated that human Rec8 rescues the cohesion defect originating from Sgo1 depletion only in the presence Sgo2 (Figure 16). In addition,

evidence exists that Sgo1 physically interacts with cohesin (Hara et al., 2014; Liu et al., 2013b). The inability of human Sgo2 to associate with cohesin rings harboring mRec8 would be a straightforward explanation for the absence of the rescuing effect. Interesting experiments would be to transfect mouse Sororin or mouse Sgo2, respectively, in the mRec8-Stag3 cell line and test again whether the cohesion defect caused by Sgo1 depletion is reduced. Assuming that mouse Sororin or mouse Sgo2 induces the rescue effect the next step would be to look for striking differences between human and murine Rec8. This could lead to the identification of the interaction sites of Rec8 and the corresponding regulator protein.

It was shown that Rec8 can be cleaved *in vitro* by Separase only when it is phosphorylated (Kudo et al., 2009). We wanted to reproduce this by isolating Rec8 from mitotically arrested cells and incubating it with active Separase, since we speculated that the high activity of mitotic kinases might transform Rec8 into a suitable substrate for the protease. Indeed, we could observe Rec8 cleavage by Separase *in vitro*. However, unexpected was that non-phosphorylatable mutants of Rec8 were only marginally less efficiently cleaved compared to the wild type protein. A straightforward explanation for this conundrum might be that the observed cleavage of all Rec8 variants is merely basal cleavage triggered by the high concentrations of substrate and protease incubated in the *in vitro* reaction. That would indicate that the correct phosphorylations were not put into place on Rec8 in our system. We do not think that the required kinases are absent in mitotic cells since human Rec8 is not toxic in our cell lines indicating that it can be transformed into a suitable Separase substrate. However, nor can we exclude that the suitable kinases are chromatin-associated and are hardly in contact with soluble Rec8 that we purified in our assay. Therefore, wild type Rec8 would be not or only poorly phosphorylated when isolated from the cell lysate and, thus, merely cleaved as efficiently as the variant that cannot be modified by kinases at all. It will be important to perform an identical cleavage assay but using chromatin bound Rec8 which might be differently modified than the soluble pool. To this end, chromatin has to be isolated from cells co-expressing Stag3 and one of the Rec8 variants. Afterwards the chromatin will be digested with DNAse and the resulting lysate will be subjected to IP of Rec8.

It is also possible that in higher eukaryotes phosphorylation of Rec8 for Separase mediated cleavage is not as crucial as it was proposed in yeast. For example, the protection mechanism of centromeric Rec8 might be mediated by Separase inhibition rather than Rec8 dephosphorylation. As mentioned earlier Sororin probably has the ability to inhibit Separase.

Furthermore, very recent work of our lab strongly suggests an inhibitory effect of Sgo2 on Separase (Susanne Hellmuth, unpublished results). Therefore, it is tempting to speculate that Sgo2's role in meiosis I is not or not exclusively to recruit PP2A but also to directly bind and inhibit Separase. However, work of Kudo et al. clearly shows Rec8 cleavage by Separase is massively enhanced by phosphorylation at least *in vitro*. In that study *in vitro* translated Rec8 was not cleaved at all when it was incubated with Separase in an unmodified state. This is in sharp contrast to our experiments, in which a variant of Rec8 lacking all serine and threonine residues is unequivocally cut although in both cases the murine kleisin was used. We cannot rule out that the S/T-free variant is somehow modified when expressed in cells for example by tyrosine phosphorylation. However, the simplest explanation is a difference in the activity of the Separase preparations that were used.

## 3.5. The role of Cyclin A in terms of sister chromatid cohesion

Intrigued by the observation that Cyclin A is required for SCS in meiosis II of mouse oocytes we asked for the effect induced by overexpression of non-degradable Cyclin A in mitotic cells. Indeed, non-physiological levels of Cyclin A or its presence in late mitosis cause a pronounced cohesion defect as determined by chromosome spreading using cells arrested in prometaphase. Several studies suggested that the cohesion protection mechanism at the centromere is abrogated by Sgo2 relocation when bipolar tension is applied across sister kinetochores in metaphase II (Gomez et al., 2007; Lee et al., 2008). The authors only addressed the localization of Sgo2 by immunostaining and assumed that PP2A would redistribute accordingly since depletion of Sgo2 leads to a complete loss of centromeric PP2A. However, in immunofluorescence experiments conducted by Chambon et al. Sgo2 indeed relocalized upon bipolar tension but the signal of PP2A and centromeric Rec8 remained overlapping (Chambon et al., 2013). This observation suggests that Sgo2 might be only responsible for the initial recruitment of PP2A to the centromere but afterwards the localization of both proteins is independent of each other. Furthermore, Chambon and colleagues showed that SCS in oocytes depends on the PP2A inhibitor I2PP2A, which co-localizes with the PP2A enzyme to centromeres at metaphase II. Interestingly, experiments studying PP2A in a different pathway revealed that phosphorylation of I2PP2A massively increased its ability to inhibit PP2A (Vasudevan et al., 2011). An attractive hypothesis is that Cyclin A is required at the centromere

in meiosis II to boost I2PP2A's inhibition capacity by phosphorylation. However, we were not able to gain evidence for an involvement of I2PP2A in the cohesion defect caused by Cyclin A overexpression in mitotic cells. Neither did I2PP2A overexpression alone cause any premature SCS nor did co-overexpression of I2PP2A and Cyclin A increase the cohesion defect compared to Cyclin A expression alone (data not shown). In addition, we were unable to detect I2PP2A at the centromere of prometaphase cells although non-degradable Cyclin A was expressed (data not shown). Moreover, a siRNA mediated depletion of I2PP2A did not rescue the Cyclin A induced cohesion defect (data not shown). This result, however, is inconclusive since we were not able to verify the knockdown efficiency due to lack of a functional antibody against I2PP2A.

Remarkably, there are even more examples for PP2A inhibitors that are regulated by phosphorylation. For example, it is well established that PP2A-B55 is regulated by the protein Ensa which has to be phosphorylated by the kinase Gwl to become inhibitory (Mochida et al., 2010). Most importantly, a very recent study described a protein, namely Bod1, that is required for the fine tuning of PP2A-B56 activity at the kinetochore. The chromosome alignment defect observed upon Bod1 depletion is not rescued by expression of a Bod1 variant in which a potential Cdk1 phosphorylation site was exchanged to alanine (Porter et al., 2013). These data suggest that inhibition of PP2A may depend on phosphorylation of Bod1 by Cdk1. The sister chromatid cohesion failures caused by Cyclin A overexpression could be attributed to hyperphosphorylation and, thus, increased activity of Bod1. A too tight inhibition of PP2A might render centromeric cohesin susceptible to Wapl activity. It will be very interesting to test the effect of Bod1 depletion or overexpression on the cohesion defect induced by non-physiological levels of Cyclin A.

Nonetheless, it is also possible that Cyclin A-Cdk inhibits PP2A by direct phosphorylation. Very recent data strongly suggest that direct phosphorylation of the phosphatase is involved in its regulation (Grallert et al., 2015). To test this, one could simply monitor the phosphatase activity of PP2A with and without pre-incubation with Cyclin A-Cdk. PP2A can be obtained by purification of the tagged and overexpressed B56 subunit, which will co-precipitate subunits A and C. Cyclin A-Cdk can be isolated as already described in this study and a standard, commercially available malachite green assay can be used to quantify phosphatase activity.

We speculated that Cyclin A might be involved in the regulation of prophase pathway signaling. Therefore, we asked whether Cyclin A-Cdk is able to phosphorylate Sororin.

Intriguingly, Cyclin A-Cdk and Cyclin B-Cdk modified Sororin to a similar extent. An interesting idea is that both Cyclins have to phosphorylate Sororin before it can be displaced from cohesin by Wapl. A straightforward experiment can help to elucidate if Cyclin A-Cdk and Cyclin B-Cdk attach phosphate groups to different residues of Sororin. Sororin has to be incubated with Cyclin B-Cdk in the presence of cold ATP. The pre-phosphorylated Sororin is subsequently incubated with Cyclin A-Cdk in the presence of radioactively labelled ATP and subjected to autoradiography. One sample with addition of new Cyclin B-Cdk serves as control. A signal in the autoradiography after incubation with Cyclin A-Cdk would indicate that Cyclin A-dependent Cdk can phosphorylate sites that cannot be targeted by Cyclin B-Cdk.

Another kinase, which might be interesting in terms of prophase pathway control is Nek2A. Similar to Cyclin A this kinase is degraded in early mitosis in an APC/C-dependent manner (Hames et al., 2001; Hayes et al., 2006). An easy and straightforward experiment is to overexpress a non-degradable variant of Nek2A and test for cohesion defects in metaphase arrested cells. Furthermore, it could be worthwhile to perform *in vitro* kinase assays to test if Sororin is a substrate of Nek2A. A positive result could point to an involvement of Nek2A in cohesin ring opening. An additional thrilling *in vivo* experiment would be to deplete Cyclin A and/or Nek2A in cells and subject the cells to chromosome spreading. An enrichment of mitotic chromosomes without resolved arm cohesion compared to control cells would suggest a defect in prophase pathway signaling upon depletion of the corresponding kinase(s).

For quite some time the biological purpose of the prophase pathway was not clear. However, very recently Rowland and coworkers could show that resolution of arm cohesion in prophase ensures correct decatenation of sister chromatids. When they shut down prophase pathway activity by Wapl depletion they observed failures during chromosome segregation such as lagging chromosomes (Haarhuis et al., 2013). Since it is important for genome integrity a comprehensive understanding of prophase pathway signaling is of great interest. In this work we provide hints that Cyclin A might be involved in the control of this vital cellular process and, hence, has the potential to shape future prophase pathway research.

# 4. Material and Methods

## 4.1. Materials

Unless otherwise mentioned, chemicals (analytical pure) and reagents were obtained from GE Healthcare, Applied Biosystems, Biomol, Bio-Rad, Difco, Fluka, Invitrogen, Stratagene, Merck, New England Bioloabs, Promega, Roth, Roche, Serva, or Sigma.

### 4.1.1. Hardware and Software

This thesis was written on a Fujitsu Desktop PC operating on “Windows 7 Professional” using the software “Microsoft Word 2016” and “EndNote X7”. “Microsoft Excel 2011” was used for the preparation of diagrams. Chemiluminescence signals of Western blots as well as Coomassie stained gels were digitized using a "LAS-4000" or a "LAS-3000" system (FUJIFILM Europe), respectively. Signals from radioactively labeled proteins were analyzed using the "FLA-7000" system (FUJIFILM Europe).
IFM was performed using a Zeiss Axioplan 2 fluorescence microscope with a Plan-Apochromat 100x/1.40 Oil DIC objective, an AxioCam MRm CCD camera and AxioVision software version 4.8.2.0.
Image processing was performed with "Adobe Photoshop CS6" and figures were prepared using "Adobe Ilustrator CS6". For Literature and database searches online services provided by the "National Center for Biotechnology Information" (http://www.ncbi.nlm.nih.gov/) were used. Sequence alignments were performed using “Clustal Omega” from the “European Bioinformatics Institute” (http://www.ebi.ac.uk/Tools/msa/clustalo/).
Centrifuges were purchased from Beckman Coulter and Eppendorf. Cell culture clean benches were purchased from Kojair and incubators from New Brunswick. Precision pipettes were provided by Eppendorf and Gilson.

### 4.1.2. Antibodies

**Primary antibodies**

| target protein | species and clonality | dilution/concentration | origin |
|---|---|---|---|
| Wapl | mouse, monoclonal | Western blot: 2 µg/ml | self-made, clone D9, raised against bacterially expressed N-terminal 88 aa of human Wapl, affinity purified |
| α-Tubulin | mouse, monoclonal | Western blot: hybridoma supernatant 1:200 | self-made hybridoma |

| | | | |
|---|---|---|---|
| | | | supernatant, hybridoma cells (clone 12G10) derived from Developmental Studies Hybridoma Bank |
| Sgo1 | rabbit, polyclonal | Western blot: 1:300 | Abcam, ab21633 |
| Sgo2 | rabbit, polyclonal | Western blot: 1:1000 | Bethyl Laboratories, A301-261A |
| GFP | mouse, monoclonal | Western blot: 4 µg/ml | self-made, hybridoma cells kindly provided by Simona Saccani, affinity purified |
| GFP | rabbit, polyclonal | IFM: 1:3000 | kindly provided by Stefan Heidmann, raised against bacterially expressed full length GFP (IS31), affinity purified |
| Scc1 | mouse, monoclonal | Western blot: 1:1000 | Millipore, 05-908 |
| Flag | mouse, monoclonal | IFM: 1:250 | Sigma-Aldrich, F3165 |
| Flag | rabbit, polyclonal | Western blot: 1:1000 | Sigma-Aldrich, F7425 |
| Myc | mouse, monoclonal | Western blot: 0.2 µg/ml | self-made, hybridoma cells (clone 9E10) derived from Developmental Studies Hybridoma Bank, affinity purified |
| Myc | mouse, monoclonal | IFM: 1:1500 | Millipore, 05-724 |
| Smc1 | rabbit, polyclonal | Western blot: 1:4000 | Bethyl Laboratories, A300-055A |
| Smc3 | rabbit, polyclonal | Western blot: 1 µg/ml | kindly provided by Susannah Rankin, affinity purified |
| Stag1 | rabbit, polyclonal | Western blot: 3.5 µg/ml | kindly provided by Susannah Rankin, affinity purified |
| Stag2 | rabbit, polyclonal | Western blot: 3.3 µg/ml | kindly provided by Jan-Michael Peters, affinity purified |
| CREST | Human, polyclonal | IFM: 1:1000 | Immunovision, hct-0100 |
| Hec1 | mouse, monoclonal | IFM: 1:500 | Genetex, 70268 |

**Secondary antibodies**

| name | use | dilution | origin |
|---|---|---|---|
| HRP-conjugated goat anti-mouse IgG | Western blot | 1:15000 | Sigma, A9917 |
| HRP-conjugated goat anti-rabbit IgG | Western blot | 1:15000 | Sigma, A0545 |
| AlexaFluor488 goat anti-rabbit IgG | IFM | 1:500 | Invitrogen, A-11008 |
| Cy3 goat anti-mouse IgG | IFM | 1:500 | Invitrogen, A-10521 |
| Cy5 goat anti-human IgG | IFM | 1:500 | Bethyl Laboratories, A80-219C5 |

For precipitation of Flag-tagged proteins, the cell lysates were incubated with Anti-Flag M2 Affinity Gel (Sigma, A2220). For targeting proteins fused to GFP single chain camel GFP antibodies (Rothbauer et al., 2008) were covalently couplet to NHS-activated sepharose (GE Healthcare)

### 4.1.3. siRNAs

The following table provides information for small interfering RNAs used in this study to deplete proteins in mammalian cells via RNA interference (Elbashir et al., 2001). All siRNAs are 21mers consisting of 19 target specific nucleotides with an additional 5'dTdT-overhang (the overhang is omitted in the table). The denoted concentration refers to the concentration of the siRNA in the cell culture medium. For the depletion of Scc1 and Wapl both siRNAs were transfected.

| name | target mRNA | sequence (5'-3') | conc. in nM | reference |
|---|---|---|---|---|
| GL2 | luciferase | CGUACGCGGAAUACUUCGA | variable | (Elbashir et al., 2001) |
| LM_Sgo1 | Sgo1 | GAUGACAGCUCCAGAAAUU | 50 | PhD thesis Lisa Mohr |
| Sgo2_Yen2 | Sgo2 | GAUGACAGCUCCAGAAAUU | 100 | (Huang et al., 2007) |
| hScc1_3'UTR1 | Scc1 | ACUCAGACUUCAGUGUAUA | 50 | (Schockel et al., 2011) |
| hScc1_3'UTR2 | Scc1 | AGGACAGACUGAUGGGAAA | 50 | (Schockel et al., 2011) |
| siWapl_1 | Wapl | CGGACUACCCUUAGCACAA | 70 | (Kueng et al., 2006) |

| | | | | |
|---|---|---|---|---|
| siWapl_2 | Wapl | GGUUAAGUGUUCCUCUUAU | 70 | (Kueng et al., 2006) |
| siSororin | Sororin | GCCUAGGUGUCCUUGAGCU | 120 | (Schmitz et al., 2007) |

### 4.1.4. *E. coli* strains

XL-1 blue (used for cloning and plasmid production):
*E. coli recA1 endA1 gyrA96 thi-1 hsdR17 supE44 relA1 lac* [F*' proAB lacI*$^{q}$*ZΔM15* Tn*10* (Tet$^{r}$)]

Rosetta 2 DE3 (used for Protein expression):
*E. coli* F$^{-}$ *omp*T *hsdS*$_{B}$*(*$r_{B}^{-}$ $m_{B}^{-}$*) gal dcm* (DE3) pRARE (Cam$^{R}$)

### 4.1.5. Mammalian cell lines

HEK 293T: human embryonic kidney cells, which were transformed with a fraction of the adenovirus 5 genom and contain in addition the SV40 large T antigen.

HEK 293 FlpIn: human embryonic kidney cells, which were transformed with a fraction of the adenovirus 5 genome and contain a genomically inserted FRT recombination site, which allows FLP recombinase-mediated transgene insertion (Life technologies). In addition, the cells obligatory express the tetracycline repressor, which binds to the tetracycline operator sequence. Upon binding to tetracycline the repressor leaves DNA and the corresponding gene is expressed.

HeLa: human cervical carcinoma cell line derived from Henrietta Lacks

### 4.1.6. Plasmids

Except for the murine Rec8 variants and the recombinases all genes were the human homologs.

| name | insert | tag(s) | backbone | origin |
|---|---|---|---|---|
| pSC1986 | Rec8 | GFP-C | pcDNAL-FRT-TO | Cornelia Schuster |
| pLG2776 | Scc1 | GFP-C | pcDNAL-FRT-TO | Laura Schöckel |
| pJBI3258 | Stag2 | N-Flag$_3$-Tev$_2$ | pcDNA5-loxP-TO | Julia Bittner |
| pJBI3227 | Stag2 | N-Flag$_3$-Tev$_2$ | pCS2 | Julia Bittner |
| pJBI3259 | Stag3 | N-Flag$_3$-Tev$_2$ | pcDNA5-loxP-TO | Julia Bittner |
| pJBI3182 | Stag3 | N-Flag$_3$-Tev$_2$ | pCS2 | Julia Bittner |

| | | | | |
|---|---|---|---|---|
| pPW3473 | Stag3 | N-$Flag_3$-$Tev_2$ | pcDNAL-FRT-TO | this study |
| pPW3397 | Separase P1127A | N-$Myc_6$-$Tev_2$ | pCS2 | this study |
| pFL3463 | Separase P1127A | N-GFP-$Tev_4$ | pCS2 | Franziska Langhammer |
| pPW3502 | Separase P1127A | N-GFP-$Tev_4$ | pCS2 | this study |
| pSX100 | Securin | - | pCS2 | Hui Zou |
| pMO636 | Sgo1 | N-$Myc_6$ | pCS2 | Michael Orth |
| pMO1172 | Sgo2 | N-$Myc_6$ | pCS2 | Michael Orth |
| pPW3645 | Meikin | N-$Myc_6$-$Tev_2$ | pCS2 | this study |
| pJBI3232 | Smc1α | N-$Myc_6$-$Tev_2$ | pCS2 | Julia Bittner |
| pPW3564 | Smc1α | N-$Myc_6$ | pcDNA3.1-attB-TO | this study |
| pPW3558 | Smc1β iso1 | N-$Myc_6$-$Tev_2$ | pCS2 | this study |
| pPW3560 | Smc1β iso1 | N-$Myc_6$ | pcDNA3.1-attB-TO | this study |
| pJBI3181 | Smc1β iso2 | N-$Myc_6$-$Tev_2$ | pCS2 | Julia Bittner |
| pPW3399 | Smc1β iso2 | N-$Myc_6$ | pcDNA3.1-attB-TO | this study |
| pPW3500 | mRec8 wt | GFP-C | pCS2 | this study |
| pPW3530 | mRec8 wt | GFP-C | pcDNA5-loxP-TO | this study |
| pPW3501 | mRec8 39A | GFP-C | pCS2 | this study |
| pPW3541 | mRec8 39A | GFP-C | pcDNA5-loxP-TO | this study |
| pPW3538 | mRec8 S/T-free | GFP-C | pCS2 | this study |
| pPW3559 | mRec8 S/T-free | GFP-C | pcDNA5-loxP-TO | this study |
| pPW3048 | Δ86-Cyclin A2 | N-$Flag_3$-$Tev_2$ | pCS2 | this study |
| pPW3068 | Δ86-Cyclin A2 | N-GFP | pcDNA5-FRT-TO | this study |
| pPW3047 | Δ90-Cyclin B1 | N-$Flag_3$-$Tev_2$ | pCS2 | this study |
| pPW3065 | Δ90-Cyclin B1 | N-GFP | pcDNA5-FRT-TO | this study |
| pPW3481 | Sororin | N-$His_6$-SUMO3 | pET28M | this study |
| pAG1786 | FLP-recombinase | - | pCS2 | Amelie Gutsmiedel |
| pIC-Cre | Cre recombinase | - | pMC1 | (Gu et al., 1993) |
| ϕC31 | ϕC31 integrase | - | pCMV-Int | Michele P. Calos |

### 4.1.7. Stable cell lines

All stable transgenic cell lines used in this study were based on Hek 293 FlpIn cells. The following table shows which plasmid(s) were used for the corresponding cell line. All cell lines can unambiguously be identified via the plasmid numbers. For the exact description of the tags see the plasmid table 4.1.6.

| transgenes integrated in the genome | integrated plasmid |
|---|---|
| Scc1-GFP | pLG2776 |
| Rec8-GFP | pSC1986 |
| Rec8-GFP + Flag-Stag2 | pSC1986 + pJBI3258 |
| Rec8-GFP + Flag-Stag3 | pSC1986 + pJBI3259 |
| Rec8-GFP + Flag-Stag3 + Myc-Smc1α | pSC1986 + pJBI3259 + pPW3564 |
| Rec8-GFP + Flag-Stag3 + Myc-Smc1β iso1 | pSC1986 + pJBI3259 + pPW3560 |
| Rec8-GFP + Flag-Stag3 + Myc-Smc1β iso2 | pSC1986 + pJBI3259 + pPW3399 |
| Flag-Stag3 | pPW3473 |
| Flag-Stag3 + mRec8 wt | pPW3473 + pPW3530 |
| Flag-Stag3 + mRec8 39A | pPW3473 + pPW3541 |
| Flag-Stag3 + mRec8 S/T-free | pPW3473 + pPW3559 |
| GFP-Δ90-Cyclin B | pPW3065 |
| GFP-Δ86-Cyclin A | pPW3068 |

## 4.2. Microbiological techniques

### 4.2.1. Cultivation and storage of *E. coli*

| | |
|---|---|
| LB-medium | 1 % tryptone (w/v)<br>0.5 % yeast extract (w/v)<br>1 % NaCl (w/v) |
| LB-plates | LB-medium with 1.5 % Agar (w/v) |

Growth media were sterilized by autoclaving. *E. coli* strains were grown in LB medium by shaking at 150 rpm at 37°C. Solid cultures were grown on agar plates at 37°C. For selection of transformed bacteria ampicillin (50 µg/ml) was added to the media.

### 4.2.2. Preparation of chemically competent *E. coli*

| | |
|---|---|
| Tbf1 buffer | 30 mM KAc<br>50 mM $MnCl_2$<br>100 mM KCl<br>15 % glycerol (v/v)<br>pH adjusted to 5.8 |

| | |
|---|---|
| Tbf2 buffer | 10 mM MOPS-NaOH<br>75 mM $CaCl_2$<br>10 mM KCl<br>15% glycerol (v/v)<br>pH adjusted to 7.0 |

For preparation of chemically competent bacteria 300 ml LB-medium was inoculated with an overnight culture to an $OD_{600}$ of 0.1 and grown at 37°C to an $OD_{600}$ of 0.5. The culture was cooled down on ice for 15 min and harvested by centrifugation (4°C, 3,000 g, 15 min). All following steps were performed with precooled sterile materials and solutions at 4°C. The bacteria were carefully resuspended in 90 ml Tbf1 buffer and incubated on ice for 15 min. After a second centrifugation (4°C, 1500 g, 15 min), bacteria were resuspended in 15 ml Tbf2 buffer and chilled on ice for 5 min. Finally, the suspension of bacteria was aliquoted, snap-frozen and stored at -80°C.

### 4.2.3. Transformation of chemically competent *E. coli*

Chemically competent bacteria were thawed on ice. 20 to 50 µl of competent bacteria were mixed with 1 µl of plasmid DNA or 20 µl ligation reaction and incubated on ice for 15 min. A heat shock at 42°C was performed for 45 s. Transformed cells were selected by streaking out the bacteria suspension on LB agar plates containing ampicillin and incubated overnight at 37°C.

### 4.2.4. Expression of proteins in *E. coli*

For the production of recombinant proteins, the *E. coli* strain Rosetta 2 DE3 was used. LB medium was inoculated with an overnight culture to an $OD_{600}$ of 0.15. The culture was grown at 37°C and expression of the protein was induced by addition of IPTG (0.5 mM final concentration) at an $OD_{600}$ of 0.5 - 0.7. After shaking for 3 h at 37°C, cells were harvested by centrifugation (4°C, 5000 g, 15 min). Pellets were either processed directly or stored at -80°C after snap-freezing.

## 4.3. Molecular biological methods

### 4.3.1. Isolation of plasmid DNA from *E. coli*

Plasmid DNA was isolated using the commercially available kit from Thermo Scientific (GeneJET Plasmid Miniprep Kit) according to the manufacturer's instructions. Usually 2 ml of an overnight culture was used for the preparation. Larger amounts of plasmid DNA were isolated out of 50-100 ml of overnight culture using a kit from Quiagen (Plasmid Plus Midi Kit).

### 4.3.2. Restriction digestion of DNA

For sequence specific cleavage of vector DNA and linear PCR products, restriction enzymes (New England Biolabs) were employed according to the manufacturer's instructions. The PCR product or 1 µg of vector DNA was digested in a 50 µl reaction mix for 1 h at 37°C. The reactions were purified by agarose gel electrophoresis or by a commercially available kit from Thermo Scientific (GeneJET PCR Purification Kit)

### 4.3.3. Separation of DNA fragments by agarose gel electrophoresis

| | |
|---|---|
| TBE buffer | 90 mM Tris<br>90 mM boric acid<br>2 mM EDTA, pH 8.0 |
| TPE buffer | 90 mM Tris<br>90 mM phosphoric acid<br>2 mM EDTA, pH 8.0 |
| DNA loading buffer 6x | 0.5 % SDS (w/v)<br>0.25 % bromophenol blue (w/v)<br>25 % glycerol (v/v)<br>25 mM EDTA, pH 8.0 |

For analytical and preparative isolation DNA, fragments were separated on 0.8-2 % agarose gels containing ethidium bromide (final concentration 0.5 µg/ml). DNA samples were mixed with 6x DNA loading buffer and electrophoretically separated at 115 volts in TBE or TPE buffer. DNA fragments could be visualized by UV light (324nm) due to intercalation of ethidium bromide into DNA.

### 4.3.4. DNA extraction from agarose gels

After gel electrophoresis DNA fragments were isolated by excising the respective piece of agarose using a scalpel. Next, DNA purification from the cut agarose block was performed using the commercially available kit from Thermo Scientific (GeneJET Gel Extraction Kit) according to the manufacturer`s instructions.

### 4.3.5. Dephosphorylation of DNA fragments

In order to avoid recircularization of linearized vectors, the ends of vector DNA were dephosphorylated by incubation with 5 U/µg Antarctic phosphatase (NEB) at 37°C for 30 min. The dephosphorylation reaction was performed in a final concentration of 1x Antarctic phosphatase buffer. The phosphatase was heat inactivated at 75°C for 5 min.

### 4.3.6. Ligation of DNA fragments

| | |
|---|---|
| 10x T4 DNA ligase buffer | 500 mM Tris-HCl |
| | 100 mM $MgCl_2$ |
| | 10 mM ATP |
| | 100 mM DTT |

For ligation, a molecular ratio of 1:3 to 1:10 of linearized vector to digested insert was used. In total, the 20 µl ligation reaction sample contained 50-100 ng of vector DNA, 1 µl T4 DNA ligase (selfmade) and 1x T4 DNA ligase buffer. The ligation reaction was performed at 14°C overnight. After ligation, the complete reaction mix was transformed into *E. coli* as described above.

### 4.3.7. DNA sequencing

0.5-1 µg plasmid DNA was supplemented with 20 pmol of a suitable sequencing primer. Sequencing services were provided from Microsynth/Seqlab (Göttingen, Germany). The software “DNASTAR Lasergene” was used for analysis of the sequencing results.

### 4.3.8. Polymerase chain reaction (PCR)

PCR reactions were performed in a total volume of 50 µl, containing 10-100 ng of template plasmid DNA or 50 to 250 ng of genomic DNA, 1 µM of forward and reverse primer, 0.5 mM of all four deoxynucleotids, 1x Phusion HF buffer, and 0.5 to 1 unit of Phusion High-Fidelity DNA polymerase (Thermo scientific). The PCR-program was adjusted to primer melting temperature and target sequence length according to the instructions of the polymerase manufacturer. A thermocycler "TC-512" (Techne) was used for the reaction.

## 4.4. Protein biochemical methods

### 4.4.1. SDS-polyacrylamide gel electrophoresis (SDS-PAGE)

| | |
|---|---|
| 17 % resolving gel | 14 ml 1 M Tris-HCl, pH 8.8 |
| (37.5 ml) | 21.3 ml 30 % acrylamide/bisacrylamide (37.5:1) |
| | 2 ml 2.5 M sucrose |
| | 20 µl 20 % SDS (w/v) |
| | 160 µl 10 % ammonium persulfate (w/v) |
| | 11 µl TEMED |
| 8 % resolving gel | 13.1 ml 1 M Tris-HCl, pH 8.8 |
| (35 ml) | 9.3 ml 30 % acrylamide/bisacrylamide (37.5:1) |
| | 12.4 ml $ddH_2O$ |
| | 20 µl 20 % SDS (w/v) |
| | 160 µl 10 % ammonium persulfate (w/v) |
| | 11 µl TEMED |
| 7 % stacking gel | 4.1 ml 1 M Tris-HCl, pH 6.8 |
| (32.5 ml) | 7.6 ml 30 % acrylamide/bisacrylamide (37.5:1) |
| | 20.6 ml $ddH_2O$ |
| | 20 µl 20 % SDS (w/v) |
| | 160 µl 10 % ammonium persulfate (w/v) |
| | 11 µl TEMED |
| 1x Laemmli running buffer | 25 mM Tris |
| | 192 mM glycine |
| | 0.1 % SDS (w/v) |

| | |
|---|---|
| 4x SDS sample buffer | 40 % glycerol<br>250 mM Tris-HCl, pH 6.8<br>8 % SDS (w/v)<br>0.04 % bromphenol blue (w/v)<br>7 % β-mercaptoethanol |

The 8-17 % gradient gels were poured with an “SG100” System (Hoefer Inc.). The gels were run in a “Mighty Small II for 8x7cm gels” chamber containing 1x Laemmli running buffer at 130 V (30 mA/gel). Samples were mixed with 1x SDS sample buffer and denatured at 95°C for 5 to 10 min prior to loading. As a molecular weight standard the PageRuler Prestained Protein Ladder (Thermo Scientific) was used.

### 4.4.2. Immunoblotting (Western blot)

| | |
|---|---|
| Transfer buffer | 25 mM Tris<br>192 mM glycine<br>20 % methanol |
| Wash buffer | 1x PBS<br>0.05 % Tween |

Proteins separated by SDS-PAGE were transferred to a polyvinylidene fluorid (PVDF) membrane (Serva) using a semi-dry blot system (BioRAD). The blotting was performed at 13 V and 120 mA/gel for 1.5 h. The PVDF membrane with immobilized proteins was blocked with 5 % milk powder in wash buffer for 30 min and incubated overnight at 4°C or 3 hours at RT with primary antibodies diluted in blocking solution. Afterwards, the membrane was washed 3 times for 8 min with wash buffer and incubated for 40 min at RT with secondary antibodies coupled to horseradish peroxidase diluted 1:15000 in blocking solution. Subsequently, the membrane was washed again 3 times for 8 min with wash buffer. The detection of the protein of interest was carried out using the chemiluminiscence detection kits "HRP Juice" (PJK) or "ECL Ultra" (Lumigen) according to the instructions of the manufacturer.

### 4.4.3. Coomassie staining

For the Colloidal Coomassie suspension 80 g $(NH_4)_2SO_4$ were dissolved in 760 ml $ddH_2O$. Then 18.8 ml 85 % phosphoric acid were added. Before the 800 mg Coomassie Brilliant Blue G-250 were added to the solution they were dissolved in 16 ml $ddH_2O$. For Coomassie staining, gels were incubated overnight in freshly mixed 80 % (v/v) Coomassie suspension with 20 % (v/v)

Methanol following SDS-PAGE. Before documentation the gels were repeatedly washed with deionized water.

### 4.4.4. $Ni^{2+}$-NTA affinity purification of $His_6$-SUMO3-Sororin

| | |
|---|---|
| Lysis buffer | 1x PBS<br>400 mM NaCl<br>5 mM imidazole<br>5 mM β-mercaptoethanol |
| Wash buffer | 1x PBS<br>400 mM NaCl<br>20 mM imidazole<br>5 mM β-mercaptoethanol |
| Elution buffer | 1x PBS<br>400 mM NaCl<br>200 mM imidazole<br>5 mM β-mercaptoethanol |
| Dialysis buffer: | 30 mM Tris pH 7.7<br>200 mM NaCl<br>5 % glycerol (v/v)<br>5 mM imidazole<br>5 mM β-mercaptoethanol |

Bacteria obtained from 1 l of *E. coli* culture were resuspended in 30 ml of ice cold Lysis Buffer. Cells were lysed using a high pressure homogenizer (Avestin) by cycling the cell suspension for 8 min. The lysate was cleared from debris by centrifugation at 13000 g and 4°C for 30 min. The lysate was incubated with 400 µl of equilibrated $Ni^{2+}$-NTA resin (Machery-Nagel) for 3 h at 4°C with gentle shaking. The beads were washed with 1.5 ml lysis buffer and 5 ml wash buffer. Subsequently, the protein was eluted with 0.7 ml elution buffer. In order to remove precipitated protein the eluate was centrifuged at 16000 g and 4°C for 10 min. After addition of Senp2 (SUMO protease) the Protein solution was dialyzed two times against 500 ml of dialysis buffer using a membrane with 3.5 kDa cut-off. To remove the $His_6$-SUMO3-Tag and the $His_6$-tagged Senp2 the dialyzed eluate was again incubated with 400 µl of equilibrated $Ni^{2+}$-NTA resin and the flow-through which is the purified protein was aliquoted, snap-frozen using liquid nitrogen and stored at -80 °C.

### 4.4.5. Immunoprecipitation

| | |
|---|---|
| LP2 buffer | 20 mM Tris-HCl, pH 7.6<br>100 mM NaCl<br>10 mM NaF<br>20 mM β-glycerophosphate<br>5 mM $MgCl_2$<br>0.1% Triton X-100 (v/v)<br>5 % glycerol (v/v)<br>1x protease inhibitor cocktail (Roche Diagnostics) |
| Cyclin storage buffer: | 50 mM Tris HCl pH 8.0<br>100 NaCl<br>20 % glycerol (v/v)<br>0.1 mM EDTA<br>2 mM DTT (added just before snap freeze) |

Usually, the nocodazole arrested cells were harvested by flushing from the culture dish with medium and pelleted at 300 g for 3 min at RT. The pellet was resuspended in LP2 buffer and transferred to a dounce homogenizer (Wheaton). After 15 strokes with the pestle the lysate was incubated on ice for 5-10 min and cleared from cell debris by centrifugation (16100 g, 30 min, 4°C). The corresponding beads were washed twice with an adequate volume of LP2 and then incubated with the lysate for 3 h at 4°C. All centrifugation steps involving beads were performed at 200 g and 4 °C. After incubation with the lysate the beads were washed three times with an adequate volume of LP2. Subsequently, the beads were mixed with 1x SDS-sample buffer (without β-mercaptoethanol) and boiled for 5 min. The eluate was separated from the beads via Mobicol microcolumns (Mobitec) and β-mercaptoethanol was added.
When Cyclin B and Cyclin A were purified a fourth wash step with Cyclin storage buffer was added. Then the cyclins were eluted with Tev protease and the eluate was separated from beads via Mobicol microcolumns. The eluate was aliquoted and snap-frozen.
For the cleavage assay with mouse Rec8 variants two additional wash steps with Tev cleavage buffer (see 4.4.7) were included. After the last wash step almost all buffer was removed from the beads and the Separase preparation was added. After 30 min at 30°C the reaction was stopped by addition of SDS-sample buffer and boiling. The samples were subjected to SDS-PAGE and Western blot.

### 4.4.6. *In vitro* kinase assay

| | |
|---|---|
| 10 x kinase buffer: | 250 mM HEPES/KOH pH 7.2 |
| | 20 mM NaF |
| | 200 mM β-glycerolphosphat |
| | 20 mM DTT |
| | 100 mM $MgCl_2$ |
| | 40 mM EGTA |

The purified Cyclin B and Cyclin A were incubated in a total volume of 30 µl with 1x kinase buffer, 1 µCi [γ-$^{33}$P]-ATP, 50 µM ATP and 1 µg of the substrate (commercially available Histone H1 or selfmade Sororin). When indicated 2 µM RO3306 or the corresponding volume of the solvent DMSO was added to the reaction mix. After 10 min at 30°C the reaction was stopped by addition of SDS-sample buffer. The samples were subjected to SDS-PAGE followed by fixation of the gel in 40 % (v/v) methanol/10 % (v/v) acetic acid for 30 min. In the following the gel was washed with $ddH_2O$ for 10 min, placed on a wet sheet of Whatman paper and dried for 1 h at 80 °C on a "Model 483" vacuum drier (BioRAD). The dried gel was covered with an imaging plate (FUJIFILM Europe). After overnight exposure, the imaging plate was analyzed.

### 4.4.7. Purification of active human Separase

| | |
|---|---|
| Tev cleavage buffer: | 10 mM HEPES/KOH 7.7 |
| | 20 % glycerol (v/v) |
| | 50 mM NaCl |
| | 25 mM NaF |
| | 1 mM EGTA |
| | 2 mM DTT (added just before snap freeze) |

GFP-$Tev_2$-tagged Separase carrying the amino acid change P1127A was co-overexpressed with Securin in Hek 293T cells. The IP was performed as described in 4.4.5 using GFP nanobodies coupled to sepharose. After 3 h at 4°C the beads were washed once with LP2 buffer and once with CSF-XB buffer (Murray, 1991). During the incubation of beads and cell lysate a *Xenopus laevis* egg extract was prepared as described (Murray, 1991). The CSF-extract was supplemented with 57 nM recombinant human Δ90-Cyclin B and released into anaphase by calcium addition. Non-degradable Cyclin B keeps the extract in an anaphase-like state with APC/C activity. The beads were incubated in tenfold volume of anaphase extract for 20 min at RT to degrade Securin and to gain active Separase. After the extract was diluted with CSF-XB buffer the beads were re-isolated and were washed once with CSF-XB buffer and once with Tev cleavage buffer. Then Separase were eluted with Tev protease and the eluate was

separated from beads via Mobicol microcolumns. The eluate was aliquoted, snap-frozen and stored at -80°C. The exactly same procedure was performed with a Separase variant carrying the amino acid change P1127A (Hellmuth et al., 2015) and C2029S (Stemmann et al., 2001). This protein lacks protease activity and serves as a negative control.

## 4.5. Cell biological methods

### 4.5.1. Cultivation of mammalian cells

Adherent mammalian cells were grown in cell culture dishes (Greiner Bio-One) using Dulbecco's Modified Eagle Medium (DMEM; Biowest) supplemented with 10 % (v/v) heat inactivated (56°C, 30 min) fetal calf serum (Biowest, Sigma-Aldrich). The dishes were kept at 37°C in a 5 % CO2 atmosphere and split in a ratio of 1:4 to 1:20 twice a week. The medium was removed and cells were washed once with 1x PBS before they were incubated with pre-warmed trypsin-EDTA (Sigma-Aldrich) for 5 min at 37°C. Trypsinized cells were resuspended in fresh, prewarmed medium, washed from the dish's surface and transferred to a 50 ml falcon tube (Greiner Bio-One, Sarstedt). The cell suspension was subsequently centrifuged at 300 g for 2-3 min at RT and the cell pellet was resuspended in fresh pre-warmed medium and seeded onto new cell culture dishes.

### 4.5.2. Storage of mammalian cells

Cells were harvested as described in 4.5.1. After centrifugation the cells were resuspended in fetal calf serum supplemented with 10 % DMSO and aliquoted in cryovials (Nalgene) which were placed in isopropanol filled freezing containers providing -1°C/min cooling. The freezing containers were placed at -80°C and after 2-3 days cryostocks were transferred into a liquid nitrogen tank for long term storage.
For use, cryostocks were thawed rapidly in a 37°C water bath and pelleted at 300 g for 2 min. The cell pellet was resuspended in fresh pre-warmed medium and seeded onto a new cell culture dish.

### 4.5.3. Transfection of Hek 293 cells

| | |
|---|---|
| 2× HBS (500 ml): | 8 g NaCl |
| | 0.37 g KCl |
| | 106.5 mg $Na_2HPO_4$ |
| | 1 g glucose |
| | 5 g HEPES |
| | pH 7.05 adjusted with NaOH; sterile-filtered |

Cells were transfected at 30-70% confluency with the calcium phosphate method. Shortly before transfection, chloroquine was added to the medium to a final concentration of 25 µM. The transfection mix was prepared as described in the following table.

| **diameter of dish** | **5.3 cm** | **10 cm** | **14.5 cm** |
|---|---|---|---|
| **volume of medium** (in dish) | 3.5 ml | 9 ml | 23 ml |
| | | | |
| **amount of DNA** | 4 µg | 16 µg | 30 µg |
| **dd$H_2O$** (add to) | 300 µl | 800 µl | 2000 µl |
| **2 M $CaCl_2$** | 37.2 µl | 99.2 µl | 248 µl |
| **2x HBS** | 300µl | 800 µl | 2000 µl |

DNA was combined with the corresponding amount of water and then $CaCl_2$ was added. The HBS was then slowly dropped into the solution while vortexing. The transfection mix was carefully dripped onto the surface of the medium within 10 minutes after preparation. 6-12 h after addition of the transfection mix the cell culture medium was changed. siRNAs were transfected into Hek 293T and Hek 293 Flp-In cells accordingly.

### 4.5.4. Transfection of HeLa cells

For the transfection of HeLa cells Lipofectamine 2000 (Invitrogen) was used. For a 5 cm dish containing 3.5 ml medium DNA-Lipofectamine 2000 complexes were prepared by individually diluting 4 µg of plasmid DNA in 250 µl Opti-MEM medium and 8 µl Lipofectamine 2000 in 250 µl Opti-MEM medium. After incubation for 5 min at RT both dilutions were combined and incubated for 20 min at RT before the transfection mix was added to the cells. After 6-8 hours growth medium was replaced.

### 4.5.5. Generation of stable mammalian cell lines

Hek 293 FlpIn cells were grown on a jumbo dish. At 60% confluency, they were co-transfected with 3 µg of a plasmid containing the gene of interest (under control of a tetracyclin operator), a hygromycin resistance cassette and an FRT-site (which allows recombination into the FLP site of the host genome), and 30 µg of a plasmid encoding Flp recombinase (pAG1786). 48 h after transfection, hygromycin B (Roth) was added (90 µg/ml endconcentration) to select for clones with stable integration of the plasmid. For 1 to 2 weeks the medium was changed when required due to dying cells. When single colonies were visible they were trypsinized using small glass cylinders and transferred into single wells of a 24-well cell culture dish. The clones were expanded under selection until they were tested for expression of the transgene.
The insertion plasmids used for stable genomic integration via FLP recombinase also contained a loxP recombination site, allowing a second round of genomic insertion utilizing Cre recombinase. A stable cell line growing on a jumbo dish was co-transfected with 3 µg of an insertion plasmid encoding a second gene of interest (under control of a tetracycline operator sequence), a G418 resistance cassette and a loxP-site and 30 µg of a plasmid encoding the Cre recombinase (pIC-Cre). Selection and cloning were performed using medium containing 120 µg/ml G418 (Gibco).
For the integration of a third transgene in the genome of Hek 293 cells we used plasmids containing an attB site that permits the ϕC31 integrase-mediated integration at pseudo-attP sites in the human genome and a puromycin resistance cassette. The generation of triple transgenic cell lines was similar to the procedure described above. For selection a puromycin (Santa Cruz) concentration of 0.8 µg/ml was used.

### 4.5.6. Immunofluorescence staining and microscopy

Cells were grown on poly-L-lysine-coated coverslips and washed once with PBS. When indicated the cells were pre-extracted with 0.2 % (v/v) Triton X-100 in PBS prior to fixation with 3.7 % (w/v) paraformaldehyde in PBS for 10 minutes. Afterwards cells were treated with 100 mM glycine in PBS to quench residual fixative followed by a PBS wash. Cells were permeabilized by incubation in 0.5 % (v/v) Triton X-100 in PBS for 5 minutes. After washing once with PBS samples were incubated in 1 % (w/v) BSA in PBS overnight at 4°C. Coverslips were transferred onto Parafilm, placed in a wet chamber and incubated at RT with the corresponding primary antibody diluted in 1 % (w/v) BSA in PBS. After 4 washes with 0.1 % (v/v) Triton X-100 in PBS (WS) coverslips were incubated with a dilution of fluorescently labeled secondary antibodies for 40 minutes. The samples were washed once with WS, once with 1 µg/ml Hoechst 33342 in WS and again 4 times with WS. Finally, the coverslips were mounted onto glass slides in mounting medium (2.33 % (w/v) diazabicyclo-[2,2,2]-octane, 20 mM Tris/HCl, pH 8.0, in 78 % (v/v) glycerol) and imaged.

### 4.5.7. Chromosome spreads

| | |
|---|---|
| Hypotonic medium | 40 % serum-free DMEM (v/v)<br>60 % dd$H_2O$ (v/v)<br>200 ng/ml nocodazole |
| Carnoy's solution | 75 % methanol (v/v)<br>25 % acetic acid (v/v) |

Nocodazole arrested cells from a 5 cm dish were resuspended in 200 µl hypotonic medium by carefully pipetting up and down. To generate Western blot samples 20 µl of the cell suspension were combined with 80 µl of 1 x SDS sample buffer. Another 300 µl and then 2 ml of hypotonic medium were added to the cell suspension. Following incubation for 5 min at RT, swollen cells were pelleted by centrifugation for 5 min at 100 g and resuspended in 20 µl of hypotonic medium by flicking the tube. Then, 250 µl, 250 µl, and 2 ml of Carnoy's Solution were added stepwise at RT. After incubation for 15-30 min at RT, cells were pelleted and washed again in 1 ml Carnoy's Solution. Finally, the cells were resuspended in 250 µl Carnoy's Solution and stored at -20°C until further use.
For spreading, 17 µl aliquots were dropped onto a microscope slide which was cooled down on an ice-submersed metal block and moisturized by breath. Afterwards the slides were dried on a wet tissue heated by a thermblock. The chromosomes were stained by incubation with Hoechst 33342 (1 µg/ml in 1x PBS) for 10 min. Then, samples were washed twice with PBS, once with dd$H_2O$ and air-dried. Finally, 7 µl of mounting medium (2.33 % (w/v) diazabicyclo-[2,2,2]-octane, 20 mM Tris/HCl, pH 8.0, in 78 % (v/v) glycerol) was applied to a 22 x 22 mm coverslip and used to cover the chromosomes.

### 4.5.8. Chromosome spreads combined with immunostaining

| | |
|---|---|
| hypotonic buffer I | 30 mM Tris/HCl, pH 8.2<br>50 mM sucrose<br>17 mM sodium citrate<br>200 ng/ml nocodazole |
| fixation solution | 1 % paraformaldehyde (w/v)<br>5 mM sodium borate, pH 9.2<br>0.15 % Triton X-100 (v/v) |

Chromosome spreading combined with IFM was basically performed as described previously (McGuinness et al., 2005). In brief, Nocodazole arrested cells were incubated in a hypotonic buffer I for 7 min and then resuspended in 100 mM sucrose. A small volume of the cell suspension was pipetted on a coverslip covered with fixation solution and dispersed by tilting. The coverslip was dried, washed by dipping in 1 x PBS and incubated in 1 % (w/v) BSA in PBS overnight at 4°C. The slides were processed for IFM as described in 4.5.6.

# 5. References

Arumugam, P., Gruber, S., Tanaka, K., Haering, C.H., Mechtler, K., and Nasmyth, K. (2003). ATP hydrolysis is required for cohesin's association with chromosomes. Curr Biol *13*, 1941-1953.

Bannister, L.A., Reinholdt, L.G., Munroe, R.J., and Schimenti, J.C. (2004). Positional cloning and characterization of mouse mei8, a disrupted allelle of the meiotic cohesin Rec8. Genesis *40*, 184-194.

Beckouet, F., Srinivasan, M., Roig, M.B., Chan, K.L., Scheinost, J.C., Batty, P., Hu, B., Petela, N., Gligoris, T., Smith, A.C*., et al.* (2016). Releasing activity disengages cohesin's Smc3/Scc1 interface in a process blocked by acetylation. Mol Cell *61*, 563-574.

Ben-Shahar, T.R., Heeger, S., Lehane, C., East, P., Flynn, H., Skehel, M., and Uhlmann, F. (2008). Eco1-dependent cohesin acetylation during establishment of sister chromatid cohesion. Science *321*, 563-566.

Bentley, A.M., Normand, G., Hoyt, J., and King, R.W. (2007). Distinct sequence elements of cyclin B1 promote localization to chromatin, centrosomes, and kinetochores during mitosis. Mol Biol Cell *18*, 4847-4858.

Biswas, U., Wetzker, C., Lange, J., Christodoulou, E.G., Seifert, M., Beyer, A., and Jessberger, R. (2013). Meiotic cohesin SMC1beta provides prophase I centromeric cohesion and is required for multiple synapsis-associated functions. PLoS Genet *9*, e1003985.

Booher, R.N., Holman, P.S., and Fattaey, A. (1997). Human Myt1 is a cell cycle-regulated kinase that inhibits Cdc2 but not Cdk2 activity. J Biol Chem *272*, 22300-22306.

Boos, D., Kuffer, C., Lenobel, R., Korner, R., and Stemmann, O. (2008). Phosphorylation-dependent binding of cyclin B1 to a Cdc6-like domain of human separase. J Biol Chem *283*, 816-823.

Brar, G.A., Kiburz, B.M., Zhang, Y., Kim, J.E., White, F., and Amon, A. (2006). Rec8 phosphorylation and recombination promote the step-wise loss of cohesins in meiosis. Nature *441*, 532-536.

Brieno-Enriquez, M.A., Moak, S.L., Toledo, M., Filter, J.J., Gray, S., Barbero, J.L., Cohen, P.E., and Holloway, J.K. (2016). Cohesin removal along the chromosome arms during the first meiotic division depends on a NEK1-PP1gamma-WAPL axis in the mouse. Cell Rep *17*, 977-986.

Buheitel, J., and Stemmann, O. (2013). Prophase pathway-dependent removal of cohesin from human chromosomes requires opening of the Smc3-Scc1 gate. Embo J *32*, 666-676.

Burkhardt, S., Borsos, M., Szydlowska, A., Godwin, J., Williams, S.A., Cohen, P.E., Hirota, T., Saitou, M., and Tachibana-Konwalski, K. (2016). Chromosome cohesion established by Rec8-cohesin in fetal oocytes is maintained without detectable turnover in oocytes arrested for months in mice. Curr Biol *26*, 678-685.

Camdere, G., Guacci, V., Stricklin, J., and Koshland, D. (2015). The ATPases of cohesin interface with regulators to modulate cohesin-mediated DNA tethering. Elife *4*, e11315.

Canudas, S., and Smith, S. (2009). Differential regulation of telomere and centromere cohesion by the Scc3 homologues SA1 and SA2, respectively, in human cells. J Cell Biol *187*, 165-173.

Cardoso, M.C., Leonhardt, H., and Nadalginard, B. (1993). Reversal of terminal differentiation and control of DNA-replication - Cyclin-a and Cdk2 specifically localize at subnuclear sites of DNA-replication. Cell *74*, 979-992.

Challa, K., Lee, M.S., Shinohara, M., Kim, K.P., and Shinohara, A. (2016). Rad61/Wpl1 (Wapl), a cohesin regulator, controls chromosome compaction during meiosis. Nucleic Acids Res *44*, 3190-3203.

Chambon, J.P., Touati, S.A., Berneau, S., Cladiere, D., Hebras, C., Groeme, R., McDougall, A., and Wassmann, K. (2013). The PP2A inhibitor I2PP2A is essential for sister chromatid segregation in oocyte meiosis II. Curr Biol *23*, 485-490.

Chan, K.L., Roig, M.B., Hu, B., Beckouet, F., Metson, J., and Nasmyth, K. (2012). Cohesin's DNA exit gate is distinct from its entrance gate and is regulated by acetylation. Cell *150*, 961-974.

Chau, V., Tobias, J.W., Bachmair, A., Marriott, D., Ecker, D.J., Gonda, D.K., and Varshavsky, A. (1989). A multiubiquitin chain is confined to specific lysine in a targeted short-lived protein. Science *243*, 1576-1583.

Chiang, T., Duncan, F.E., Schindler, K., Schultz, R.M., and Lampson, M.A. (2010). Evidence that weakened centromere cohesion is a leading cause of age-related aneuploidy in oocytes. Curr Biol *20*, 1522-1528.

Ciosk, R., Shirayama, M., Shevchenko, A., Tanaka, T.U., Toth, A., Shevchenko, A., and Nasmyth, K. (2000). Cohesin's binding to chromosomes depends on a separate complex consisting of Scc2 and Scc4 proteins. Mol Cell *5*, 243-254.

Colegrave, N. (2012). The evolutionary success of sex. Embo Rep *13*, 774-778.

Coverley, D., Pelizon, C., Trewick, S., and Laskey, R.A. (2000). Chromatin-bound Cdc6 persists in S and G2 phases in human cells, while soluble Cdc6 is destroyed in a cyclin A-cdk2 dependent process. J Cell Sci *113* 1929-1938.

Crasta, K., Huang, P., Morgan, G., Winey, M., and Surana, U. (2006). Cdk1 regulates centrosome separation by restraining proteolysis of microtubule-associated proteins. Embo J *25*, 2551-2563.

Crawley, O., Barroso, C., Testori, S., Ferrandiz, N., Silva, N., Castellano-Pozo, M., Jaso-Tamame, A.L., and Martinez-Perez, E. (2016). Cohesin-interacting protein WAPL-1 regulates meiotic chromosome structure and cohesion by antagonizing specific cohesin complexes. Elife *5*, e10851.

Davidson, I.F., Goetz, D., Zaczek, M.P., Molodtsov, M.I., Huis In 't Veld, P.J., Weissmann, F., Litos, G., Cisneros, D.A., Ocampo-Hafalla, M., Ladurner, R.*, et al.* (2016). Rapid movement and transcriptional re-localization of human cohesin on DNA. Embo J *35*, 2671-2685.

De Boer, L., Oakes, V., Beamish, H., Giles, N., Stevens, F., Somodevilla-Torres, M., DeSouza, C., and Gabrielli, B. (2008). Cyclin A/cdk2 coordinates centrosomal and nuclear mitotic events. Oncogene *27*, 4261-4268.

De, K., Sterle, L., Krueger, L., Yang, X., and Makaroff, C.A. (2014). Arabidopsis thaliana WAPL is essential for the prophase removal of cohesin during meiosis. PLoS Genet *10*, e1004497.

den Elzen, N., and Pines, J. (2001). Cyclin a is destroyed in prometaphase and can delay chromosome alignment and anaphase. J Cell Biol *153*, 121-135.

Di Fiore, B., and Pines, J. (2010). How cyclin A destruction escapes the spindle assembly checkpoint. J Cell Biol *190*, 501-509.

Dreier, M.R., Bekier, M.E., 2nd, and Taylor, W.R. (2011). Regulation of sororin by Cdk1-mediated phosphorylation. J Cell Sci *124*, 2976-2987.

Duro, E., and Marston, A.L. (2015). From equator to pole: splitting chromosomes in mitosis and meiosis. Genes Dev *29*, 109-122.

Eichinger, C.S., Kurze, A., Oliveira, R.A., and Nasmyth, K. (2013). Disengaging the Smc3/kleisin interface releases cohesin from Drosophila chromosomes during interphase and mitosis. Embo J *32*, 656-665.

Eijpe, M., Offenberg, H., Jessberger, R., Revenkova, E., and Heyting, C. (2003). Meiotic cohesin REC8 marks the axial elements of rat synaptonemal complexes before cohesins SMC1beta and SMC3. J Cell Biol *160*, 657-670.

Elbashir, S.M., Harborth, J., Lendeckel, W., Yalcin, A., Weber, K., and Tuschl, T. (2001). Duplexes of 21-nucleotide RNAs mediate RNA interference in cultured mammalian cells. Nature *411*, 494-498.

Elbatsh, A.M., Haarhuis, J.H., Petela, N., Chapard, C., Fish, A., Celie, P.H., Stadnik, M., Ristic, D., Wyman, C., Medema, R.H.*, et al.* (2016). Cohesin releases DNA through asymmetric ATPase-driven ring opening. Mol Cell *61*, 575-588.

Finley, D. (2009). Recognition and processing of ubiquitin-protein conjugates by the proteasome. Annu Rev Biochem *78*, 477-513.

Finley, D., Ulrich, H.D., Sommer, T., and Kaiser, P. (2012). The ubiquitin-proteasome system of Saccharomyces cerevisiae. Genetics *192*, 319-360.

Foley, E.A., and Kapoor, T.M. (2013). Microtubule attachment and spindle assembly checkpoint signalling at the kinetochore. Nat Rev Mol Cell Bio *14*, 25-37.

Fu, S.C., Imai, K., and Horton, P. (2011). Prediction of leucine-rich nuclear export signal containing proteins with NESsential. Nucleic Acids Res *39*, e111.

Fukuda, T., Fukuda, N., Agostinho, A., Hernandez-Hernandez, A., Kouznetsova, A., and Hoog, C. (2014). STAG3-mediated stabilization of REC8 cohesin complexes promotes chromosome synapsis during meiosis. Embo J *33*, 1243-1255.

Fung, T.K., Ma, H.T., and Poon, R.Y.C. (2007). Specialized roles of the two mitotic cyclins in somatic cells: Cyclin a as an activator of M phase-promoting factor. Mol Biol Cell *18*, 1861-1873.

Furuya, K., Takahashi, K., and Yanagida, M. (1998). Faithful anaphase is ensured by Mis4, a sister chromatid cohesion molecule required in S phase and not destroyed in G(1) phase. Genes Dev *12*, 3408-3418.

Gandhi, R., Gillespie, P.J., and Hirano, T. (2006). Human Wapl is a cohesin-binding protein that promotes sister-chromatid resolution in mitotic prophase. Curr Biol *16*, 2406-2417.

Gause, M., Webber, H.A., Misulovin, Z., Haller, G., Rollins, R.A., Eissenberg, J.C., Bickel, S.E., and Dorsett, D. (2008). Functional links between Drosophila Nipped-B and cohesin in somatic and meiotic cells. Chromosoma *117*, 51-66.

Gautier, J., Minshull, J., Lohka, M., Glotzer, M., Hunt, T., and Maller, J.L. (1990). Cyclin is a component of maturation-promoting factor from Xenopus. Cell *60*, 487-494.

Gautier, J., Norbury, C., Lohka, M., Nurse, P., and Maller, J. (1988). Purified maturation-promoting factor contains the product of a Xenopus homolog of the fission yeast-cell cycle control gene Cdc2+. Cell *54*, 433-439.

Gautier, J., Solomon, M.J., Booher, R.N., Bazan, J.F., and Kirschner, M.W. (1991). Cdc25 is a specific tyrosine phosphatase that directly activates P34cdc2. Cell *67*, 197-211.

Gerlich, D., Koch, B., Dupeux, F., Peters, J.M., and Ellenberg, J. (2006). Live-cell imaging reveals a stable cohesin-chromatin interaction after but not before DNA replication. Curr Biol *16*, 1571-1578.

Girard, F., Strausfeld, U., Fernandez, A., and Lamb, N.J.C. (1991). Cyclin-a is required for the onset of DNA-replication in mammalian fibroblasts. Cell *67*, 1169-1179.

Gligoris, T.G., Scheinost, J.C., Burmann, F., Petela, N., Chan, K.L., Uluocak, P., Beckouet, F., Gruber, S., Nasmyth, K., and Lowe, J. (2014). Closing the cohesin ring: structure and function of its Smc3-kleisin interface. Science *346*, 963-967.

Gomez, R., Felipe-Medina, N., Ruiz-Torres, M., Berenguer, I., Viera, A., Perez, S., Barbero, J.L., Llano, E., Fukuda, T., Alsheimer, M.*, et al.* (2016). Sororin loads to the synaptonemal complex central region independently of meiotic cohesin complexes. Embo Rep *17*, 695-707.

Gomez, R., Valdeolmillos, A., Parra, M.T., Viera, A., Carreiro, C., Roncal, F., Rufas, J.S., Barbero, J.L., and Suja, J.A. (2007). Mammalian SGO2 appears at the inner centromere domain and redistributes depending on tension across centromeres during meiosis II and mitosis. Embo Rep *8*, 173-180.

Gong, D.Q., Pomerening, J.R., Myers, J.W., Gustavsson, C., Jones, J.T., Hahn, A.T., Meyer, T., and Ferrell, J.E. (2007). Cyclin A2 regulates nuclear-envelope breakdown and the nuclear accumulation of cyclin B1. Curr Biol *17*, 85-91.

Gorr, I.H., Boos, D., and Stemmann, O. (2005). Mutual inhibition of separase and Cdk1 by two-step complex formation. Molecular cell *19*, 135-141.

Grallert, A., Boke, E., Hagting, A., Hodgson, B., Connolly, Y., Griffiths, J.R., Smith, D.L., Pines, J., and Hagan, I.M. (2015). A PP1-PP2A phosphatase relay controls mitotic progression. Nature *517*, 94-98.

Gregan, J., Polakova, S., Zhang, L.J., Tolic-Norrelykke, I.M., and Cimini, D. (2011). Merotelic kinetochore attachment: causes and effects. Trends Cell Biol *21*, 374-381.

Gruber, S., Arumugam, P., Katou, Y., Kuglitsch, D., Helmhart, W., Shirahige, K., and Nasmyth, K. (2006). Evidence that loading of cohesin onto chromosomes involves opening of its SMC hinge. Cell *127*, 523-537.

Gruber, S., Haering, C.H., and Nasmyth, K. (2003). Chromosomal cohesin forms a ring. Cell *112*, 765-777.

Gu, H., Zou, Y.R., and Rajewsky, K. (1993). Independent control of immunoglobulin switch recombination at individual switch regions evidenced through Cre-loxp-mediated gene targeting. Cell *73*, 1155-1164.

Gutierrez-Caballero, C., Herran, Y., Sanchez-Martin, M., Suja, J.A., Barbero, J.L., Llano, E., and Pendas, A.M. (2011). Identification and molecular characterization of the mammalian alpha-kleisin RAD21L. Cell Cycle *10*, 1477-1487.

Haarhuis, J.H.I., Elbatsh, A.M.O., van den Broek, B., Camps, D., Erkan, H., Jalink, K., Medema, R.H., and Rowland, B.D. (2013). WAPL-mediated removal of cohesin protects against segregation errors and aneuploidy. Curr Biol *23*, 2071-2077.

Haering, C.H., Farcas, A.M., Arumugam, P., Metson, J., and Nasmyth, K. (2008). The cohesin ring concatenates sister DNA molecules. Nature *454*, 297-U219.

Haering, C.H., Lowe, J., Hochwagen, A., and Nasmyth, K. (2002). Molecular architecture of SMC proteins and the yeast cohesin complex. Mol Cell *9*, 773-788.

Haering, C.H., Schoffnegger, D., Nishino, T., Helmhart, W., Nasmyth, K., and Lowe, J. (2004). Structure and stability of cohesin's Smc1-kleisin interaction. Mol Cell *15*, 951-964.

Hagting, A., den Elzen, N., Vodermaier, H.C., Waizenegger, I.C., Peters, J.M., and Pines, J. (2002). Human securin proteolysis is controlled by the spindle checkpoint and reveals when the APC/C switches from activation by Cdc20 to Cdh1. J Cell Biol *157*, 1125-1137.

Hames, R.S., Wattam, S.L., Yamano, H., Bacchieri, R., and Fry, A.M. (2001). APC/C-mediated destruction of the centrosomal kinase Nek2A occurs in early mitosis and depends upon a cyclin A-type D-box. Embo J *20*, 7117-7127.

Hara, K., Zheng, G., Qu, Q., Liu, H., Ouyang, Z., Chen, Z., Tomchick, D.R., and Yu, H. (2014). Structure of cohesin subcomplex pinpoints direct shugoshin-Wapl antagonism in centromeric cohesion. Nat Struct Mol Biol *21*, 864-870.

Hassold, T., and Hunt, P. (2001). To ERR (meiotically) is human: The genesis of human aneuploidy. Nat Rev Genet *2*, 280-291.

Hauf, S., Roitinger, E., Koch, B., Dittrich, C.M., Mechtler, K., and Peters, J.M. (2005). Dissociation of cohesin from chromosome arms and loss of arm cohesion during early mitosis depends on phosphorylation of SA2. Plos Biol *3*, 419-432.

Hauf, S., Waizenegger, I.C., and Peters, J.M. (2001). Cohesin cleavage by separase required for anaphase and cytokinesis in human cells. Science *293*, 1320-1323.

Hayes, M.J., Kimata, Y., Wattam, S.L., Lindon, C., Mao, G.J., Yamano, H., and Fry, A.M. (2006). Early mitotic degradation of Nek2A depends on Cdc20-indedpenent interaction with the APC/C. Nat Cell Biol *8*, 607-614.

Heald, R., and Mckeon, F. (1990). Mutations of phosphorylation sites in lamin-a that prevent nuclear lamina disassembly in mitosis. Cell *61*, 579-589.

Heidinger-Pauli, J.M., Unal, E., Guacci, V., and Koshland, D. (2008). The kleisin subunit of cohesin dictates damage-induced cohesion. Mol Cell *31*, 47-56.

Heidinger-Pauli, J.M., Unal, E., and Koshland, D. (2009). Distinct targets of the Eco1 acetyltransferase modulate cohesion in S phase and in response to DNA damage. Mol Cell *34*, 311-321.

Hellmuth, S., Rata, S., Brown, A., Heidmann, S., Novak, B., and Stemmann, O. (2015). Human chromosome segregation involves multi-layered regulation of separase by the peptidyl-prolyl-isomerase Pin1. Molecular cell *58*, 495-506.

Hershko, A., and Ciechanover, A. (1998). The ubiquitin system. Annu Rev Biochem *67*, 425-479.

Hoffmann, I., Clarke, P.R., Marcote, M.J., Karsenti, E., and Draetta, G. (1993). Phosphorylation and activation of human Cdc25-C by Cdc2 Cyclin-B and its involvement in the self-amplification of Mpf at mitosis. Embo J *12*, 53-63.

Holland, A.J., and Taylor, S.S. (2006). Cyclin-B1-mediated inhibition of excess separase is required for timely chromosome disjunction. J Cell Sci *119*, 3325-3336.

Holloway, K., Roberson, E.C., Corbett, K.L., Kolas, N.K., Nieves, E., and Cohen, P.E. (2011). NEK1 facilitates cohesin removal during mammalian spermatogenesis. Genes (Basel) *2*, 260-279.

Hopkins, J., Hwang, G., Jacob, J., Sapp, N., Bedigian, R., Oka, K., Overbeek, P., Murray, S., and Jordan, P.W. (2014). Meiosis-specific cohesin component, Stag3 is essential for maintaining centromere chromatid cohesion, and required for DNA repair and synapsis between homologous chromosomes. PLoS Genet *10*, e1004413.

Hsu, J.Y., Reimann, J.D., Sorensen, C.S., Lukas, J., and Jackson, P.K. (2002). E2F-dependent accumulation of hEmi1 regulates S phase entry by inhibiting APC(Cdh1). Nat Cell Biol *4*, 358-366.

Hu, B., Itoh, T., Mishra, A., Katoh, Y., Chan, K.L., Upcher, W., Godlee, C., Roig, M.B., Shirahige, K., and Nasmyth, K. (2011). ATP hydrolysis is required for relocating cohesin from sites occupied by its Scc2/4 loading complex. Curr Biol *21*, 12-24.

Huang, H., Feng, J., Famulski, J., Rattner, J.B., Liu, S.T., Kao, G.D., Muschel, R., Chan, G.K., and Yen, T.J. (2007). Tripin/hSgo2 recruits MCAK to the inner centromere to correct defective kinetochore attachments. J Cell Biol *177*, 413-424.

Huang, X.X., Andreu-Vieyra, C.V., York, J.P., Hatcher, R., Lu, T., Matzuk, M.M., and Zhang, P.M. (2008). Inhibitory phosphorylation of separase is essential for genome stability and viability of murine embryonic germ cells. Plos Biol *6*, 52-62.

in 't Veld, P.J.H., Herzog, F., Ladurner, R., Davidson, I.F., Piric, S., Kreidl, E., Bhaskara, V., Aebersold, R., and Peters, J.M. (2014). Characterization of a DNA exit gate in the human cohesin ring. Science *346*, 968-972.

Ishiguro, K., Kim, J., Fujiyama-Nakamura, S., Kato, S., and Watanabe, Y. (2011). A new meiosis-specific cohesin complex implicated in the cohesin code for homologous pairing. EMBO Rep *12*, 267-275.

Ishiguro, K., Kim, J., Shibuya, H., Hernandez-Hernandez, A., Suzuki, A., Fukagawa, T., Shioi, G., Kiyonari, H., Li, X.C., Schimenti, J.*, et al.* (2014). Meiosis-specific cohesin mediates homolog recognition in mouse spermatocytes. Genes Dev *28*, 594-607.

Ishimi, Y., Komamura-Kohno, Y., You, Z., Omori, A., and Kitagawa, M. (2000). Inhibition of Mcm4,6,7 helicase activity by phosphorylation with cyclin A/Cdk2. J Biol Chem *275*, 16235-16241.

Ito, M., Kugou, K., Fawcett, J.A., Mura, S., Ikeda, S., Innan, H., and Ohta, K. (2014). Meiotic recombination cold spots in chromosomal cohesion sites. Genes Cells *19*, 359-373.

Ivanov, D., and Nasmyth, K. (2005). A topological interaction between cohesin rings and a circular minichromosome. Cell *122*, 849-860.

Ivanov, D., and Nasmyth, K. (2007). A physical assay for sister chromatid cohesion in vitro. Mol Cell *27*, 300-310.

Jaspersen, S.L., Charles, J.F., and Morgan, D.O. (1999). Inhibitory phosphorylation of the APC regulator Hct1 is controlled by the kinase Cdc28 and the phosphatase Cdc14. Curr Biol *9*, 227-236.

Jin, L.Y., Williamson, A., Banerjee, S., Philipp, I., and Rape, M. (2008). Mechanism of ubiquitin-chain formation by the human anaphase-promoting complex. Cell *133*, 653-665.

Katis, V.L., Lipp, J.J., Imre, R., Bogdanova, A., Okaz, E., Habermann, B., Mechtler, K., Nasmyth, K., and Zachariae, W. (2010). Rec8 phosphorylation by casein kinase 1 and Cdc7-Dbf4 kinase regulates cohesin cleavage by separase during meiosis. Dev Cell *18*, 397-409.

Kerscher, O., Felberbaum, R., and Hochstrasser, M. (2006). Modification of proteins by ubiquitin and ubiquitin-like proteins. Annu Rev Cell Dev Biol *22*, 159-180.

Kim, J., Ishiguro, K.I., Nambu, A., Akiyoshi, B., Yokobayashi, S., Kagami, A., Ishiguro, T., Pendas, A.M., Takeda, N., Sakakibara, Y.*, et al.* (2015). Meikin is a conserved regulator of meiosis-I-specific kinetochore function. Nature *517*, 466-471.

Kitajima, T.S., Sakuno, T., Ishiguro, K., Iemura, S., Natsume, T., Kawashima, S.A., and Watanabe, Y. (2006). Shugoshin collaborates with protein phosphatase 2A to protect cohesin. Nature *441*, 46-52.

Klug, W.S. (2012). Concepts of genetics, 10th edn (San Francisco: Pearson Education).

Komander, D., and Rape, M. (2012). The ubiquitin code. Annu Rev Biochem *81*, 203-229.

Koshland, D., and Hartwell, L.H. (1987). The Structure of sister minichromosome DNA before anaphase in Saccharomyces cerevisiae. Science *238*, 1713-1716.

Kosugi, S., Hasebe, M., Tomita, M., and Yanagawa, H. (2009). Systematic identification of cell cycle-dependent yeast nucleocytoplasmic shuttling proteins by prediction of composite motifs. Proc Natl Acad Sci U S A *106*, 10171-10176.

Kouznetsova, A., Novak, I., Jessberger, R., and Hoog, C. (2005). SYCP2 and SYCP3 are required for cohesin core integrity at diplotene but not for centromere cohesion at the first meiotic division. J Cell Sci *118*, 2271-2278.

Kraft, C., Herzog, F., Gieffers, C., Mechtler, K., Hagting, A., Pines, J., and Peters, J.M. (2003). Mitotic regulation of the human anaphase-promoting complex by phosphorylation. Embo J *22*, 6598-6609.

Kudo, N.R., Anger, M., Peters, A.H., Stemmann, O., Theussl, H.C., Helmhart, W., Kudo, H., Heyting, C., and Nasmyth, K. (2009). Role of cleavage by separase of the Rec8 kleisin subunit of cohesin during mammalian meiosis I. J Cell Sci *122*, 2686-2698.

Kueng, S., Hegemann, B., Peters, B.H., Lipp, J.J., Schleiffer, A., Mechtler, K., and Peters, J.M. (2006). Wapl controls the dynamic association of cohesin with chromatin. Cell *127*, 955-967.

Kugou, K., Fukuda, T., Yamada, S., Ito, M., Sasanuma, H., Mori, S., Katou, Y., Itoh, T., Matsumoto, K., Shibata, T.*, et al.* (2009). Rec8 guides canonical Spo11 distribution along yeast meiotic chromosomes. Mol Biol Cell *20*, 3064-3076.

Kuleszewicz, K., Fu, X., and Kudo, N.R. (2013). Cohesin loading factor Nipbl localizes to chromosome axes during mammalian meiotic prophase. Cell Div *8*, 12.

Kumagai, A., and Dunphy, W.G. (1992). Regulation of the Cdc25 protein during the cell cycle in Xenopus extracts. Cell *70*, 139-151.

Kuroda, M., Oikawa, K., Ohbayashi, T., Yoshida, K., Yamada, K., Mimura, J., Matsuda, Y., Fujii-Kuriyama, Y., and Mukai, K. (2005). A dioxin sensitive gene, mammalian WAPL, is implicated in spermatogenesis. FEBS Lett *579*, 167-172.

la Cour, T., Kiemer, L., Molgaard, A., Gupta, R., Skriver, K., and Brunak, S. (2004). Analysis and prediction of leucine-rich nuclear export signals. Protein Eng Des Sel *17*, 527-536.

Ladurner, R., Kreidl, E., Ivanov, M.P., Ekker, H., Idarraga-Amado, M.H., Busslinger, G.A., Wutz, G., Cisneros, D.A., and Peters, J.M. (2016). Sororin actively maintains sister chromatid cohesion. Embo J *35*, 635-653.

Lafont, A.L., Song, J.H., and Rankin, S. (2010). Sororin cooperates with the acetyltransferase Eco2 to ensure DNA replication-dependent sister chromatid cohesion. Proc Natl Acad Sci U S A *107*, 20364-20369.

Lammens, A., Schele, A., and Hopfner, K.P. (2004). Structural biochemistry of ATP-driven dimerization and DNA-stimulated activation of SMC ATPases. Curr Biol *14*, 1778-1782.

Lara-Gonzalez, P., Westhorpe, F.G., and Taylor, S.S. (2012). The spindle assembly checkpoint. Curr Biol *22*, R966-R980.

Lee, J., and Hirano, T. (2011). RAD21L, a novel cohesin subunit implicated in linking homologous chromosomes in mammalian meiosis. J Cell Biol *192*, 263-276.

Lee, J., Kitajima, T.S., Tanno, Y., Yoshida, K., Morita, T., Miyano, T., Miyake, M., and Watanabe, Y. (2008). Unified mode of centromeric protection by shugoshin in mammalian oocytes and somatic cells. Nat Cell Biol *10*, 42-52.

Lengronne, A., Katou, Y., Mori, S., Yokobayashi, S., Kelly, G.P., Itoh, T., Watanabe, Y., Shirahige, K., and Uhlmann, F. (2004). Cohesin relocation from sites of chromosomal loading to places of convergent transcription. Nature *430*, 573-578.

Lin, W., Jin, H., Liu, X., Hampton, K., and Yu, H.G. (2011). Scc2 regulates gene expression by recruiting cohesin to the chromosome as a transcriptional activator during yeast meiosis. Mol Biol Cell *22*, 1985-1996.

Lindon, C., and Pines, J. (2004). Ordered proteolysis in anaphase inactivates Plk1 to contribute to proper mitotic exit in human cells. J Cell Biol *164*, 233-241.

Lindqvist, A., Rodriguez-Bravo, V., and Medema, R.H. (2009). The decision to enter mitosis: feedback and redundancy in the mitotic entry network. J Cell Biol *185*, 193-202.

Lister, L.M., Kouznetsova, A., Hyslop, L.A., Kalleas, D., Pace, S.L., Barel, J.C., Nathan, A., Floros, V., Adelfalk, C., Watanabe, Y.*, et al.* (2010). Age-related meiotic segregation errors in mammalian oocytes are preceded by depletion of cohesin and Sgo2. Curr Biol *20*, 1511-1521.

Liu, D., Matzuk, M.M., Sung, W.K., Guo, Q.X., Wang, P., and Wolgemuth, D.J. (1998). Cyclin A1 is required for meiosis in the male mouse. Nat Genet *20*, 377-380.

Liu, H., Jia, L.Y., and Yu, H.T. (2013a). Phospho-H2A and Cohesin Specify Distinct Tension-Regulated Sgo1 Pools at Kinetochores and Inner Centromeres. Curr Biol *23*, 1927-1933.

Liu, H., Rankin, S., and Yu, H. (2013b). Phosphorylation-enabled binding of SGO1-PP2A to cohesin protects sororin and centromeric cohesion during mitosis. Nat Cell Biol *15*, 40-49.

Llano, E., Gomez, R., Gutierrez-Caballero, C., Herran, Y., Sanchez-Martin, M., Vazquez-Quinones, L., Hernandez, T., de Alava, E., Cuadrado, A., Barbero, J.L.*, et al.* (2008). Shugoshin-2 is essential for the completion of meiosis but not for mitotic cell division in mice. Genes Dev *22*, 2400-2413.

Llano, E., Herran, Y., Garcia-Tunon, I., Gutierrez-Caballero, C., de Alava, E., Barbero, J.L., Schimenti, J., de Rooij, D.G., Sanchez-Martin, M., and Pendas, A.M. (2012). Meiotic cohesin

complexes are essential for the formation of the axial element in mice. J Cell Biol *197*, 877-885.

Loidl, J. (2016). Conservation and variability of meiosis across the eukaryotes. Annu Rev Genet *50*, 293-316.

Losada, A., Yokochi, T., Kobayashi, R., and Hirano, T. (2000). Identification and characterization of SA/Scc3p subunits in the Xenopus and human cohesin complexes. J Cell Biol *150*, 405-416.

Masui, Y., and Markert, C.L. (1971). Cytoplasmic control of nuclear behavior during meiotic maturation of frog oocytes. J Exp Zool *177*, 129-145.

McGowan, C.H., and Russell, P. (1995). Cell cycle regulation of human WEE1. Embo J *14*, 2166-2175.

McGuinness, B.E., Hirota, T., Kudo, N.R., Peters, J.M., and Nasmyth, K. (2005). Shugoshin prevents dissociation of cohesin from centromeres during mitosis in vertebrate cells. PLos Biol *3*, e86.

McNicoll, F., Stevense, M., and Jessberger, R. (2013). Cohesin in Gametogenesis. Curr Top Dev Biol *102*, 1-34.

Melby, T.E., Ciampaglio, C.N., Briscoe, G., and Erickson, H.P. (1998). The symmetrical structure of structural maintenance of chromosomes (SMC) and MukB proteins: Long, antiparallel coiled coils, folded at a flexible hinge. J Cell Biol *142*, 1595-1604.

Michaelis, C., Ciosk, R., and Nasmyth, K. (1997). Cohesins: Chromosomal proteins that prevent premature separation of sister chromatids. Cell *91*, 35-45.

Miftakhova, R., Hedblom, A., Batkiewicz, L., Anagnosaki, L., Zhang, Y., Sjolander, A., Wingren, A.G., Wolgemuth, D.J., and Persson, J.L. (2015). Cyclin A1 regulates the interactions between mouse haematopoietic stem and progenitor cells and their niches. Cell Cycle *14*, 1948-1960.

Minamino, M., Ishibashi, M., Nakato, R., Akiyama, K., Tanaka, H., Kato, Y., Negishi, L., Hirota, T., Sutani, T., Bando, M.*, et al.* (2015). Esco1 acetylates cohesin via a mechanism different from that of Esco2. Curr Biol *25*, 1694-1706.

Mitra, J., and Enders, G.H. (2004). Cyclin A/Cdk2 complexes regulate activation of Cdk1 and Cdc25 phosphatases in human cells. Oncogene *23*, 3361-3367.

Mochida, S., Maslen, S.L., Skehel, M., and Hunt, T. (2010). Greatwall phosphorylates an inhibitor of protein phosphatase 2A that is essential for mitosis. Science *330*, 1670-1673.

Moldovan, G.L., Pfander, B., and Jentsch, S. (2006). PCNA controls establishment of sister chromatid cohesion during S phase. Mol Cell *23*, 723-732.

Morgan, D.O. (2007). The cell cycle : principles of control (London Sunderland, MA: Published by New Science Press in association with Oxford University Press; Distributed inside North America by Sinauer Associates, Publishers).

Mueller, P.R., Coleman, T.R., and Dunphy, W.G. (1995a). Cell cycle regulation of a Xenopus Wee1-like kinase. Mol Biol Cell *6*, 119-134.

Mueller, P.R., Coleman, T.R., Kumagai, A., and Dunphy, W.G. (1995b). Myt1 - a membrane-associated inhibitory kinase that phosphorylates Cdc2 on both threonine-14 and tyrosine-15. Science *270*, 86-90.

Murayama, Y., and Uhlmann, F. (2014). Biochemical reconstitution of topological DNA binding by the cohesin ring. Nature *505*, 367-371.

Murayama, Y., and Uhlmann, F. (2015). DNA entry into and exit out of the cohesin ring by an interlocking gate mechanism. Cell *163*, 1628-1640.

Murphy, M., Stinnakre, M.G., SenamaudBeaufort, C., Winston, N.J., Sweeney, C., Kubelka, M., Carrington, M., Brechot, C., and SobczakThepot, J. (1997). Delayed early embryonic lethality following disruption of the murine cyclin A2 gene. Nature Genet *15*, 83-86.

Murray, A.W. (1991). Cell cycle extracts. Methods Cell Biol *36*, 581-605.

Murray, A.W. (2004). Recycling the cell cycle: cyclins revisited. Cell *116*, 221-234.

Murray, A.W., Solomon, M.J., and Kirschner, M.W. (1989). The role of cyclin synthesis and degradation in the control of maturation promoting factor activity. Nature *339*, 280-286.

Musacchio, A. (2015). The molecular biology of spindle assembly checkpoint signaling dynamics. Curr Biol *25*, R1002-R1018.

Nasmyth, K. (2011). Cohesin: a catenase with separate entry and exit gates? Nat Cell Biol *13*, 1170-1177.

Nasmyth, K., and Haering, C.H. (2009). Cohesin: Its roles and mechanisms. Annu Rev Genet *43*, 525-558.

Nishiyama, T., Ladurner, R., Schmitz, J., Kreidl, E., Schleiffer, A., Bhaskara, V., Bando, M., Shirahige, K., Hyman, A.A., Mechtler, K.*, et al.* (2010). Sororin mediates sister chromatid cohesion by antagonizing Wapl. Cell *143*, 737-749.

Nishiyama, T., Sykora, M.M., Huis in 't Veld, P.J., Mechtler, K., and Peters, J.M. (2013). Aurora B and Cdk1 mediate Wapl activation and release of acetylated cohesin from chromosomes by phosphorylating Sororin. Proc Natl Acad Sci U S A *110*, 13404-13409.

O'Farrell, P.H. (2001). Triggering the all-or-nothing switch into mitosis. Trends Cell Biol *11*, 512-519.

Pagano, M., Pepperkok, R., Verde, F., Ansorge, W., and Draetta, G. (1992). Cyclin A is required at two points in the human cell cycle. Embo J *11*, 961-971.

Panizza, S., Tanaka, T.U., Hochwagen, A., Eisenhaber, F., and Nasmyth, K. (2000). Pds5 cooperates with cohesin in maintaining sister chromatid cohesion. Curr Biol *10*, 1557-1564.

Parker, L.L., Athertonfessler, S., and Piwnicaworms, H. (1992). P107(Wee1) is a dual-specificity kinase that phosphorylates-P34(Cdc2) on tyrosine-15. Proc Natl Acad Sci U S A *89*, 2917-2921.

Petersen, B.O., Lukas, J., Sorensen, C.S., Bartek, J., and Helin, K. (1999). Phosphorylation of mammalian CDC6 by cyclin A/CDK2 regulates its subcellular localization. Embo J *18*, 396-410.

Pines, J. (2011). Cubism and the cell cycle: the many faces of the APC/C. Nat Rev Mol Cell Biol *12*, 427-438.

Porter, I.M., Schleicher, K., Porter, M., and Swedlow, J.R. (2013). Bod1 regulates protein phosphatase 2A at mitotic kinetochores. Nat Commun *4*, 2677.

Qiao, H., Lohmiller, L.D., and Anderson, L.K. (2011). Cohesin proteins load sequentially during prophase I in tomato primary microsporocytes. Chromosome Res *19*, 193-207.

Rankin, S. (2015). Complex elaboration: making sense of meiotic cohesin dynamics. Febs J *282*, 2426-2443.

Rankin, S., Ayad, N.G., and Kirschner, M.W. (2005). Sororin, a substrate of the anaphase-promoting complex, is required for sister chromatid cohesion in vertebrates. Mol Cell *18*, 185-200.

Ravnik, S.E., and Wolgemuth, D.J. (1999). Regulation of meiosis during mammalian spermatogenesis: The A-type cyclins and their associated cyclin-dependent kinases are differentially expressed in the germ-cell lineage. Dev Biol *207*, 408-418.

Revenkova, E., Eijpe, M., Heyting, C., Gross, B., and Jessberger, R. (2001). Novel meiosis-specific isoform of mammalian SMC1. Mol Cell Biol *21*, 6984-6998.

Revenkova, E., Eijpe, M., Heyting, C., Hodges, C.A., Hunt, P.A., Liebe, B., Scherthan, H., and Jessberger, R. (2004). Cohesin SMC1 beta is required for meiotic chromosome dynamics, sister chromatid cohesion and DNA recombination. Nat Cell Biol *6*, 555-562.

Ricke, R.M., Jeganathan, K.B., Malureanu, L., Harrison, A.M., and van Deursen, J.M. (2012). Bub1 kinase activity drives error correction and mitotic checkpoint control but not tumor suppression. J Cell Biol *199*, 931-949.

Robbins, J.A., and Cross, F.R. (2010). Regulated degradation of the APC coactivator Cdc20. Cell Div *5*, 23.

Rothbauer, U., Zolghadr, K., Muyldermans, S., Schepers, A., Cardoso, M.C., and Leonhardt, H. (2008). A versatile nanotrap for biochemical and functional studies with fluorescent fusion proteins. Mol Cell Proteomics *7*, 282-289.

Rudner, A.D., and Murray, A.W. (2000). Phosphorylation by Cdc28 activates the Cdc20-dependent activity of the anaphase-promoting complex. J Cell Biol *149*, 1377-1390.

Sacristan, C., and Kops, G.J.P.L. (2015). Joined at the hip: kinetochores, microtubules, and spindle assembly checkpoint signaling. Trends Cell Biol *25*, 21-28.

Saeki, Y., Kudo, T., Sone, T., Kikuchi, Y., Yokosawa, H., Toh-e, A., and Tanaka, K. (2009). Lysine 63-linked polyubiquitin chain may serve as a targeting signal for the 26S proteasome. Embo J *28*, 359-371.

Santaguida, S., and Musacchio, A. (2009). The life and miracles of kinetochores. Embo J *28*, 2511-2531.

Schmitz, J., Watrin, E., Lenart, P., Mechtler, K., and Peters, J.M. (2007). Sororin is required for stable binding of cohesin to chromatin and for sister chromatid cohesion in interphase. Curr Biol *17*, 630-636.

Schockel, L., Mockel, M., Mayer, B., Boos, D., and Stemmann, O. (2011). Cleavage of cohesin rings coordinates the separation of centrioles and chromatids. Nat Cell Biol *13*, 966-972.

Seitan, V.C., Banks, P., Laval, S., Majid, N.A., Dorsett, D., Rana, A., Smith, J., Bateman, A., Krpic, S., Hostert, A*., et al.* (2006). Metazoan Scc4 homologs link sister chromatid cohesion to cell and axon migration guidance. Plos Biol *4*, 1411-1425.

Shintomi, K., and Hirano, T. (2009). Releasing cohesin from chromosome arms in early mitosis: opposing actions of Wapl-Pds5 and Sgo1. Genes Dev *23*, 2224-2236.

Shintomi, K., Takahashi, T.S., and Hirano, T. (2015). Reconstitution of mitotic chromatids with a minimum set of purified factors. Nat Cell Biol *17*, 1014-1023.

Sigl, R., Wandke, C., Rauch, V., Kirk, J., Hunt, T., and Geley, S. (2009). Loss of the mammalian APC/C activator FZR1 shortens G1 and lengthens S phase but has little effect on exit from mitosis. J Cell Sci *122*, 4208-4217.

Sobczakthepot, J., Harper, F., Florentin, Y., Zindy, F., Brechot, C., and Puvion, E. (1993). Localization of Cyclin A at the sites of cellular DNA-replication. Exp Cell Res *206*, 43-48.

Stemmann, O., Zou, H., Gerber, S.A., Gygi, S.P., and Kirschner, M.W. (2001). Dual inhibition of sister chromatid separation at metaphase. Cell *107*, 715-726.

Strom, L., Karlsson, C., Lindroos, H.B., Wedahl, S., Katou, Y., Shirahige, K., and Sjogren, C. (2007). Postreplicative formation of cohesion is required for repair and induced by a single DNA break. Science *317*, 242-245.

Strom, L., Lindroos, H.B., Shirahige, K., and Sjogren, C. (2004). Postreplicative recruitment of cohesin to double-strand breaks is required for DNA repair. Mol Cell *16*, 1003-1015.

Sumara, I., Vorlaufer, E., Gieffers, C., Peters, B.H., and Peters, J.M. (2000). Characterization of vertebrate cohesin complexes and their regulation in prophase. J Cell Biol *151*, 749-761.

Sun, X., Huang, L., Markowitz, T.E., Blitzblau, H.G., Chen, D., Klein, F., and Hochwagen, A. (2015). Transcription dynamically patterns the meiotic chromosome-axis interface. Elife *4*, e07424.

Sun, Y.X., Kucej, M., Fan, H.Y., Yu, H., Sun, Q.Y., and Zou, H. (2009). Separase is recruited to mitotic chromosomes to dissolve sister chromatid cohesion in a DNA-dependent manner. Cell *137*, 123-132.

Tachibana-Konwalski, K., Godwin, J., van der Weyden, L., Champion, L., Kudo, N.R., Adams, D.J., and Nasmyth, K. (2010). Rec8-containing cohesin maintains bivalents without turnover during the growing phase of mouse oocytes. Genes Dev *24*, 2505-2516.

Tarnowski, L.J., Kowalec, P., Milewski, M., Jurek, M., Plochocka, D., Fronk, J., and Kurlandzka, A. (2012). Nuclear import and export signals of human cohesins SA1/Stag1 and SA2/Stag2 expressed in Saccharomyces cerevisiae. PLos One *7*, e38740.

Tedeschi, A., Wutz, G., Huet, S., Jaritz, M., Wuensche, A., Schirghuber, E., Davidson, I.F., Tang, W., Cisneros, D.A., Bhaskara, V.*, et al.* (2013). Wapl is an essential regulator of chromatin structure and chromosome segregation. Nature *501*, 564-568.

Touati, S.A., Cladiere, D., Lister, L.M., Leontiou, I., Chambon, J.P., Rattani, A., Bottger, F., Stemmann, O., Nasmyth, K., Herbert, M.*, et al.* (2012). Cyclin A2 is required for sister chromatid segregation, but not separase control, in mouse oocyte meiosis. Cell Rep *2*, 1077-1087.

Tsutsumi, M., Fujiwara, R., Nishizawa, H., Ito, M., Kogo, H., Inagaki, H., Ohye, T., Kato, T., Fujii, T., and Kurahashi, H. (2014). Age-related decrease of meiotic cohesins in human oocytes. PLos One *9*, e96710.

Uhlmann, F., Lottspeich, F., and Nasmyth, K. (1999). Sister-chromatid separation at anaphase onset is promoted by cleavage of the cohesin subunit Scc1. Nature *400*, 37-42.

Uhlmann, F., Wernic, D., Poupart, M.A., Koonin, E.V., and Nasmyth, K. (2000). Cleavage of cohesin by the CD clan protease separin triggers anaphase in yeast. Cell *103*, 375-386.

Unal, E., Arbel-Eden, A., Sattler, U., Shroff, R., Lichten, M., Haber, J.E., and Koshland, D. (2004). DNA damage response pathway uses histone modification to assemble a double-strand break-specific cohesin domain. Mol Cell *16*, 991-1002.

Unal, E., Heidinger-Pauli, J.M., Kim, W., Guacci, V., Onn, I., Gygi, S.P., and Koshland, D.E. (2008). A molecular determinant for the establishment of sister chromatid cohesion. Science *321*, 566-569.

Unal, E., Heidinger-Pauli, J.M., and Koshland, D. (2007). DNA double-strand breaks trigger genome-wide sister-chromatid cohesion through Eco1 (Ctf7). Science *317*, 245-248.

Valdeolmillos, A.M., Viera, A., Page, J., Prieto, I., Santos, J.L., Parra, M.T., Heck, M.M., Martinez, A.C., Barbero, J.L., Suja, J.A.*, et al.* (2007). Sequential loading of cohesin subunits during the first meiotic prophase of grasshoppers. PLos Genet *3*, e28.

Vasudevan, N.T., Mohan, M.L., Gupta, M.K., Hussain, A.K., and Naga Prasad, S.V. (2011). Inhibition of protein phosphatase 2A activity by PI3Kgamma regulates beta-adrenergic receptor function. Mol Cell *41*, 636-648.

Vaur, S., Feytout, A., Vazquez, S., and Javerzat, J.P. (2012). Pds5 promotes cohesin acetylation and stable cohesin-chromosome interaction. Embo Rep *13*, 645-652.

Visnes, T., Giordano, F., Kuznetsova, A., Suja, J.A., Lander, A.D., Calof, A.L., and Strom, L. (2014). Localisation of the SMC loading complex Nipbl/Mau2 during mammalian meiotic prophase I. Chromosoma *123*, 239-252.

Voitenleitner, C., Fanning, E., and Nasheuer, H.P. (1997). Phosphorylation of DNA polymerase alpha-primase by cyclin A-dependent kinases regulates initiation of DNA replication in vitro. Oncogene *14*, 1611-1615.

Waizenegger, I.C., Hauf, S., Meinke, A., and Peters, J.M. (2000). Two distinct pathways remove mammalian cohesin from chromosome arms in prophase and from centromeres in anaphase. Cell *103*, 399-410.

Ward, G.E., and Kirschner, M.W. (1990). Identification of cell cycle-regulated phosphorylation sites on nuclear lamin C. Cell *61*, 561-577.

Watrin, E., Schleiffer, A., Tanaka, K., Eisenhaber, F., Nasmyth, K., and Peters, J.M. (2006). Human Scc4 is required for cohesin binding to chromatin, sister-chromatid cohesion, and mitotic progression. Curr Biol *16*, 863-874.

Webster, A., and Schuh, M. (2016). Mechanisms of aneuploidy in human eggs. Trends Cell Biol *27*, 55–68.

Weng, K.A., Jeffreys, C.A., and Bickel, S.E. (2014). Rejuvenation of meiotic cohesion in oocytes during prophase I is required for chiasma maintenance and accurate chromosome segregation. Plos Genet *10*, e1004607.

Westhorpe, F.G., and Straight, A.F. (2013). Functions of the centromere and kinetochore in chromosome segregation. Curr Opin Cell Biol *25*, 334-340.

Winters, T., McNicoll, F., and Jessberger, R. (2014). Meiotic cohesin Stag3 is required for chromosome axis formation and sister chromatid cohesion. Embo J *33*, 1256-1270.

Xu, H., Beasley, M.D., Warren, W.D., van der Horst, G.T., and McKay, M.J. (2005). Absence of mouse REC8 cohesin promotes synapsis of sister chromatids in meiosis. Dev Cell *8*, 949-961.

Xu, P., Duong, D.M., Seyfried, N.T., Cheng, D.M., Xie, Y., Robert, J., Rush, J., Hochstrasser, M., Finley, D., and Peng, J. (2009a). Quantitative proteomics reveals the function of unconventional ubiquitin chains in proteasomal degradation. Cell *137*, 133-145.

Xu, Z., Cetin, B., Anger, M., Cho, U.S., Helmhart, W., Nasmyth, K., and Xu, W.Q. (2009b). Structure and function of the PP2A-shugoshin interaction. Mol Cell *35*, 426-441.

Yam, C.H., Fung, T.K., and Poon, R.Y.C. (2002). Cyclin A in cell cycle control and cancer. Cell Mol Life Sci *59*, 1317-1326.

Yamamoto, A., Guacci, V., and Koshland, D. (1996). Pds1p is required for faithful execution of anaphase in the yeast, Saccharomyces cerevisiae. J Cell Biol *133*, 85-97.

Yang, R., Nakamaki, T., Lubbert, M., Said, J., Sakashita, A., Freyaldenhoven, B.S., Spira, S., Huynh, V., Muller, C., and Koeffler, H.P. (1999). Cyclin A1 expression in leukemia and normal hematopoietic cells. Blood *93*, 2067-2074.

Zhang, J., Hakansson, H., Kuroda, M., and Yuan, L. (2008a). Wapl localization on the synaptonemal complex, a meiosis-specific proteinaceous structure that binds homologous chromosomes, in the female mouse. Reprod Domest Anim *43*, 124-126.

Zhang, J.L., Shi, X.M., Li, Y.H., Kim, B.J., Jia, J.L., Huang, Z.W., Yang, T., Fu, X.Y., Jung, S.Y., Wang, Y.*, et al.* (2008b). Acetylation of Smc3 by Eco1 is required for S phase sister chromatid cohesion in both human and yeast. Mol Cell *31*, 143-151.

Zhang, N., Panigrahi, A.K., Mao, Q., and Pati, D. (2011). Interaction of Sororin protein with polo-like kinase 1 mediates resolution of chromosomal arm cohesion. J Biol Chem *286*, 41826-41837.

Zickler, D., and Kleckner, N. (1999). Meiotic chromosomes: Integrating structure and function. Annu Rev Genet *33*, 603-754.

Zickler, D., and Kleckner, N. (2015). Recombination, pairing, and synapsis of homologs during meiosis. Csh Perspect Biol *7*, a016626.

Zindy, F., Lamas, E., Chenivesse, X., Sobczak, J., Wang, J., Fesquet, D., Henglein, B., and Brechot, C. (1992). Cyclin A is required in S-Phase in normal epithelial cells. Biochem Bioph Res Co *182*, 1144-1154.

Zou, H., McGarry, T.J., Bernal, T., and Kirschner, M.W. (1999). Identification of a vertebrate sister-chromatid separation inhibitor involved in transformation and tumorigenesis. Science *285*, 418-422.

# 6. Abbreviations

| | |
|---|---|
| aa | amino acids |
| AE | axial element |
| APC/C | anaphase promoting complex/cyclosome |
| BSA | bovine serum albumin |
| Cdk | cyclin-dependent kinase |
| CSF | cytostatic factor |
| DMSO | dimethylsulfoxide |
| dNTP | deoxynucleotide triphosphate |
| Dox | doxycycline |
| DSB | DNA double strand breaks |
| DTT | dithiothreitol |
| EDTA | ethylendiamine tetraacetic acid |
| EGTA | ethylene glycol-bis(2-aminoethylether)-N,N,N’,N’-tetraacetic acid |
| HECT | homologous to E6-AP C-terminus |
| Hek | human embryonic kidney |
| HeLa | Henrietta Lacks (patient from whom cell line is derived) |
| HEPES | 4-(2-hydroxyethyl)-1-piperazineethansulfonic acid |
| HRP | horseradish peroxidase |
| IFM | immunofluorescence microscopy |
| IP | immunoprecipitation |
| IPTG | isopropyl-β-D-thiogalactopyranoside |
| IVT | coupled *in vitro* transcription/translation in reticulocyte lysate |
| kDa | kilo dalton |
| LB | Luria-Bertani |
| MCC | mitotic checkpoint complex |
| mRec8 | mouse Rec8 |
| mRNA | messenger RNA |
| NBD | nucleotide binding domain |
| NES | nuclear export signal |
| NHS | N-Hydroxysuccinimide |

| | |
|---|---|
| NLS | nuclear localization signal |
| OD | optical density |
| PAGE | polyacrylamide gel electrophoresis |
| PBS | phosphate buffered saline |
| PD | protease dead |
| PP2A | protein phosphatase 2A |
| PVDF | polyvinylidene fluoride |
| RING | really interesting new gene |
| RNAi | RNA interference |
| RT | room temperature |
| SAC | spindle assembly checkpoint |
| SC | synaptonemal complex |
| Scc | sister chromatid cohesion |
| SCS | sister chromatid separation |
| SDS | sodium dodecylsulfate |
| Sgo | shugoshin |
| Smc | structural maintenance of chromosomes |
| siRNA | small interfering RNA |
| Stag | stromalin antigen |
| TEMED | N,N,N',N'-tetramethylethylenediamine |
| Tev | tobacco etch virus |
| Tris | tris(hydroxymethyl)aminomethane |
| v/v | volume per volume |
| w/v | weight per volume |
| Wapl | wings apart-like |

# 7. Danksagung

An erster Stelle danke ich Herrn Prof. Dr. Olaf Stemmann für die Möglichkeit in seinem Lehrstuhl forschen zu dürfen.
Er hat mir durch vielerlei Unterstützung eine spannende und lehrreiche Doktorarbeit ermöglicht, wofür ich ausgesprochen dankbar bin.

Weiterhin gilt mein Dank dem Zweitgutachter und allen Mitgliedern des Prüfungsausschusses für ihr Interesse und ihre Zeit.

Des Weiteren möchte ich mich bei Julia Bittner und Alexander Cuba Ramos bedanken, die während ihrer Master- bzw. Bachelorarbeit einen wertvollen Beitrag zu dieser Arbeit geleistet haben.

Ein besonderer Dank ergeht an Philip Kahlen, Kristina Seel und Brigitte Neumann für das Korrekturlesen dieser Arbeit. Weiterhin bedanken möchte ich mich Monika Ohlraun und Jutta Hübner für hervorragende technische Assistenz.

Abschließend bedanke ich mich bei allen aktuellen und ehemaligen Mitgliedern des Lehrstuhls Genetik für ihre Unterstützung und ständige Hilfsbereitschaft.

Die Experimente bei denen die Interaktionen der Cohesin Untereinheiten mittels Co-Immunpräzipitation untersucht wurden, wurden unter meiner Anleitung in Zusammenarbeit mit der Masterstudentin Julia Bittner durchgeführt. Daher finden sich diese Ergebnisse auch in der entsprechenden Masterarbeit.
Die Experimente mit Cyclin A Überexpression (Abbildungen 29-31) wurden unter meiner Anleitung in Zusammenarbeit mit dem Bachelorstudenten Alexander Cuba Ramos durchgeführt. Daher finden sich diese Ergebnisse auch in der entsprechenden Bachelorarbeit.

Die Verwendung der Zeichnung in Abbildung 35 wurde durch den Verlag „John Wiley and Sons“ genehmigt.

**(Eidesstattliche) Versicherungen und Erklärungen**

(§ 5 Nr. 4 PromO)

*Hiermit erkläre ich, dass keine Tatsachen vorliegen, die mich nach den gesetzlichen Bestimmungen über die Führung akademischer Grade zur Führung eines Doktorgrades unwürdig erscheinen lassen.*

(§ 8 S. 2 Nr. 5 PromO)

*Hiermit erkläre ich mich damit einverstanden, dass die elektronische Fassung meiner Dissertation unter Wahrung meiner Urheberrechte und des Datenschutzes einer gesonderten Überprüfung hinsichtlich der eigenständigen Anfertigung der Dissertation unterzogen werden kann.*

(§ 8 S. 2 Nr. 7 PromO)

*Hiermit erkläre ich eidesstattlich, dass ich die Dissertation selbständig verfasst und keine anderen als die von mir angegebenen Quellen und Hilfsmittel benutzt habe.*

(§ 8 S. 2 Nr. 8 PromO)

*Ich habe die Dissertation nicht bereits zur Erlangung eines akademischen Grades anderweitig eingereicht und habe auch nicht bereits diese oder eine gleichartige Doktorprüfung endgültig nicht bestanden.*

(§ 8 S. 2 Nr. 9 PromO)

*Hiermit erkläre ich, dass ich keine Hilfe von gewerblichen Promotionsberatern bzw. -vermittlern in Anspruch genommen habe und auch künftig nicht nehmen werde.*

…….

Ort, Datum, Unterschrift